Faculty of Pharmaceutical Sciences

Synthesis and Biological Evaluation of Modified Adenosine and Thymidine Nucleoside Analogues

Philippe Van Rompaey

Thesis submitted to the Faculty of Pharmaceutical Sciences in order to obtain the degree of Doctor in the Pharmaceutical Sciences

Promotor

Prof. Dr. Serge Van Calenbergh

October 2004

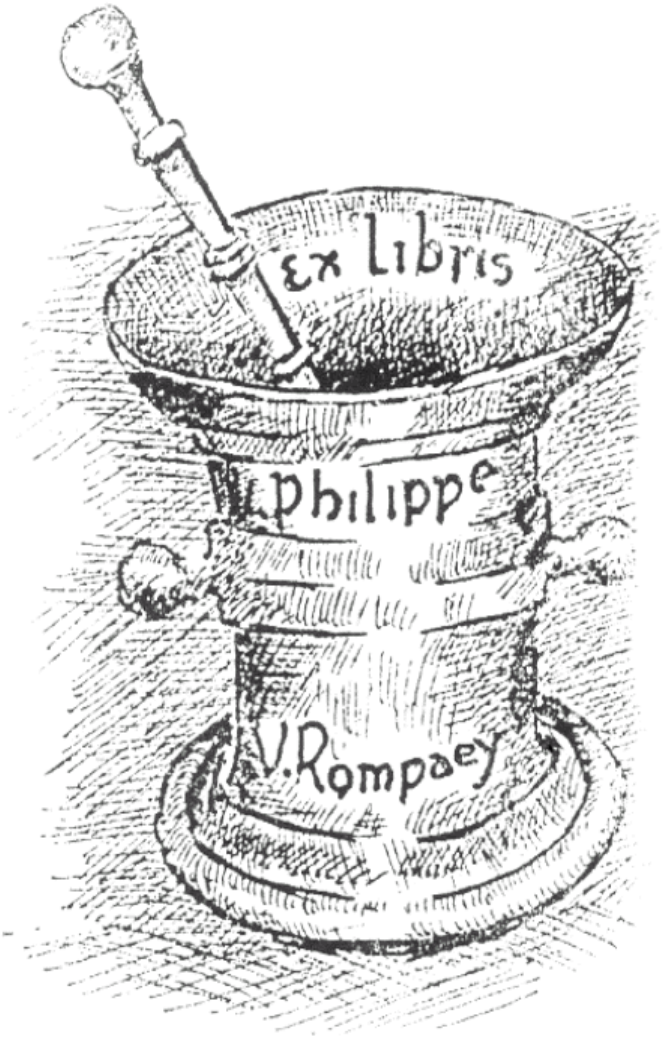

In memory of
Frans Van Rompaey and Armand Van de Mosselaer

ACKNOWLEDGEMENTS

In vele opzichten doet het raar deze woorden te schrijven, omdat ik ze altijd voor het laatst bewaard heb. Het is een open deur intrappen, maar een doctoraat haal je nooit alleen. Velen zijn erbij betrokken.

Tijdens mijn opleiding tot apotheker raakte ik gefascineerd door wetenschappelijk onderzoek, maar het schrok me ook af, want: “Wat is namelijk wetenschappelijk onderzoek? En kan ik dat wel?” Een tip van de sluier werd opgelicht tijdens mijn onderzoeksstage op het Laboratorium voor Farmacognosie en Fytochemie onder leiding van Prof. dr. Sc. Denis De Keukeleire. Hem ben ik dankbaar om mijn eerste (wankele) stappen als wetenschapper te begeleiden en de eerste versies van mijn thesis om te toveren tot de haast beruchte rode-inkt-picasso’s.

Mijn promotor Prof. dr. apr. Serge Van Calenbergh, ben ik in vele opzichten dankbaar. Hij heeft me de tijd en ruimte geboden om me wetenschappelijk te ontplooien. Gedurende de afgelopen vier jaar vormden zijn wetenschappelijk inzicht en enthousiasme een stevige houvast. Wat ik ga missen zijn onze gesprekken, al of niet in de “Take a Bite”, die zeker niet altijd over Medicinale Scheikunde gingen. Serge, voor meer redenen dan ik kan noemen, mijn welgemeende dank. Ook Prof. dr. apr. Piet Herdewijn zou ik hier willen danken voor de *long distance support* en zijn nuttige ideeën in de nucleosidenchemie.

In many ways this thesis would not have been possible without the scientific input of Dr. Kenneth A. Jacobson and his group at the NIH, Maryland, USA. I wish to express my sincere gratitude for introducing me into the challenging field of adenosine receptor (bio)chemistry. Although the study of the neoceptor was in many ways troublesome, it was nevertheless very exciting.

Voor de financiering van dit onderzoek dank ik het Instituut voor de Aanmoediging van Innovatie door de Wetenschap en Technologie in Vlaanderen (IWT-Vlaanderen).

Graag zou ik mijn collega's van het Laboratorium voor Medicinale Scheikunde (Veerle, Ineke, Liesbet, Izet, Ulrik, Timo, Vincent) danken voor de fijne samenwerking en hulp bij problemen allerhande. Ook heb ik altijd kunnen rekenen op de steun van verschillende fijne mensen, verspreid over de Labo's voor Farmacognosie en Fytochemie, Toxicologie en Medische Biochemie, waarvoor dank.

Everybody at the deVGen chemistry department that supports me: thank you.

Mijn ouders, familie en vrienden, … Hoe bedank je mensen die er altijd, in alle omstandigheden, staan. Jullie hebben me allemaal gesteund, getroost, geholpen, doen lachen, ontspannen en groen zien. Jullie allemaal, bedankt!

Beste mensen, voor mij is dit doctoraat geen eindpunt, maar eerder een nieuw begin. Ik ben klaar voor de volgende zet.

ABBREVIATIONS

AR	adenosine receptor
CHO	Chinese hamster ovary
DMAP	dimethylaminopyridine
DMF	dimethylformamide
DMSO	dimethylsulfoxide
DNA	deoxy ribo nucleic acid
EDC	*N*-ethyl-*N*'-(3-dimethylaminopropyl)carbodiimide
EL	extracellular loop
ESI	electron spray ionisation
EtOAc	ethyl acetate
EtOH	ethanol
GPCR / 7TM	G-protein coupled receptor
HMDS	hexamethyldisilazane
HOAc	acetic acid
IL	intracellular loop
MDR	multi drug resistant
MeOH	methanol
MS	mass spectrometry
N	north
NMR	nuclear magnetic resonance
PKA	protein kinase A
RNA	ribo nucleic acid
S	south
SAR	structure-activity-relationship
SDM	site-directed mutagenisis
TB	tuberculosis
TBSCl	*tert*-butyldimethylsilyl chloride
TEA	triethylamine
THF	tetrahydrofuran
TMPKmt	thymidine monophosphate kinase of Mycobacterium *tuberculosis*
TMSCl	chlorotrimethylsilane
TMSOTf	trimethylsilyl triflate

TABLE OF CONTENTS

OBJECTIVES

Structure-based drug discovery relies on the three dimensional interactions of ligand molecules with their target. Generally, by inserting themselves in the binding site of the target protein, (drug) molecules can influence protein activity. Affinity of these ligands to their respective target proteins is due to their structural and chemical complementarity.

Today, fundamental understanding of the molecular details of ligand/G-protein coupled receptor (GPCR) interactions remain very rudimentary. In absence of high-resolution structural knowledge of different GPCRs, this matter can only be addressed by building (homology) models, which are validated through biochemical and pharmacological studies.

In this thesis, we will focus on the design of novel ligands for the adenosine receptors (ARs), an interesting family of GPCRs. Four AR subtypes have been identified today, i.e. A_1, A_{2A}, A_{2B} and A_3. We will evaluate the potential (i.e. binding properties, intrinsic activity and selectivity) of synthetic adenosine analogues, modified at the 3'- and 5'-positions of the ribofuranosyl moiety and at the purine 2- and N^6-positions as human A_3AR ligands.

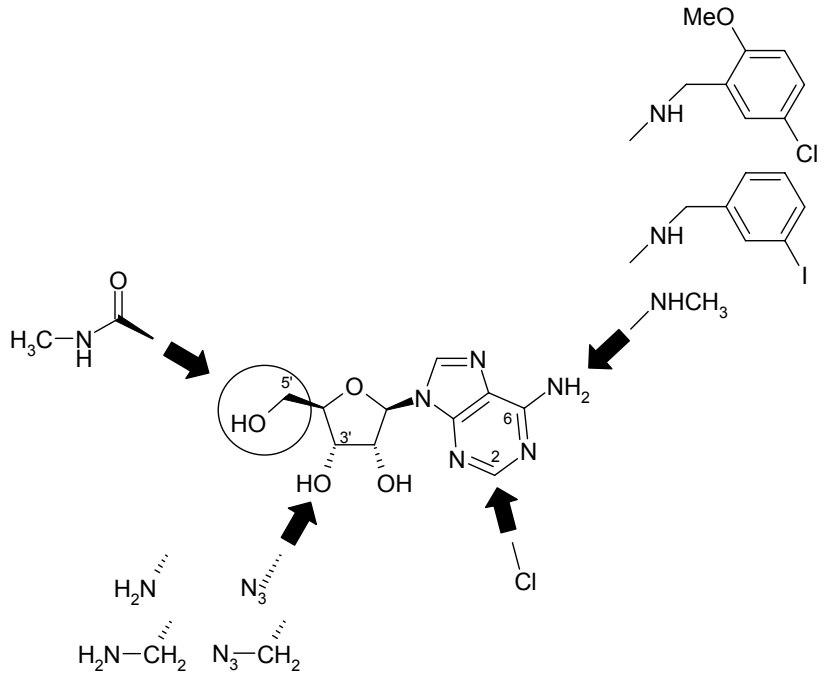

All planned analogues are characterised by an azido/amino(methyl) modification at the 3'-position (i.e. 3'-(CH_2)-N_3 or 3'-(CH_2)-NH_2) of the ribofuranose moiety. Since such structural modifications have not been explored intensively for ARs, they might open interesting perspectives towards tuning the efficacy and selectivity for the human A_3AR.

The envisaged adenosine analogues will also be valuable tools to explore a "chemical genetics" approach on ARs. In such approach individual proteins are modified so that they can be modulated with small molecules and hence improve our understanding of target function. In collaboration with the group of Dr. Kenneth A. Jacobson, we aim to integrate organic synthesis and molecular engineering to explore the "neoceptor concept", i.e. investigation of molecular complementarity at both wild-type and mutant A_3 and A_{2A} adenosine receptors.

In another part of this thesis, we will design and evaluate a number of 2'- and 3'-modified thymidine analogues as *Mycobacterium tuberculosis* thymidine monophosphate kinase (TMPKmt) inhibitors, based on its crystal structure.

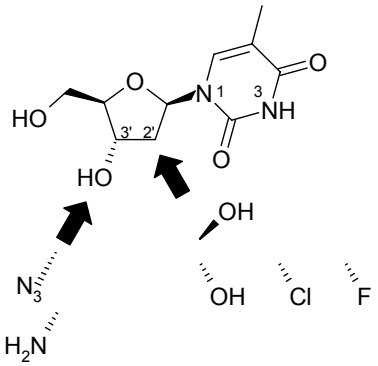

PART I

SYNTHESIS OF MODIFIED ADENOSINE AND THYMIDINE ANALOGUES

Synthesis discussed in this part gives an overview of the chemistry published in:

Bioorg. Med. Chem. **2004**, *Accepted*.

J. Med. Chem. **2003**, *46*, 4847.

Eur. J. Org. Chem. **2003**, *15*, 2911.

J. Med. Chem. **2001**, *44*, 4125.

CHAPTER 1

GENERAL BACKGROUND

1.1 Nucleoside synthesis

> "*Nucleosides and their analogues are of enormous importance. They are an established class of clinically useful medicinal agents, possessing antiviral and anticancer activity.*"[1]

The potential activity of the modified nucleoside analogues, of which the synthesis is discussed in this part, will be biologically evaluated on adenosine receptor (AR) subtypes A_{2A} and A_3 (Part II) and as inhibitors of thymidine monophosphate kinase of Mycobacterium *tuberculosis* (TMPKmt, Part III).

From a chemical point of view, in this work, we focus on the synthesis of **adenosine** and **thymidine** nucleoside analogues (Figure 1.1). Both the ribofuranose or 2'-deoxyribofuranose moieties of adenosine and thymidine are extensively modified, i.e. at the 3'- and 5'-position for the former and at the 2'- and 3'-position for the latter. In the adenosine nucleoside series the purine base was also altered at the 2- and N^6-position. The rationale for the synthesis of the reported analogues in Part I will be explained in Parts II and III.

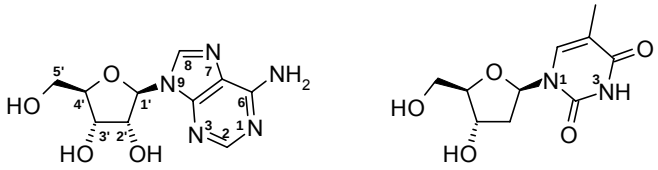

adenosine **thymidine**

Figure 1.1 The adenosine and thymidine nucleosides and their sugar and base numbering.

In general, for the *de novo* synthesis of modified nucleosides, two synthetic strategies are employed. A first approach, uses the parent nucleoside scaffold to introduce the intended modifications. When the nucleoside scaffold is not compatible with the conditions of the reactions used, a second (more elaborate) approach consists of the glycosylation of a (modified) sugar synthon with the desired (modified) heterocyclic base.

In the method developed by Vorbrüggen, the glycosidic bond formation is driven by the use of a silylated nucleobases in combination with strong Lewis acids, like trimethylsilyl triflate (**2** in Scheme 1.1).[2] This Vorbrüggen coupling reaction is "the" reference in nucleoside synthesis and provides a highly reproducible method for nucleoside formation in high yield with reliable and predictable stereochemistry, i.e. orientation of the glycosidic bond.[1,2]

Scheme 1.1

The Vorbrüggen coupling reaction for the formation of β-ribonucleosides.

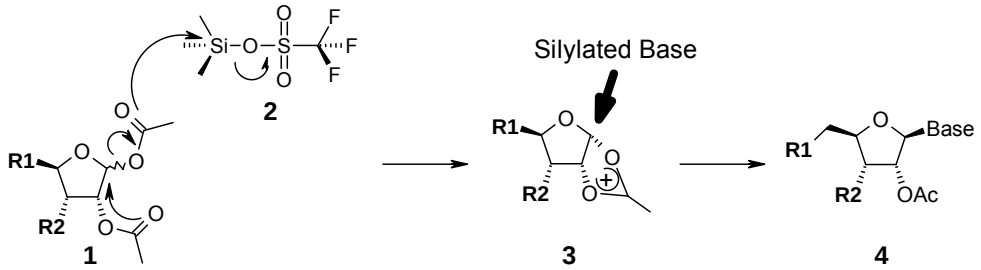

In the presence of a 2-α-acetyl group (as in **1**), the trimethylsilyl triflate catalyst **2** converts the 1,2-diacetylated ribofuranosyl sugar **1** into the 1,2-acetyloxonium intermediate **3** (as a triflate salt).[3] Under these conditions the nucleophilic silylated base can only attack the sugar cation from the top (β-side), resulting in the exclusive formation of β-nucleoside **4**.

Silylation of the base is needed to:

- convert these quite polar heterocycles into more lipophilic compounds, to become soluble in organic solvent and permitting homogeneous reactions;
- promote the nucleophilicity of the heterocycles, due to the electron-releasing properties of silicon.[4]

The preferred strategy for the synthesis of adenosine and thymidine analogues described in this work, was to couple the modified ribofuranosyl moieties (**5**-**8**) with the desired purine (**9**-**11**) or pyrimidine (**12**) heterocycles (Scheme 1.2). This approach allowed us to keep the main synthetic route as common as possible and permitted time-effective and efficient preparation of divergent nucleoside analogues.

Scheme 1.2
Ribofuranose, purine and pyrimidine moieties used for nucleoside formation.

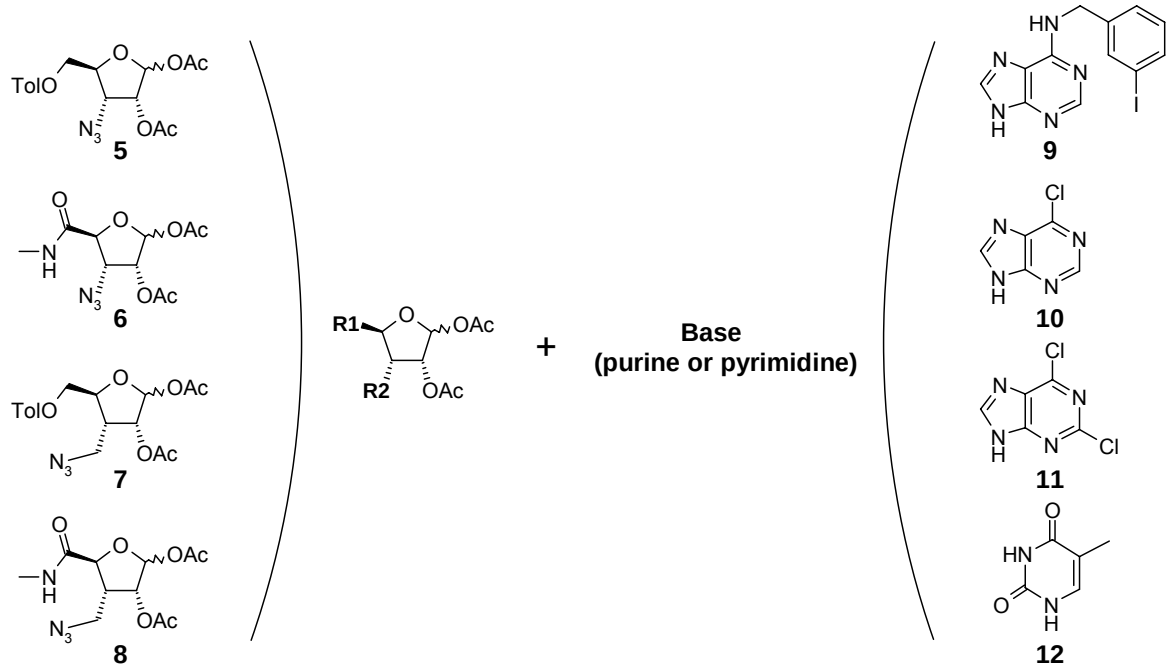

The stereoselective introduction of both key modifications, i.e. an azido (**13**) and azidomethyl (**14**) group at the 3-position of the ribofuranose ring (Scheme 1.3), was accomplished via appropriate protection/deprotection strategies, described in detail in Chapter 2. The commercially available 1,2-*O*-isopropylidene-α-D-xylo-furanose sugar (**15**) was used as starting material for both modifications.

Using the key azido (**13**) and azidomethyl (**14**) synthons as a secondary starting point we could:

- easily get access to the desired 1,2-diacetylated intermediates **5** and **7** after isopropylidene deprotection and acetylation;
- further modify the ribofuranosyl moiety, i.e. introduction of the uronamide (methylcarbamoyl) functionality at the 5-position,[5] to give **6** and **8** after isopropylidene deprotection and acetylation.

1.2 Comments on the synthesis of the key azido synthons

Throughout this work we used the Ph_3P azido reduction as a final step in the synthesis of the modified adenosine and thymidine nucleoside derivatives. Azido

reduction reactions are of wide applicability and have been effected with a variety of reagents, including $LiAlH_4$, $NaBH_4$, catalytic hydrogenation, Ph_3P, diborane, Bu_3SnH, Zn/HCl.[6] However, one the mildest and most selective routes to convert azides to amines is the Staudinger[7] reaction (with Ph_3P).[6,8]

Scheme 1.3

Retrosynthetic overview for the preparation of the 1,2-diacetylated modified ribofuranose sugar scaffolds.

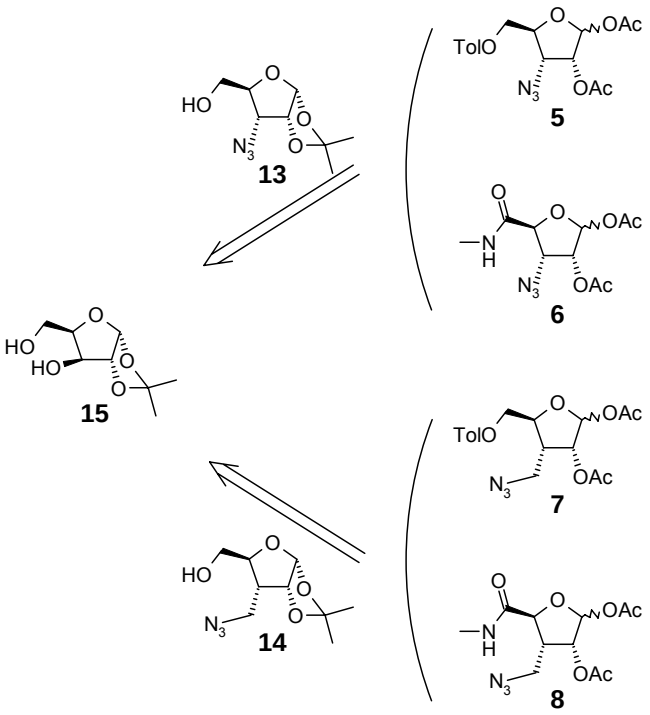

The crucial stage in the preparation of the azido modified 1,2-diacetylated sugar synthons **5** and **6** (Scheme 1.2 and Scheme 1.3), was the stereoselective introduction of the 3-α-oriented azide (**13**). Synthetic routes to **puromycine** (and its analogues) via **3'-amino-3'-deoxyadenosine** (Figure 1.2) have already been reported.[9] Most of these procedures however suffer from a high number of steps and a low overall yield. Moreover, these synthetic strategies all use adenosine as a starting point, which, contrary to our approach, limits their use for the preparation of nucleosides derived from **5**-**8**.

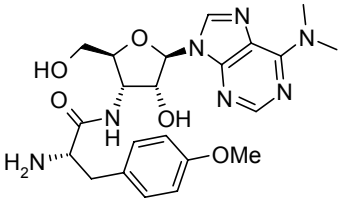

puromycine

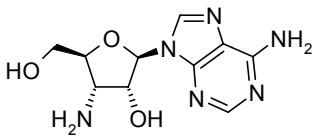

3'-aminoadenosine

Figure 1.2 The puromycine and 3'-amino-3'-deoxyadenosine nucleosides.

Based on the work of Azhayev *et al.*,[10] we developed a procedure that made the regio- and stereoselective azido functionalisation possible (Chapter 2), starting from the isopropylidene protected α-D-xylofuranose sugar.

Formation of the 3-α-oriented azidomethyl intermediate **14** (Scheme 1.3), to give access to the 1,2-diacetylated "3-*C*-branched chain" intermediates **7** and **8**, was based on the method of Lin *et al.*[11] (Chapter 2). This approach also allowed us to start from the isopropylidene protected α-D-xylofuranose **15**. Other methods to introduce this type of branching have been reported:

- Acton *et al.*,[12] starting from 1,2:5,6-di-*O*-isopropylidene-α-D-glucofuranose;
- An *et al.*,[13] formation of the 3'-α-hydroxymethyl on 2'-deoxythymidine and cytidine derivatives;
- Filichev *et al.*,[14] via reduction of 3'-α-cyano or 3'-α-nitromethyl as amino precursor groups.

During the course of our work, a procedure for the synthesis of the simple 3'-amino / azido modified series has been patented[15] and published[16] by *Pfizer* in parallel to our reports.[17] Based on the work of Acton *et al.*,[12] they prepared their 3'-amino modified nucleosides (like **CP-608039**) through azide displacement of the triflate derived from **glucose diacetonide** (Scheme 1.4).

Scheme 1.4

Pfizer approach towards the synthesis of the 3'-amino modified analogue CP-608039.

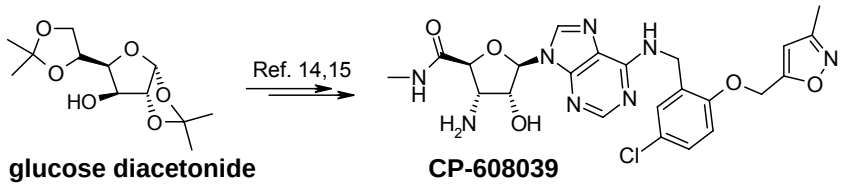

glucose diacetonide **CP-608039**

Recently Rozners *et al.* communicated a novel and general approach to 3',5'-C-branched pyrimidine ribonucleosides[18] **16** and **17** (Figure 1.3) that show high similarity to our envisaged purine nucleoside analogues.

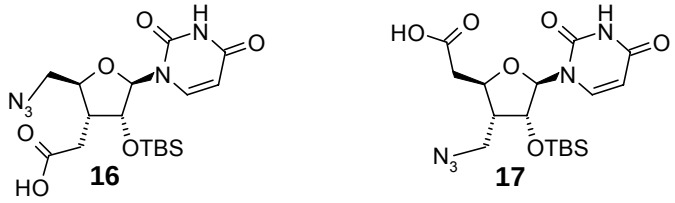

16 **17**

Figure 1.3 3',5'-C-branched pyrimidine nucleosides analogues reported by Rozners *et al.*[18]

Note on the nucleoside nomenclature used in this work

In nucleosides, as already demonstrated for adenosine and thymidine in Scheme 1.1, the ribofuranose ring numbering can be distinguished from purine heterocycle numbering by the use of the prime after the arabic numerals. Moreover, this "generic" nucleoside notation, i.e. not according to IUPAC conventions, is used to indicate the positions of the nucleoside that are chemically modified (like the 3'-branching) or to pinpoint particular regions of the nucleoside that interact with the biological (target) system (like the N^6-substituent in the human A_3AR binding site, see Part II).

These conventions can lead to serious misinterpretations when modifications on the nucleoside significantly alter the parent nucleoside structure. In this work, such a modification is the replacement of the 4'-CH_2OH group of the parent nucleoside (**18**) by a uronamide functionality (**19**) (Figure 1.4). Although the methylcarbamoyl group in **19** can be seen as a 4'-substituent, it is dubiously called a 5'-uronamide modification. Hence, the generic name of **19** is **5'-methylcarbamoyladenosine** or

9-[(5-methylcarbamoyl)-β-D-ribofuranosyl]adenosine. However the latter can easily be mistaken for compound **20**.

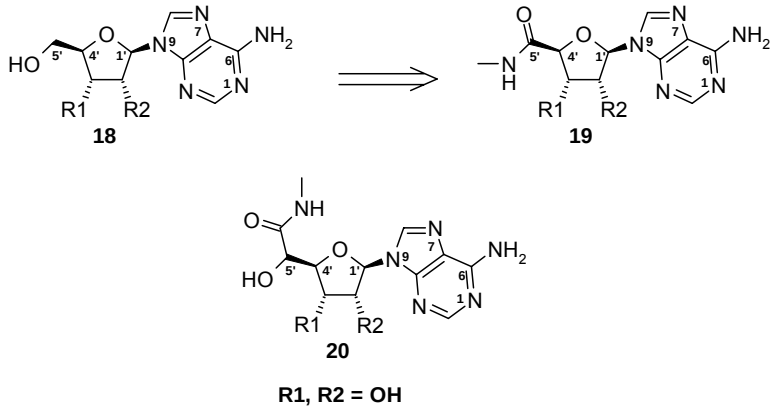

Figure 1.4 Nomenclature in nucleoside chemistry for modifications at the 5'-position.

In fact to accurately describe structure **19** its IUPAC-name should be used, i.e. **(2*S*,3*R*,4*R*,5*R*)-5-(6-amino-9*H*-purin-9-yl)-tetrahydro-3,4-dihydroxy-N-methylfuran-2-carboxamide**. Since IUPAC nomenclature does not allow rapid visualisation of the described structures, the "generic" nomenclature is generally accepted in the nucleoside (bio)chemistry and pharmacology field and will therefore be used throughout this work.

1.3 References

[1] Ichikawa, E.; Kato, K. *Curr. Med. Chem.* **2001**, *8*, 385.

[2] (i) Vorbrüggen, H.; Krolikiewicz, K.; Bennua, B. *Chem. Ber.* **1981**, *114*, 1234. (ii) Vorbrüggen, H.; Ruh-Pohlenz, C. *Handbook of Nucleoside Synthesis*, John Wiley & Sons, **2001**.

[3] Vorbrüggen, H.; Höfle, G. *Chem. Ber.* **1981**, *114*, 1256.

[4] Colvin, E. N. *Silicon in Organic chemistry*, Butterworths: London, **1981**.

[5] (i) Kim, H. O.; Ji, X.-D.; Siddiqi, S. M.; Olah, M. E.; Stiles, G. L.; Jacobson, K. A. *J. Med. Chem.* **1994**, *37*, 3614. (ii) Jacobson, K. A.; Siddiqi, S. M.; Olah, M. E.; Ji, X.-D.; Melman, N.; Bellamkonda, K.; Meshulam, Y.; Stiles, G. L.; Kim, H. O. *J. Med. Chem.* **1995**, *38*, 1720. (iii) Dauban, P.; Chiaroni, A.; Riche, C.; Dodd, R. H. *J. Org. Chem. 1996*, *61*, 2488.

[6] Scriven, E. F. V.; Turnbull, K. *Chemical Reviews* **1988**, *88*, 351.

[7] Staudinger, H.; Meyer, J. *Helv. Chim. Acta* **1919**, *2*, 635.

[8] Alajarin, M.; Conesa, C.; Rzepa, H. *Perkin Trans. 2* **1999**, 1811.

[9] (i) Gerber, N. N.; Lechevalier, H. A. *J. Org. Chem.* **1962**, *27*, 1731. (ii) Sowa, W. *Can. J. Chem.* **1968**, *46*, 1586. (iii) McDonald, F. E.; Gleason, M. M. *J. Am. Chem. Soc.* **1996**, *118*, 6648. (iv) Robins, M. J.; Miles, R. W.; Samano, M. C.; Kaspar, R. L. *J. Org. Chem.* **2001**, *66*, 8204. (v) Nguyen-Trung, N. Q.; Botta, O.; Terenzi, S.; Strazewski, P. *J. Org. Chem.* **2003**, *68*, 2038. (iii) Takatsuki, K.-I.; Yamamoto, M.; Ohgushi, S.; Kohmoto, S.; Kishikawa, K.; Yamashita, H. *Tetrahedron Lett.* **2004**, *45*, 137.

[10] (i) Azhayev, A. V.; Smrt, J. *Collect. Czech. Chem. Commun.* **1978**, *43*, 1520. (ii) Azhayev, A. V. Nucleic Acids Res. **1979**, *6*, 625. (iii) Ozols, A. M.; Azhayev, A. V.; Dyatkina, N. B.; Krayevski, A. A. *Synthesis* **1980**, 557. (iv) Ozols, A. M.; Azhayev, A. V.; Krayevski, A. A.; Ushakov, A. S.; Gnuchev, N. V.; Gottikh, B. P. *Synthesis* **1980**, 559.

[11] Lin, T.-S.; Zhu, J.-L.; Dutschman, G. E.; Cheng, Y.-C.; Prusoff, W. H. *J. Med. Chem.* **1993**, *36*, 353.

[12] (i) Acton, E. M.; Goerner, R. N.; Uh, H. S.; Ryan, K. J.; Henry, D. W. *J. Med. Chem.* **1979**, *22*, 518. (ii) Mikhailopulo, I. A.; Poopeiko, N. E.; Tsvetkova, T. M.; Marochkin, A. P.; Balzarini, J.; De Clercq, E. *Carbohydr. Res.* **1996**, *285*, 17.

[13] An, H.; Wang, T.; Maier, M. A.; Manoharan, M.; Ross, B. S.; Cook, P. D. *J. Org. Chem.* **2001**, *66*, 2789.

[14] Filichev, V. V.; Brandt, M.; Pedersen, E. B. *Carbohydrate Res.* **2001**, *333*, 115.

[15] (i) Masumane, H.; DeNinno, M. P.; Scott, R. W. *PCT Int. Appl.* WO 2001023399 A1 **2001**, 194 pp. (ii) DeNinno, M. P.; Masumane, H. *Eur. Pat. Appl.* EP 1241176 A1 **2002**, 55 pp.

[16] DeNinno, M. P.; Masumane, H.; Chenard, L. K.; DiRico, K. J.; Eller, C.; Etienne, J. B.; Tickner, J. E.; Kennedy, S. P.; Knight, D. R.; Kong, J.; Oleynek, J. J.; Tracey, W. R.; Hill, R. J. *J. Med. Chem.* **2003**, *46*, 353.

[17] (i) Jacobson, K.A.; Gao, Z.-G.; Chen, A.; Barak, D.; Kim, S.-A.; Lee, K.; Link, A.; Van Rompaey, P.; Van Calenbergh, S.; Liang, B.T. *J. Med. Chem.* **2001**, *44*, 4125. (ii) Van Rompaey, P.; Nauwelaerts, K.; Vanheusden, V.; Rozenski, J.; Munier-Lehmann, H.; Herdwijn, P.; Van Calenbergh, S. *Eur. J. Org. Chem.* **2003**, *15*, 2911. (iii) Kim, S.-K.; Gao, Z.-G.; Van Rompaey, P.; Gross, A. S.; Chen, A.; Van Calenbergh, S.; Jacobson, K. A. *J. Med. Chem.* **2003**, *46*, 4847.

[18] (i) Rozners, E.; Liu, Y. *Org. Lett.* **2003**, *5*, 181. (ii) Rozners, E; Xu, Q. *Org. Lett.* **2003**, *5*, 3999.

CHAPTER 2

SYNTHESIS AND PREPARATION OF MODIFIED
ADENOSINE AND THYMIDINE ANALOGUES

2.1 Synthesis of 3'-azido / amino modified iodobenzyladenosine

3-Azido-3-deoxy-1,2-di-*O*-acetyl-5-*O*-(toluoyl)-D-ribofuranose (**4**) was prepared in five steps from the commercially available 1,2-*O*-isopropylidene-α-D-xylofuranose (**1**) following a slightly altered procedure described by *Ozols et al* (Scheme 2.1).[1] *Vorbrüggen*[2] coupling with N^6-(3-iodobenzyl)adenine[3] followed by alkaline deprotection, gave the β-anomer **5** in low yield. Reduction of the azido moiety of **5** with triphenylphosphine led to smooth conversion to the desired amine **6**, without detectable loss of the benzylic N^6-substituent.

Scheme 2.1[a]

Synthesis of 3'-azido / amino modified iodobenzyladenosine.

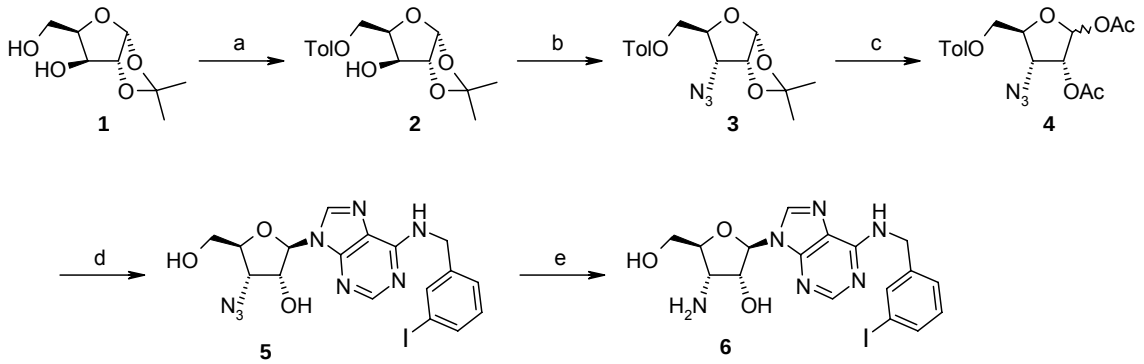

[a]**Reagents and conditions:** (a) toluoyl chloride, dry pyridine, dry CH_2Cl_2, 0 °C, 71%; (b) (i) $(CF_3SO_2)_2O$, dry pyridine, dry CH_2Cl_2, -10 °C (ii) NaN_3, DMF, rt, 40%; (c) (i) 75 % HCOOH, 50 °C (ii) $(CH_3CO)_2O$, pyridine, rt, 90%; (d) (i) silylated 3-iodobenzyladenine, $(CH_3)_3SiOSO_2CF_3$, ClC_2H_4Cl, 85 °C (ii) 0.1 N $NaOCH_3$ in MeOH, rt, 18%; (e) Ph_3P, NH_4OH, pyridine, rt, 70%.

2.2 Synthesis of the 3'-azido-5'-methylcarbamoyl nucleoside scaffolds

For the synthesis of the fully modified nucleoside scaffolds, the 3-azido intermediate **7**[4], was obtained by simple 5-deprotection of **3** (Scheme 2.2). Periodate oxidation[5] followed by esterification of the carboxylic acid and subsequent treatment with methylamine[3] in a sealed tube afforded the ribofuronamide **8**[6]. One pot deprotection-acetylation gave the 1,2-diacetylated 3,5-modified sugar **9**. Vorbrüggen-

glycosylation[2] with silylated 6-chloropurine and 2,6-dichloropurine[7] quantitatively yielded the key nucleoside scaffolds **10**[6] and **11**.

Scheme 2.2[a]

Synthesis of the 3'-azido-5'-methylcarbamoyl nucleoside scaffolds.

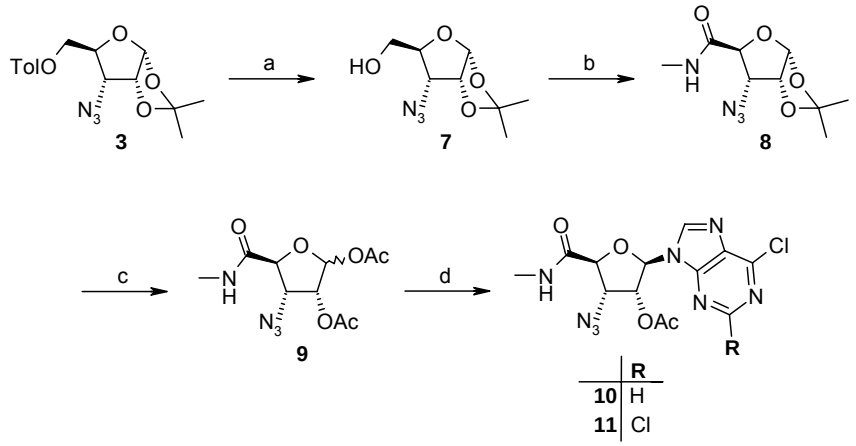

[a]**Reagents and conditions:** (a) 0.1 N $NaOCH_3$ in MeOH, rt, 88%; (b) (i) $NaIO_4$, $RuCl_3$, H_2O, $CHCl_3$, CH_3CN, rt (ii) EDC, DMAP, anhydrous MeOH, rt (iii) 2 M CH_3NH_2 in THF, 55 °C, 33%; (c) H_2SO_4, $(CH_3CO)_2O$, CH_3COOH, 55%; (d) silylated 6-chloropurine or 2,6-dichloropurine, $(CH_3)_3SiOSO_2CF_3$, ClC_2H_4Cl, 85 °C, 95% and 70%.

The one pot deprotection-acetylation strategy was needed for the preparation of the 1,2-diacetylated 3,5-modified sugar moiety **9**. As pointed out in Scheme 2.3, deprotection of **8** with 75% acetic acid and simple acetylation, using an acetic anhydride-pyridine (1:2) mixture, resulted in a rearrangement to compound **12**, which yielded the isolated six-membered nucleoside **13** after Vorbrüggen coupling[2] with 6-chloropurine.

Scheme 2.3[a]

Rearrangement upon deprotection / acetylation of the isopropylidene group.

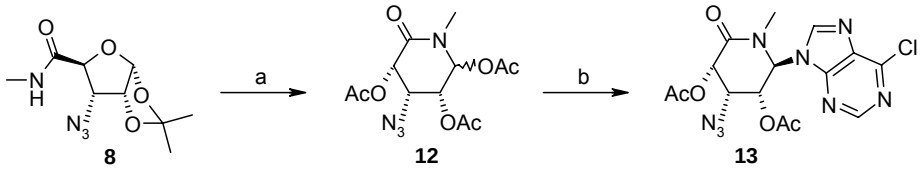

[a]**Reagents and conditions:** (a) (i) 75 % CH_3COOH, 60 °C (ii) $(CH_3CO)_2O$, pyridine, rt, 61%; (b) silylated 6-chloropurine, $(CH_3)_3SiOSO_2CF_3$, ClC_2H_4Cl, 85 °C, 93%.

2.3 Synthesis of the 3'-azidomethyl modified nucleoside scaffold

The 3-*C*-azidomethyl sugar **17** was prepared in six steps from **1** by reported procedures (Scheme 2.4).[8,9] Removal of the 5-*O*-(*tert*-butyldimethyl)silyl (TBS) group of **17** with tetrabutylammonium fluoride (TBAF) and protection of the 5-hydroxyl group of **18**[10] as a toluoyl ester gave **19**. Acidic deblocking of the 1,2-*O*-isopropyl moiety of **19**, followed by acetylation furnished the 1,2-diacetylated 3-*C*-azidomethyl sugar **20**. The protecting group exchange was necessary to avoid pyranose ring formation that, in our hands, occurred upon acidic deprotection (contrary to what is reported[9]). Vorbrüggen-type coupling[2] of **20** with silylated 6-chloropurine[7] gave the nucleoside scaffold **21**.

Scheme 2.4[a]

Synthesis of the 3'-azidomethyl modified nucleoside scaffold.

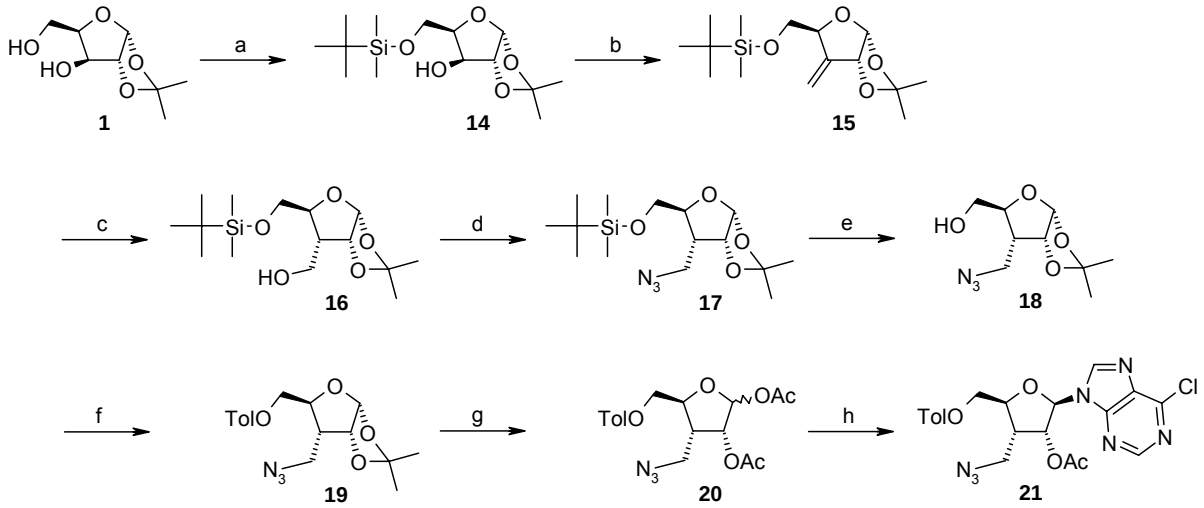

[a]**Reagents and conditions:** (a) TBSCl, DMAP, pyridine, 0°C, 73%; (b) (i) $(COCl)_2$, DMSO, dry CH_2Cl_2, -55 °C (ii) NaH, methyltriphenylphosphonium bromide, DMSO, rt, 56%; (c) (i) 1 M BH_3 in THF, rt (ii) THF, H_2O, NaOH, H_2O_2, 0 °C, 65%; (d) (i) CH_3SOCl, dry pyridine, rt (ii) NaN_3, DMF, 95 °C, 77%; (e) 1 M TBAF in THF, rt, 96%; (f) toluoyl chloride, dry pyridine, rt, 94%; (g) (i) 75 % CH_3COOH, 60 °C (ii) $(CH_3CO)_2O$, pyridine, rt, 63%; (h) silylated 6-chloropurine, $(CH_3)_3SiOSO_2CF_3$, ClC_2H_4Cl, 85 °C, 81%.

2.4 Synthesis of the 3'-azidomethyl-5'-methylcarbamoyl nucleoside scaffold

The synthesis of the 3'-azidomethyl-5'-methylcarbamoyl nucleoside scaffold **24** is outlined (Scheme 2.5). In analogy to the procedure described under paragraph 2.2, intermediate **18**[10] was converted to the 5-methylcarbamoyl derivative **22**. One pot

deprotection-acetylation afforded the 1,2-diacetylated 3,5-modified sugar **23**, which after Vorbrüggen-glycosylation[2] with silylated 6-chloropurine quantitatively yielded **24**.

Scheme 2.5[a]

Synthesis of the 3'-azidomethyl-5'-methylcarbamoyl nucleoside scaffold.

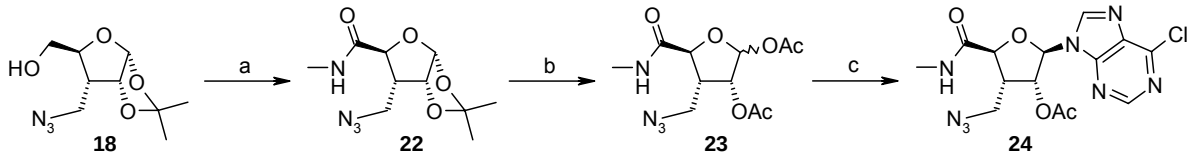

[a]**Reagents and conditions:** (a) (i) $NaIO_4$, $RuCl_3$, H_2O, $CHCl_3$, CH_3CN, rt (ii) EDC, DMAP, anhydrous MeOH, rt (iii) 2 M CH_3NH_2 in THF, 55 °C, 32%; (b) H_2SO_4, $(CH_3CO)_2O$, CH_3COOH, 40%; (c) silylated 6-chloropurine, $(CH_3)_3SiOSO_2CF_3$, ClC_2H_4Cl, 85 °C, 95%.

2.5 Synthesis of the *N*^{6}-substituted adenosine analogues

Displacement of the 6-chloro atom in **21** with ammonia, methylamine, 3-iodobenzylamine and 5-chloro-2-methoxybenzylamine[11], followed by deprotection in 7 N NH_3 in MeOH produced the 3'-C-azidomethyl nucleosides **25**-**28** (Scheme 2.6). Triphenylphosphine reduction of the azido moiety gave the 3'-C-aminomethyl nucleosides **29**-**32**. Amidation of **31** and **32** was performed with acetyl chloride under Schotten-Baumann conditions and furnished derivatives **33** and **34**.

Following the same strategy, the 3'-amino / azido(methyl)- 5'-methylcarbamoyl nucleoside scaffolds **10**, **11** and **24** produced the *N*^{6}-substituted 3'-azido(methyl)-5'-methylcarbamoyl adenosine analogues **35**-**37**, **41** and **42** after nucleophilic displacement with 3-iodobenzylamine or 5-chloro-2-methoxybenzylamine and subsequent deprotection in 7 N NH_3 in MeOH (Scheme 2.7). Here also, triphenylphosphine reduction of the azido moiety gave smooth conversion to the amino-nucleosides **38**-**40**, **43** and **44**.

2.6 Synthesis of the thymidine analogues modified at the 2'- and 3'-position

The conversion of 1,2-*O*-isopropylidene-α-D-xylofuranose **1** into **4** (Scheme 2.8) is discussed under paragraph 2.1.

Scheme 2.6[a]

Synthesis of the N^6-substituted 3'-amino / azidomethyl adenosine analogues.

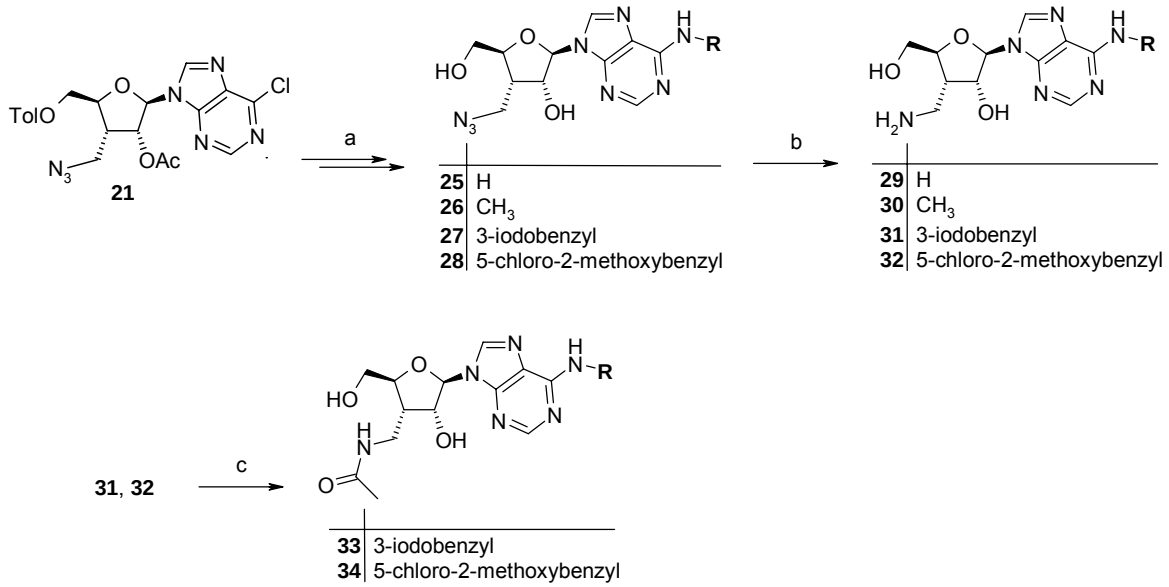

[a]**Reagents and conditions:** (a) (i) amine HCl (or ammonia for **25**), Et_3N, EtOH, reflux (ii) 7 N NH_3 in MeOH, rt, 35%-68%; (b) Ph_3P, NH_4OH, pyridine, rt, 64%-70%; (c) CH_3COCl, 50% aqueous NaOAc, THF, rt, 63% and 60%.

Scheme 2.7[a]

Synthesis of the N^6-substituted 3'-amino / azido(methyl)- 5'-methylcarbamoyl adenosine analogues.

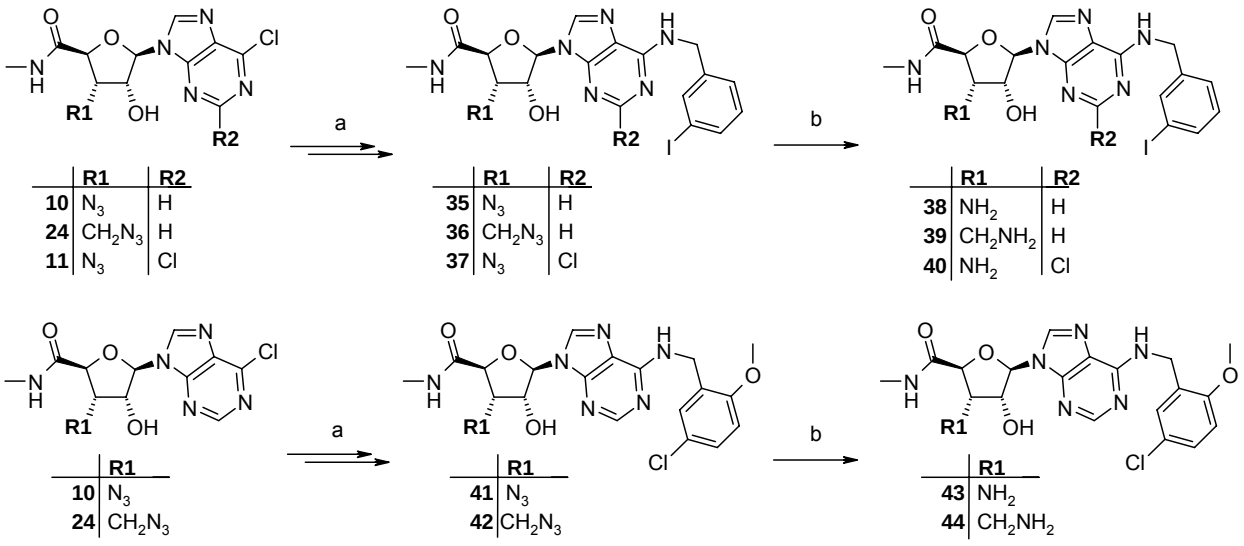

[a]**Reagents and conditions:** (a) (i) amine HCl, Et_3N, EtOH, reflux (ii) 7 N NH_3 in MeOH, rt, 60%-82%; (b) Ph_3P, NH_4OH, pyridine, rt, 18%-74%.

Scheme 2.8[a]

Synthesis of the thymidine analogues modified at the 2'- and 3'-position.

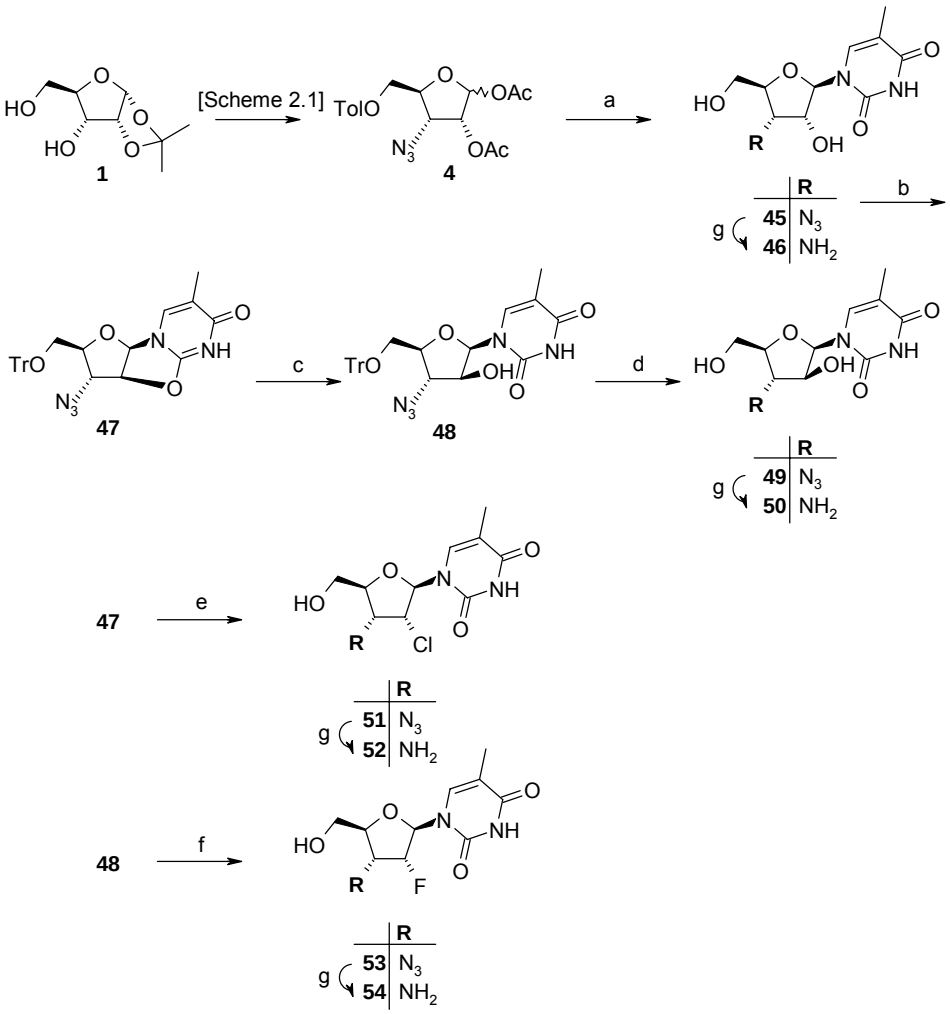

[a]**Reagents and conditions:** (a) (i) silylated thymine, $(CH_3)_3SiOSO_2CF_3$, ClC_2H_4Cl, 85 °C (ii) 0.1 N $NaOCH_3$ in MeOH, rt, 80%; (b) (i) triphenylmethyl chloride, pyridine, 65°C (ii) CF_3SO_2Cl, DMAP, CH_2Cl_2, 4°C, 75%; (c) (i) 1 N NaOH, EtOH:H_2O (1:1), rt (ii) adjusted to ~pH 7 with CH_3COOH, 88%; (d) 80 % CH_3COOH, 90°C, 79%; (e) 4 M HCl in 1,4-dioxane, 92%; (f) (i) DAST, pyridine, toluene, 50°C (ii) 80 % CH_3COOH, 90°C, 58%; (g) Ph_3P, NH_4OH, pyridine, rt, 30%-71%.

Vorbrüggen[2] glycosylation with silylated thymine, followed by alkaline deprotection afforded the azido nucleoside **45**[12]. After tritylation of the primary hydroxyl group, **45** was converted into the 2,2'-*anhydro*-analogue **47**.[13] Alkaline treatment of **47** yielded intermediate **48** with the 2'-hydroxyl group in the *arabino* ("UP") configuration.[14] Detritylation with 80 % acetic acid quantitatively yielded nucleoside **49**[15]. Nucleophilic chlorination of **47** using 4 M HCl in dioxane[16] resulted in the formation of **51**. Analogue **48** was treated with DAST[17] and, after detritylation, afforded nucleoside **53**[18] with the fluor atom at the 2'-position in *ribo* ("DOWN") configuration. Our synthesis is superior to the methods previously described, in that our method starts

from the key azide synthon **45** and avoids the troublesome opening a 2',3'-*lyxo*-epoxide.[18] Selective triphenylphosphine reduction of the azido moieties of nucleosides **45**, **49**, **51** and **53** smoothly afforded the novel 3'-amine analogues **46**, **50**, **52** and the known **54**[19].

2.7 Experimental part

General Remarks

^{1}H and ^{13}C spectra were obtained with a Varian 300 MHz spectrometer. The residual solvent signal of $CDCl_3$ and DMSO-d_6 was used as a secondary reference. Assignment of all ^{1}H-resonances was confirmed by 2D ^{1}H-^{1}H COSY experiments. Signals assigned to amino and hydroxyl groups were exchangeable with D_2O. Abbreviations used are s = singulet, d = doublet, t = triplet, q = quadruplet, m = multiplet, dd = double doublet, app = apparent and br = broad signal. Coupling constants (*J*) are expressed in Hz.

Exact mass measurements were performed on a quadrupole/orthogonal-acceleration time-of-flight (Q/oaTOF) tandem mass spectrometer (qTOF 2, Micromass, Manchester, UK) equipped with a standard electrospray ionisation (ESI) interface. Samples were infused in a 2-propanol:water (1:1) mixture at 3 μl/min. Elemental analyses were performed at the University of Konstanz, Germany, and are within ±0.4% of theoretical values unless otherwise specified.

Precoated MACHEREY-NAGEL ALUGRAM® SIL G/UV_{254} silica gel plates were used for TLC and spots were examined with UV-light at 254 nm and/or a sulfuric acid-anisaldehyde solution or a ninhydrine (0.5 % in EtOH) solution. Column Chromatography was performed on 560 (0.06-0.2 mm) Uetikon Chemie silicagel.

1,2-*O*-isopropylidene-α-D-xylofuranose (**1**), all reagents and (anhydrous) solvents were purchased from ACROS ORGANICS. CH_2Cl_2, $ClCH_2CH_2Cl$ and MeOH were obtained by distillation after refluxing overnight on CaH_2.

2.7.1 Preparation of 3'-azido / amino modified iodobenzyladenosine

1,2-*O*-Isopropylidene-5-*O*-(toluoyl)-α-D-xylofuranose (2)

A solution of toluoyl chloride (13.2 mL, 100 mmol) in dry CH_2Cl_2 (40 mL) was added dropwise to a solution of 1,2-*O*-isopropylidene-α-D-xylofuranose **1** (20 g, 105.15 mmol) in dry pyridine (50 mL) and dry CH_2Cl_2 (150 mL). The reaction mixture was stirred at 0 °C for 2 h and quenched afterwards in water (250 mL). After extraction with CH_2Cl_2, the organic phase was evaporated in vacuo. The residue was dissolved in a minimal amount of warm EtOAc and the product was crystallized upon treatment with hexane. The crystals were isolated by filtration to yield 23g (71 %) of **2**.

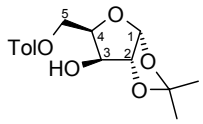

Molecular formula: $C_{16}H_{20}O_6$

Molecular weight: 308.33

^{1}H-NMR (300 MHz, $CDCl_3$):

δ 1.32 and 1.51 (2 x s, 6H, 2 x CH_3), 2.42 (s, 3H, Ar-CH_3), 2.78 (d, 1H, *J* = 4.1 Hz, 3-OH), 4.18 (dd, 1H, *J* = 2.5 Hz and 5.2 Hz, H-3), 4.24-4.90 (m, 4H, H-2, H-4, H-5B and H-5A), 5.96 (d, *J* = 3.6 Hz, H-1), 7.26 and 8.00 (2 x d, 4H, *J* = 8.0 Hz, Ar-H).

Exact mass (ESI-MS, *i*PrOH:H_2O):

calculated for $C_{16}H_{21}O_6$ $[M+H]^+$ 309.1338, found 309.1343

3-Azido-3-deoxy-1,2-*O*-isopropylidene-5-*O*-(toluoyl)-α-D-ribofuranose (3)

To a stirred solution of **2** (23g, 74.6 mmol) in CH_2Cl_2 (250 mL) and pyridine (20 mL) trifluoromethanesulfonic anhydride (15 mL, 89.5 mmol) was added and the reaction mixture was held at -10 °C for 2 h. 7 % $NaHCO_3$ was added and stirring continued for 20 min. The organic phase was washed with H_2O, dried over $MgSO_4$, filtered and evaporated to dryness. The residue was dissolved in DMF (250 mL) and NaN_3 (34g, 522 mmol) was added. The reaction mixture was stirred overnight at room temperature. DMF was evaporated in vacuo, and 7 % $NaHCO_3$ (250 mL) and EtOAc (250 mL) were added. The organic phase was dried over $MgSO_4$, filtered, evaporated to dryness and purified by column chromatography (Pentane/EtOAc, 95/5→85/15) to yield 10 g (40 %) of **3**.

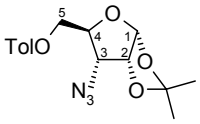

Molecular formula: $C_{16}H_{19}N_3O_5$

Molecular weight: 333.34

^{1}H-NMR (300 MHz, $CDCl_3$):

δ1.36 and 1.58 (2 x s, 6H, 2 x CH_3), 2.38 (s, 3H, Ar-CH_3), 3.38 (dd, 1H, *J* = 8.6 Hz, H-3), 4.21-4.61 (m, 3H, H-4, H-5A and H-5B), 4.73 (dd, 1H, *J* = 4.5 Hz and 8.5 Hz, H-2), 5.79 (d, 1H, *J* = 3.6 Hz, H-1), 7.16 and 7.86 (2 x d, 4H, *J* = 7.9 Hz, Ar-H).

Exact mass (ESI-MS, *i*PrOH:H_2O):

calculated for $C_{16}H_{19}N_3O_5Na$ $[M+Na]^+$ 356.1222, found 356.1235

3-Azido-3-deoxy-1,2-di-*O*-acetyl-5-*O*-(toluoyl)- D-ribofuranose (4)

The azido derivative **3** (5 g, 15 mmol) was added to a 75 % HCOOH solution (150 mL). The mixture was heated to 50 °C for 2 h and evaporated to dryness. The residue was dissolved in a mixture of acetic anhydride/pyridine (125 mL, 2:3, v/v) at room temperature. Stirring was continued for 3 h and CH_2Cl_2 (100 mL) and 7 % $NaHCO_3$ (100 mL) were added. The aqueous phase was washed with CH_2Cl_2 (100 mL) and the combined organic phases were dried over $MgSO_4$, filtered and evaporated in vacuo. The residue was precipitated from methanol to give **4** as a white solid (5.1 g, 90 %).

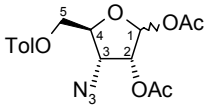

Molecular formula: $C_{17}H_{19}N_3O_7$

Molecular weight: 377.35

^{1}H-NMR (300 MHz, $CDCl_3$) ***of most polar anomer***:

δ1.90 and 2.15 (2 x s, 6H, 2 x CH_3), 2.48 (s, 3H, Ar-CH_3), 4.10-4.68 (m, 4H, H-3, H-4, H-5B and H-5A), 5.31 (d, 1H, *J* = 4.6 Hz, H-2), 6.09 (s, 1H, H-1), 7.16 and 7.88 (2 x d, 4H, *J* = 8.1 Hz, Ar-H).

Exact mass (ESI-MS, *i*PrOH:H_2O):

calculated for $C_{17}H_{19}N_3O_7Na$ $[M+Na]^+$ 400.1120, found 400.1198

General procedure for the silylation of the bases

The appropriate base (1.0 mmol) was treated with hexamethyldisilazane (HMDS, 5 mL). Chlorotrimethylsilane (TMSCl, 1.0 mmol) was added and the reaction mixture was refluxed at 134 °C under N_2 for 20 hours. Solvents were removed in vacuo and the concentrated silylated base was used without further purification.

9-(3-Azido-3-deoxy-α-D-ribofuranosyl)-*N*^{6}-(3-iodobenzyl)adenine (5)

4 (725 mg, 1.92 mmol) in 1,2-dichloroethane (35 mL) was added to silylated *N*^{6}-(3-iodobenzyl)adenine (810 mg, 2.31 mmol). TMSOTf (417 μL, 2.31 mmol) was added dropwise under continuous stirring under nitrogen atmosphere to give a clear solution after approximately 30 min at 83 °C. After 6 h at 83 °C the reaction mixture was cooled and CH_2Cl_2 (50 mL) and a 7 % $NaHCO_3$ solution (100 mL) were added. The organic phase was separated, dried with $MgSO_4$, filtered, and evaporated to dryness. The residue was dissolved in 0.1 N $NaOCH_3$ in CH_3OH (100 mL), stirred for 2 h, neutralized with a 9:1 H_2O-CH_3COOH mixture, evaporated in vacuo, purified by column chromatography (CH_2Cl_2/MeOH, 100/0 → 97/3) and precipitated from CH_3OH to yield 176 mg (18 %) of **5** as a white solid.

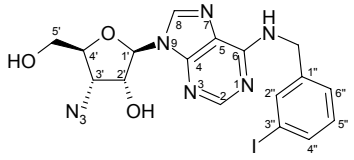

Molecular formula: $C_{17}H_{17}IN_8O_3$

Molecular weight: 508.28

^{1}H NMR (300 MHz, DMSO-d_6)

δ 3.58 (app dd, 1H, *J* = 3.6 Hz and -12.3 Hz, H-5B'), 3.69 (app dd, 1H, *J* = 3.5 Hz, H-5A'), 4.00 (app q, 1H, *J* = 3.5 Hz and 7.0 Hz, H-4'), 4.33 (q, 1H, *J* = 3.8 Hz and 5.2 Hz, H-3'), 4.67 (s, 2H, CH_2-Ar), 5.02 (t, 1H, *J* = 5.6 Hz, H-2'), 5.54 (br s, 1H, 5'-OH), 5.92 (d, 1H, *J* = 6.0 Hz, H-1'), 6.24 (br s, 1H, 2'-OH), 7.11 (t, 1H, *J* = 7.8 Hz, H-5''), 7.36 (d, 1H, *J* = 7.6 Hz, H-6''), 7.59 (d, 1H,*J* = 7.8 Hz, H-4''), 7.73 (s, 1H, H-2''), 8.23 (s, 1H, H-2), 8.42 (s, 1H, H-8), 8.55 (br s, 1H, N(6)-H).

Exact mass (ESI-MS, *i*PrOH:H_2O):

calculated for $C_{17}H_{18}IN_8O_3$ $[M+H]^+$: 509.0548, found 509.0547.

Elemental analysis ($C_{17}H_{17}IN_8O_3$) C,H,N.

9-(3-Amino-3-deoxy-α-D-ribofuranosyl)-N^6-(3-iodobenzyl)adenine (6)

5 (100 mg, 0.197 mmol) was dissolved in pyridine (10 mL), and Ph_3P (100 mg, 0.381 mmol) was added to the solution. After stirring for 1 h at room temperature, concentrated NH_4OH (5 mL) was added. The reaction mixture was stirred for another 2 h, evaporated to dryness and purified by column chromatography (CH_2Cl_2/MeOH, 9/1) to yield 67 mg (70 %) of **6** as a white solid.

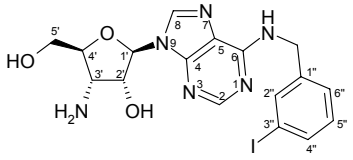

Molecular formula: $C_{17}H_{19}IN_6O_3$

Molecular weight: 482.28

^{1}H NMR (300 MHz, DMSO-d_6)

δ 1.69 (br s,2H, 3'-NH_2), 3.47 (app t, 1H, J = 6.1 Hz, H-3'), 3.57 (app dd, 1H, J = 4.3 Hz and -12.6 Hz, H-5B'), 3.73 (m, 2H, H-5A'and H-4'), 4.29 (m, 1H, H-2'), 4.65 (s, 2H, CH_2-Ar), 5.14 (br s, 1H, 5'-OH), 5.77 (br s, 1H, 2'-OH), 5.93 (d, 1H, J = 2.8 Hz, H-1'), 7.11 (t, 1H, J = 7.8 Hz, H-5''), 7.35 (d, 1H, J = 7.6 Hz, H-6''), 7.58 (d, 1H, J = 7.8 Hz, H-4'''), 7.71 (s, 1H, H-2''), 8.21 (s, 1H, H-2), 8.44 (s, 1H, H-8), 8.48 (br s, 1H, N(6)-H).

Exact mass (ESI-MS, *i*PrOH:H_2O):

calculated for $C_{17}H_{20}IN_6O_3$ $[M+H]^+$: 483.0643, found 483.0631.

Elemental analysis ($C_{17}H_{19}IN_6O_3$) C,H,N.

	calculated %				found %		
Compound	C	H	N		C	H	N
5	40.17	3.37	22.05		39.83	3.02	22.27
6	41.56	4.10	17.11		41.33	3.97	17.01

Table 2.1 Elemental analysis of final products **5** and **6**.

2.7.2 Preparation of the 3'-azido-5'-methylcarbamoyl nucleoside scaffolds

3-Azido-3-deoxy-1,2-*O*-isopropylidene-α-D-ribofuranose (7)

3 (6 g, 15 mmol) was dissolved in 0.1 N $NaOCH_3$ in CH_3OH (150 mL), stirred for 2 h, neutralized with a 9:1 H_2O-CH_3COOH solution, evaporated in vacuo and purified by column chromatography (CH_2Cl_2/MeOH, 99/1) to yield 3.4 g (88 %) of **7** as a solid.

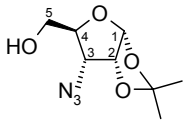

Molecular formula: $C_8H_{13}N_3O_4$

Molecular weight: 215.21

^{1}H-NMR (300 MHz, DMSO-d_6):

δ 1.28 and 1.44 (2 x s, 6H, 2 x CH_3), 3.45-3.52 (m, 2H, H-3 and H-5B), 3.64 (ddd, 1H, *J* = 2.9 Hz, 5.3 Hz and -12.3 Hz, H-5A), 3.94 (ddd, 1H, *J* = 2.9 Hz, 4.3 Hz and 9.8 Hz, H-4), 4.77 (t, 1H, *J* = 4.3 Hz, H-2), 4.90 (dd, 1H, *J* = 5.4 Hz and 6.0 Hz, 5-OH), 5.77 (d, 1H, *J* = 3.5 Hz, H-1).

Exact mass (ESI-MS, *i*PrOH:H_2O):

calculated for $C_8H_{13}N_3O_4Na$ $[M+Na]^+$ 238.0803, found 238.0801

Methyl 3-azido-3-deoxy-1,2-isopropylidene-α-D-ribofuronamide (8)

A biphasic mixture of water (46 mL), $CHCl_3$ (31 mL) and acetonitrile (31 mL) containing compound **7** (3.3 g, 15.33 mmol), $RuCl_3$ hydrate (160 mg, 0.77 mmol) and $NaIO_4$ (13.45 g, 62.87 mmol) was vigorously stirred for 4.5 h at room temperature. The reaction mixture was then diluted with water (100 mL) and extracted with CH_2Cl_2 (3 x 200 mL). The combined organic phase was dried over $MgSO_4$, filtered and evaporated. A dark green oily residue was triturated with diethyl ether to precipitate the ruthenium salts, that were removed by filtration through celite. The filtrate was concentrated in vacuo, leaving 2.7 g (77 %) of 3-azido-3-deoxy-1,2-isopropylidene-α-D-ribofuronic acid as a lightly coloured oil that was used without further purification. A mixture of this ribofuronic acid (2.5 g, 11.78 mmol), EDC (5.2 mL, 29.5 mmol) and DMAP (145 mg, 1.2 mmol) in anhydrous methanol (50 mL) was stirred at room temperature for 24 h. The reaction mixture was concentrated to dryness and the residue was dissolved in CH_2Cl_2 (200 mL) and water (100 mL). The aqueous phase was extracted with CH_2Cl_2 (3 x 200 mL) and the combined organic phase was dried over $MgSO_4$, filtered and evaporated. The residue was dissolved in 2 M methylamine in THF (20 mL) and was heated for 24 h at 55 °C in a sealed tube. After cooling, the reaction mixture was concentrated to dryness and purified by silica gel chromatography (pentane/EtOAc, 9/1) to give **8** (1.2 g, 33 % from **7**) as a transparent oil.

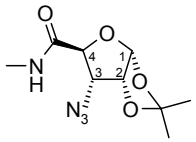

Molecular formula: $C_9H_{14}N_4O_4$

Molecular weight: 242.24

^{1}H-NMR (300 MHz, DMSO-d_6):

δ 1.29 and 1.46 (2s, 6H, 2 x CH_3) 2.62 (d, 3H, *J* = 4.7 Hz, CH_3-N), 3.75 (dd, 1H, *J* = 4.5 Hz and 9.5 Hz, H-3), 4.27 (d, 1H, *J* = 9.7 Hz, H-4), 4.77 (app t, 1H, *J* = 4.0 Hz, H-2), 5.85 (d, 1H, *J* = 3.5 Hz, H-1), 8.12 (d, 1H, *J* = 4.4 Hz, NH).

Exact mass (ESI-MS, *i*PrOH:H_2O):

calculated for $C_9H_{14}N_4O_4Na$ $[M+Na]^+$: 265.0912, found 265.0917.

Methyl 3-azido-3-deoxy-1,2-di-*O*-acetyl-D-ribofuronamide (9)

A mixture of **8** (1.2 g, 5 mmol), concentrated sulphuric acid (1.47 mL, 27.5 mmol) and acetic anhydride (4.95 mL, 52.4 mmol) in glacial acid (25 mL) was stirred for 18 h at room temperature. After cooling in an ice bath, a saturated $NaHCO_3$ solution (50 mL) and CH_2Cl_2 (50 mL) were slowly added and the mixture was stirred for another 10 min. After separation the aqueous phase was extracted with CH_2Cl_2 (3 x 100 mL). The combined organic phase was washed with saturated $NaHCO_3$ solution and brine, dried over $MgSO_4$, filtered and evaporated to dryness to yield 787 mg (55 %) of crude **9** as a yellowish foam.

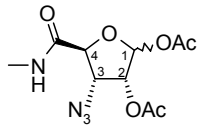

Molecular formula: $C_{10}H_{14}N_4O_6$

Molecular weight: 286.25

^{1}H-NMR (300 MHz, $CDCl_3$) ***of most polar anomer***:

δ 2.01 and 2.10 (2s, 6H, 2 x CH_3), 2.79 (d, 3H, *J* = 5.0 Hz, CH_3-N), 4.33-4.43 (m, 2H, H-3 and H-4), 5.24 (dd, 1H, *J* = 0.8 Hz and 5.0 Hz, H-2), 6.07 (br s, 1H, H-1), 6.53 (d, 1H, *J* = 4.7 Hz, NH).

Exact mass (ESI-MS, *i*PrOH:H_2O):

calculated for $C_{10}H_{15}N_4O_6$ $[M+H]^+$: 287.0991, found 287.0987.

9-[2-*O*-Acetyl-3-azido-3-deoxy-5-(methylcarbamoyl)-β-D-ribofuranosyl]-6-chloropurine (10)

9 (0.87 g, 3.0 mmol) in dry 1,2-dichloroethane (35 mL) was added to silylated 6-chloropurine (0.61 g, 4.0 mmol) under N_2-atmosphere. Under continuous stirring TMSOTf (0.3 mL, 1.5 mmol) was added dropwise to the resulting suspension to give a clear solution after ± 30 min. The temperature was raised to 83 °C. After 2 h the mixture was cooled and CH_2Cl_2 (40 mL) and cold 7 % $NaHCO_3$ solution (80 mL) were added. The organic layer was separated, dried with $MgSO_4$, filtered and the filtrate evaporated to dryness. The residue was purified by column chromatography (CH_2Cl_2/MeOH, 9/1) and precipitated from hexane to yield **10** (2.2 g, 95 %) as a yellow-white solid.

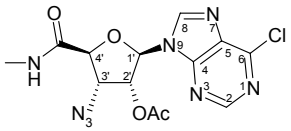

Molecular formula: $C_{13}H_{13}ClN_8O_4$

Molecular weight: 380.75

^{1}H-NMR (300 MHz, $CDCl_3$):

δ2.12 (s, 3H, CH_3), 2.92 (d, 3H, *J* = 5.0 Hz, CH_3-N), 4.57 (d, 1H, *J* = 2.9 Hz, H-4'), 4.86 (dd, 1H, *J* = 2.9 Hz and 5.6 Hz, H-3'), 5.87 (dd, 1H, *J* = 5.6 Hz and 7.0 Hz, H-2'), 6.14 (d, 1H, *J* = 7.0 Hz, H-1'), 7.66 (d, 1H, *J* = 4.1 Hz, NH), 8.23 and 8.77 (2 x s, 2H, H-2 and H-8).

Exact mass (ESI-MS, *i*PrOH:H_2O):

calculated for $C_{13}H_{14}ClN_8O_4$ $[M+H]^+$: 381.0826, found 381.0825.

9-[2-*O*-Acetyl-3-azido-3-deoxy-5-(methylcarbamoyl)-β-D-ribofuranosyl]-2,6-dichloropurine (11)

9 (200 mg, 0.69 mmol) was coupled with silylated 2,6-dichloropurine in analogy to the procedure described for **10**, to yield the the title compound **11** (200 mg, 70 %).

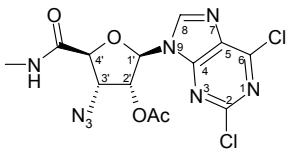

Molecular formula: $C_{13}H_{12}Cl_2N_8O_4$

Molecular weight: 415.20

^{1}H-NMR (300 MHz, $CDCl_3$):

δ 2.10 (s, 3H, CH_3), 2.63 (d, 3H, *J* = 4.7 Hz, CH_3-N), 4.52 (d, 1H, *J* = 5.6 Hz, H-4'), 4.93 (t, 1H, *J* = 5.6 Hz, H-3'), 5.96 (t, 1H, *J* = 4.7 Hz, H-2'), 6.37 (d, 1H, *J* = 3.8 Hz, H-1'), 8.16 (d, 1H, *J* = 4.4 Hz, NH),8.99 (s, 1H, H-8).

Exact mass (ESI-MS, *i*PrOH:H_2O):

calculated for $C_{13}H_{12}Cl_2N_8O_4Na$ $[M+Na]^+$: 437.0256, found 437.0252.

(3*S*,4*S*,5*R*)-4-azido-5,6-diacetyl-1-methyl-2-oxopiperidin-3-yl acetate (12)

8 (0.75 g, 3.0 mmol) was dissolved in 75 % HOAc (30 mL). The solution was kept at 60 °C and after 48 h the reaction mixture was evaporated to dryness. The residue was dissolved in a mixture of acetic anhydride/pyridine (50 mL, 2:3, v/v). After 3 h, the mixture was partitioned between CH_2Cl_2 (100 mL) and 7 % $NaHCO_3$ (150 mL). The aqueous layer was washed with CH_2Cl_2 (150 mL) and the combined organic layers were dried with $MgSO_4$, filtered and evaporated in vacuo. Treatment with a hexane-EtOAc mixture allowed precipitation of **12** (0.6 g, 61 %) as a white solid.

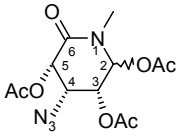

Molecular formula: $C_{12}H_{16}N_4O_7$

Molecular weight: 328.28

^{1}H-NMR (300 MHz, $CDCl_3$):

δ 2.11, 2.16 and 2.34 (3s, 9H, CH_3), 2.91 (s, 3H, CH_3-N), 4.35 (t, 1H, *J* = 3.4 Hz, H-4), 5.24 (dd, 1H, *J* = 3.8 Hz and 4.7 Hz, H-3), 5.57 (d, 1H, *J* = 2.9 Hz, H-5), 6.09 (d, 1H, *J* = 5.0 Hz, H-2).

(3*S*,4*S*,5*R*,6*S*)-5-acetyl-4-azido-6-(6-chloropurin-9-yl)-1-methyl-2-oxopiperidin-3-yl acetate (13)

Coupling reaction of **12** (0.58 g, 1.8 mmol) using the procedure described for **10** yielded **13** (710 mg, 93 %).

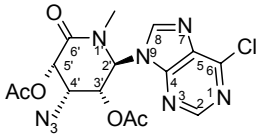

Molecular formula: $C_{15}H_{15}ClN_8O_5$

Molecular weight: 422.79

^{1}H-NMR (300 MHz, $CDCl_3$):

δ 1.99 and 2.30 (2s, 6H, 2 x CH_3), 2.66 (s, 3H, CH_3-N), 4.51 (t, 1H, *J* = 2.8 Hz, H-3'), 5.82 (d, 1H, *J* = 7.9 Hz, H-5'), 5.97 (dd, 1H, *J* = 2.6 Hz and 7.9 Hz, H-4'), 6.01 (d, 1H, *J* = 2.9 Hz, H-2'), 8.24 and 8.79 (2 x s, 2H, H-2 and H-8).

Exact mass (ESI-MS, *i*PrOH:H_2O):

calculated for $C_{15}H_{16}ClN_8O_5$ $[M+H]^+$: 423.0932, found 423.0934.

2.7.3 Preparation of the 3'-azidomethyl modified nucleoside scaffold

1,2-*O*-Isopropylidene-5-*O*-(*tert*-butyldimethylsilyl)-α-D-xylofuranose (14)

1,2-*O*-Isopropylidene-α-D-xylofuranose **1** (35.4 g, 186mmol) and DMAP (5.6 g, 46 mmol) were dissolved in pyridine (300 mL), cooled in an ice bath and TBSCl (28 g, 186 mmol) was added. The reaction mixture was stirred at 0 °C for 30 min and then allowed to warm to rt. After 2 h H_2O (40 mL) was added and the reaction mixture was evaporated in vacuo. The residue was extracted with EtOAc, washed with H_2O, dried over $MgSO_4$, filtered, evaporated to dryness and chromatographed on silica gel (pentane/EtOAc, 6/4) to give **14** (41.4g, 73 %) as a colourless oil.

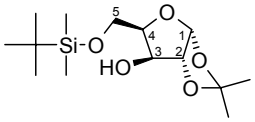

Molecular formula: $C_{14}H_{28}SiO_5$

Molecular weight: 304.46

^{1}H-NMR (300 MHz, DMSO-d_6):

δ 0.00 (s, 6H, $(CH_3)_2Si$), 0.82 (s, 9H, *tert*-Bu), 1.18 and 1.32 (2 x s, 6H, 2 x CH_3), 3.61 (dd, 1H, *J* = 6.3 Hz and -10.7 Hz, H-5B), 3.77 (dd, 1H, *J* = 5.2 Hz, H-5A), 3.93 (m, 2H, H-3 and H-4), 4.32 (d, 1H, *J* = 3.7 Hz, H-2), 5.16 (d, 1H, *J* = 4.8 Hz, 3-OH), 5.76 (d, 1H, *J* = 3.7 Hz, H-1).

Exact mass (ESI-MS, *i*PrOH:H_2O):

calculated for $C_{14}H_{29}SiO_5$ $[M+H]^+$: 305.1784, found 305.1785.

3-Deoxy-1,2-*O*-isopropylidene-3-methylene-5-*O*-(*tert*-butyldimethylsilyl)-α-D-ribofuranose (15)

Oxalyl chloride (6.5 mL, 74.8 mmol) was dissolved in dry CH_2Cl_2 (200 mL) and cooled to -55 °C. DMSO (10.6 mL, 150 mmol) was added (temperature kept below -55 °C) and the mixture was stirred for 5 min. A solution of **14** (20.72 g, 68 mmol) in dry CH_2Cl_2 (100 mL) was added dropwise over 5 min and stirring continued at -55 °C for 30 min. Subsequently, TEA (31.3 mL, 225 mmol) in dry CH_2Cl_2 (60 mL) was added and the reaction mixture was kept at -55 °C for 40 min. After warming to rt over a 2.5 h period the reaction mixture was quenched with H_2O and extracted with CH_2Cl_2. The organic phase was washed with brine, dried over $MgSO_4$, filtered and evaporated. The resulting brown oily residue was used for the next reaction without further purification.

A suspension of NaH (5.7 g, 238 mmol) in DMSO (310 mL) was heated at 65 °C under N_2-atmosphere until all the NaH had dissolved. The solution was cooled to room temperature and methyltriphenylphosphonium bromide (95 g, 265 mmol) was added under vigorous stirring. After 1.5 h, a mixture of the crude keton (previous reaction) in DMSO (100 mL) was added and the reaction mixture was stirred for 2.5 h. The reaction was quenched by pouring it in ice-water (1.5 L) and extracted with pentane (4 x 500 mL). The combined organic phase was dried over $MgSO_4$, filtered, evaporated and chromatographed on silica gel (pentane/EtOAc, 97/3) to afford **15** (11.3 g, 56 %) as a foam.

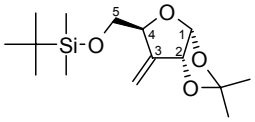

Molecular formula: $C_{15}H_{28}SiO_4$

Molecular weight: 300.47

^{1}H-NMR (300 MHz, $CDCl_3$):

δ 0.00 (s, 6H, $(CH_3)_2Si$), 0.83 (s, 9H, *tert*-Bu), 1.34 and 1.45 (2 x s, 6H, 2 x CH_3), 3.63 (dd, 1H, *J* = 3.8 Hz and -10.7 Hz, H-5B), 3.71 (dd, 1H, *J* = 4.1 Hz, H-5A), 4.71 (m, 1H, H-4), 4.84 (dq, 1H, *J* = 1.5 Hz, 2.6 Hz and 4.1 Hz, H-2), 5.22 (t, 1H, *J* = 1.8 Hz, 3-CH_b), 5.38 (dd, 1H, *J* = 1.2 Hz and 2.4 Hz, 3-CH_a), 5.81 (d, 1H, *J* = 4.1 Hz, H-1).

Exact mass (ESI-MS, *i*PrOH:H_2O):

calculated for $C_{15}H_{29}SiO_4$ $[M+H]^+$: 301.1834, found 301.1829.

3-Deoxy-3-*C*-hydroxymethyl-1,2-*O*-isopropylidene-5-*O*-(*tert*-butyldimethylsilyl)-α-D-ribofuranose (16)

To a stirring solution of 1 M borane/THF complex (68 mL) in anhydrous THF at 0 °C under N_2-atmosphere and was added dropwise**15** (8.7g, 29 mmol) in THF (60 mL). The mixture was kept at rt for 3 h and after cooling a THF/H_2O (1/1) solution (45 mL), 2 N NaOH (54 mL) and 30 % H_2O_2 (45 mL) were subsequently added. The turbid mixture was stirred at rt for 2 h when Et_2O (300 mL) was added. The Et_2O phase was separated, washed with H_2O (100 mL) and brine (100 mL), dried over $MgSO_4$, filtered, concentrated in vacuo and purified by silica gel chromatography (pentane/EtOAc, 9/1 → 6/4) to give **16** (6 g, 65 %) as a semi-solid.

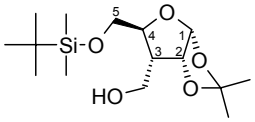

Molecular formula: $C_{15}H_{30}SiO_5$

Molecular weight: 318.49

^{1}H-NMR (300 MHz, $CDCl_3$):

δ 0.00 (s, 6H, $(CH_3)_2Si$), 0.81 (s, 9H, *tert*-Bu), 1.23 and 1.43 (2 x s, 6H, 2 x CH_3), 2.02-2.11 (m, 1H, H-3), 3.57 (dd, 1H, *J* = 6.6 Hz and -10.6 Hz, 3-CH_b), 3.76-3.82 (m, 3H, 3-CH_a, H-5B and H-5A), 3.96-4.02 (m, 1H, H-4), 4.66 (t, 1H, *J* = 4.3 Hz, H-2), 5.70 (d, 1H, *J* = 4.0 Hz, H-1).

Exact mass (ESI-MS, *i*PrOH:H_2O):

calculated for $C_{15}H_{31}SiO_5$ $[M+H]^+$: 319.1940, found 319.1935.

3-*C*-Azidomethyl-3-deoxy-1,2-*O*-isopropylidene-5-*O*-(*tert*-butyldimethylsilyl)-α-D-ribofuranose (17)

Methanesulfonyl chloride (2 ml, 25 mmol) was added to a solution of **16** (3g, 9.5 mmol) in pyridine (40 mL). The reaction mixture was stirred for 3h and the solvent was evaporated to dryness. The residue was dissolved in CH_2Cl_2 (150 mL), washed with 7 % $NaHCO_3$ solution (75 mL), H_2O (75 mL), dried over $MgSO_4$, filtered and evaporated to dryness to give a yellow syrup that was used without further purification. This syrup was dissolved in DMF (150 mL) and NaN_3 (6.2 g, 95 mmol) was added. The reaction mixture was heated at 95 °C for 2 h. After concentration in vacuo, the residue was dissolved in CH_2Cl_2 (200 mL). The organic phase was

washed with H_2O, dried over $MgSO_4$, filtered, evaporated and chromatographed on silica gel (pentane/EtOAc, 97/3) to give **17** (2.5 g, 77 %) as a yellowish syrup.

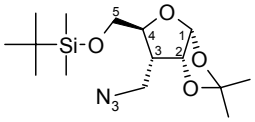

Molecular formula: $C_{15}H_{29}SiN_3O_4$

Molecular weight: 343.50

^{1}H-NMR (300 MHz, $CDCl_3$):

δ 0.00 (s, 6H, $(CH_3)_2Si$), 0.81 (s, 9H, *tert*-Bu), 1.28 and 1.45 (2 x s, 6H, 2 x CH_3), 2.20-2.30 (m, 1H, H-3), 3.37 (dd, 1H, J = 5.6 Hz and -12.2 Hz, 3-CH_b), 3.54 (dd, 1H, J = 9.7 Hz, 3-CH_a), 3.67 (dd, 1H, J = 3.8 Hz and -11.4 Hz, H-5B), 3.73 (dd, 1H, J = 4.1 Hz, H-5A), 3.81 (dt, 1H, J = 3.9 Hz and 9.9 Hz, H-4), 4.66 (t, 1H, J = 4.3 Hz, H-2), 5.75 (d, 1H, J = 3.52 Hz, H-1).

Exact mass (ESI-MS, *i*PrOH:H_2O):

calculated for $C_{15}H_{30}SiN_3O_4$ $[M+H]^+$: 344.2005, found 344.2011.

3-*C*-Azidomethyl-3-deoxy-1,2-*O*-isopropylidene-α-D-ribofuranose (18)

To a solution of **17** (2.5 g, 7.28 mmol) in THF (80 mL), a 1M TBAF solution in THF (10 mL) was added. After 3h the reaction mixture was evaporated to dryness and the residue dissolved in EtOAc (200 mL). The organic layer was washed with water, dried over $MgSO_4$, filtered, evaporated and purified by silica gel chromatography (pentane/EtOAc, 85/15) to give crude **18** (1.6 g, 96 %) as a colourless oil.

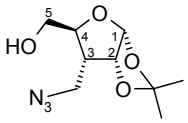

Molecular formula: $C_9H_{15}N_3O_4$

Molecular weight: 229.24

^{1}H-NMR (300 MHz, DMSO-d_6):

δ 1.25 and 1.40 (2 x s, 6H, 2 x CH_3), 2.11-2.21 (m, 1H, H-3), 3.38-3.60 (m, 4H, H-5B, H-5A, 3-CH_b and 3-CH_a), 3.73 (ddd, 1H, J = 3.4 Hz, 4.3 Hz and 10.2 Hz, H-4), 4.68 (t, 1H, J = 4.4 Hz, H-2), 4.72 (t, 1H, J = 5.7 Hz, 5-OH), 5.75 (d, 1H, J = 3.8 Hz, H-1).

Exact mass (ESI-MS, *i*PrOH:H_2O):

calculated for $C_9H_{16}N_3O_4$ $[M+H]^+$: 230.1140, found 230.1133.

3-*C*-Azidomethyl-3-deoxy-1,2-*O*-isopropylidene-5-*O*-toluoyl-α-D-ribofuranose (19)

A solution of **18** (1.55 g, 6.7 mmol) in dry pyridine (90 mL) was treated with toluoyl chloride (1.3 mL, 10 mmol). After 2h sovents were evaporated in vacuo and the residue was partitioned between CH_2Cl_2 (200 mL) and H_2O (80 mL). The organic layer was washed with 7 % $NaHCO_3$, dried over $MgSO_4$ and evaporated. Purification of the residue by column chromatography (pentane/EtOAc, 95/5) afforded **19** (2.2 g, 94 %) as a white solid.

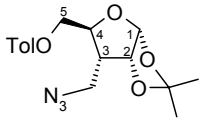

Molecular formula: $C_{17}H_{21}N_3O_5$

Molecular weight: 347.37

^{1}H-NMR (300 MHz, $CDCl_3$):

δ 1.35 and 1.53 (2s, 6H, 2 x CH_3), 2.22 (m, 1H, H-3), 2.41 (s, 3H, Ar-CH_3), 3.48 (dd, 1H, *J* = 6.0 Hz and -12.2 Hz, 3-CH_b), 3.70 (dd, 1H, *J* = 9.1 Hz, 3-CH_a), 4.17 (m, 1H, H-4), 4.38 (dd, 1H, *J* = 5.0 Hz and -12.3 Hz, H-5B), 4.58 (dd, 1H, *J* = 2.9 Hz, H-5A), 4.75 (t, 1H, *J* = 4.3 Hz, H-2), 5.88 (d, 1H, *J* = 3.8 Hz, H-1), 7.24 and 7.97 (2d, 4H, *J* = 8.0 Hz, Ar-H).

Exact mass (ESI-MS, *i*PrOH:H_2O):

calculated for $C_{17}H_{21}N_3O_5Na$ $[M+Na]^+$: 370.1379, found 370.1384.

3-*C*-Azidomethyl-3-deoxy-1,2-di-*O*-acetyl-5-*O*-toluoyl-D-ribofuranose (20)

19 (2 g, 5.76 mmol) was dissolved in 75 % HOAc (40 mL) and heated overnight at 60 °C. The reaction mixture was evaporated to dryness and the residue was dissolved in a mixture of acetic anhydride/pyridine (60 mL, 2:3, v/v). After 3 h the mixture was partitioned between CH_2Cl_2 (150 mL) and 7 % $NaHCO_3$ (200 mL). The aqueous layer was washed with CH_2Cl_2 (200 mL) and the combined organic layers were dried with $MgSO_4$, filtered and evaporated in vacuo. Treatment with a hexane/EtOAc mixture allowed precipitation of **20** (1.42 g, 63 %) as a white solid.

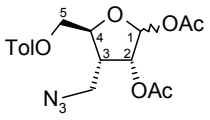

Molecular formula: $C_{18}H_{21}N_3O_7$

Molecular weight: 391.38

^{1}H-NMR (300 MHz, $CDCl_3$) ***of most polar anomer***:

δ 1.96 and 2.14 (2s, 6H, 2 x CH_3), 2.41 (s, 3H, Ar-CH_3), 2.71-2.80 (m, 1H, H-3), 3.50 (dd, 1H, *J* = 6.6 Hz and -12.4 Hz, 3-CH_b), 3.63 (dd, 1H, *J* = 8.5 Hz, 3-CH_a), 4.33-4.60 (2m, 3H, H-4 and 2 x H-5), 5.29 (d, 1H, *J* = 4.7 Hz, H-2), 6.14 (s, 1H, H-1), 7.24 and 7.95 (2d, 4H, *J* = 8,1 Hz, Ar-H).

Exact mass (ESI-MS, *i*PrOH:H_2O):

calculated for $C_{18}H_{21}N_3O_7Na$ $[M+Na]^+$: 414.1277, found 414.1268.

9-(2-*O*-Acetyl-3-*C*-azidomethyl-3-deoxy-5-*O*-toluoyl-β-D-ribofuranosyl)-6-chloropurine (21)

20 (500 mg, 1.27 mmol) was coupled with silylated 6-chloropurine and purified in analogy to the procedure described for **10**, to yield the the title compound **21** (503 mg, 81 %).

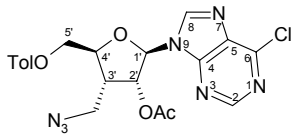

Molecular formula: $C_{21}H_{20}ClN_7O_5$

Molecular weight: 485.89

^{1}H-NMR (300 MHz, $CDCl_3$):

δ 2.18 (s, 3H, CH_3), 2.39 (s, 3H, Ar-CH_3), 3.39-3.49 (m, 1H, H-3'), 3.62 (dd, 1H, *J* = 6.0 Hz and -12.5 Hz, 3-CH_b), 3.70 (dd, 1H, *J* = 7.9 Hz, 3-CH_a), 4.43-4.48 (m, 1H, H-4'), 4.53 (dd, 1H, *J* = 4.1 Hz and -12.3 Hz, H-5B'), 4.70 (dd, 1H, *J* = 2.6 Hz, H-5A'), 5.97 (dd, 1H, *J* = 1.5 Hz and 5.8 Hz, H-2'), 6.01 (d, 1H, *J* = 1.5 Hz, H-1'), 7.16 and 7.71 (2d, 4H, *J* = 8.1 Hz, Ar-H), 8.20 and 8.57 (2 x s, 2H, H-2 and H-8).

Exact mass (ESI-MS, *i*PrOH:H_2O):

calculated for $C_{21}H_{21}ClN_7O_5$ $[M+H]^+$: 486.1292, found 486.1295.

2.7.4 Preparation of the 3'-azidomethyl-5'-methylcarbamoyl nucleoside scaffold

Methyl 3-azidomethyl-3-deoxy-1,2-isopropylidene-α-D-ribofuronamide (22)

22 (1.3 g, 32 %) was prepared from **18** (3.6 g, 15.7 mmol) in analogy to the procedure described for **8**.

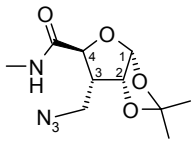

Molecular formula: $C_{10}H_{16}N_4O_4$

Molecular weight: 256.26

^{1}H-NMR (300 MHz, $CDCl_3$):

^{1}H NMR ($CDCl_3$) δ1.34 and 1.49 (2s, 6H, 2 x CH_3), 2.15-2.25 (m, 1H, H-3), 2.80 (d, 3H, *J* = 5.0 Hz, CH_3-N), 3.64 (dd, 1H, *J* = 11.1 Hz and -12.1 Hz, 3-CH_b), 3.87 (dd, 1H, *J* = 4.3 Hz, 3-CH_a), 4.15 (d, 1H, *J* = 10.6 Hz, H-4), 4.73 (t, 1H, *J* = 3.8 Hz, H-2), 5.85 (d, 1H, *J* = 5.5 Hz, H-1), 6.50 (br s, 1H, NH).

Exact mass (ESI-MS, *i*PrOH:H_2O):

calculated for $C_{10}H_{17}N_4O_4$ $[M+H]^+$: 257.1249, found 257.1253.

Methyl 3-azidomethyl-3-deoxy-1,2-di-*O*-acetyl-D-ribofuronamide (23)

23 (0.6 g, 40 %) was prepared from **22** (1.3 g, 5 mmol) in analogy to the procedure described for **9**.

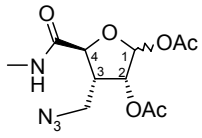

Molecular formula: $C_{11}H_{16}N_4O_6$

Molecular weight: 300.27

^{1}H-NMR (300 MHz, $CDCl_3$) ***of most polar anomer***:

δ2.06 and 2.13 (2 x s, 6H, 2 x CH_3), 2.74-2.77 (m, 1H, H-3), 2.81 (d, 3H, *J* = 5.0 Hz, CH_3-N), 3.55 (dd, 1H, *J* = 10.5 Hz and -12.3 Hz, 3-CH_b), 3.91 (dd, 1H, *J* = 4.4 Hz, 3-CH_a), 4.28 (d, 1H, *J* = 9.7 Hz, H-4), 5.23 (d, 1H, *J* = 4.7 Hz, H-2), 6.12 (s, 1H, H-1), 6.41 (d, 1H, *J* = 4.1 Hz, NH).

Exact mass (ESI-MS, *i*PrOH:H_2O):

calculated for $C_{11}H_{17}N_4O_6$ $[M+H]^+$: 301.1147, found 301.1141.

9-[2-*O*-Acetyl-3-*C*-azidomethyl-3-deoxy-5-(methylcarbamoyl)-β-D-ribofuranosyl]-6-chloropurine (24)

23 (0.6 g, 2 mmol) was used to prepare **24** (750 mg, 95 %) in analogy to the procedure described for **10**.

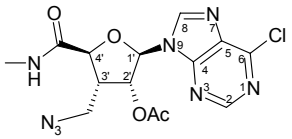

Molecular formula: $C_{14}H_{15}ClN_8O_4$

Molecular weight: 394.78

^{1}H-NMR (300 MHz, $CDCl_3$):

δ2.20 (s, 3H, CH_3), 2.83 (d, 3H, *J* = 5.0 Hz, CH_3-N), 3.38-3.48 (m, 1H, H-3'), 3.73 (dd, 1H, *J* = 9.1 Hz and -12.6 Hz, 3'-CH_b), 3.87 (dd, 1H, *J* = 4.4 Hz, 3'-CH_a), 4.48 (d, 1H, *J* = 9.4 Hz, H-4'), 5.62 (dd, 1H, *J* = 2.5 Hz and 6.6 Hz, H-2'), 6.09 (d, 1H, *J* = 2.3 Hz, H-1'), 6.98 (d, 1H, *J* = 4.4 Hz, NH), 8.22 and 8.75 (2 x s, 2H, H-2 and H-8).

Exact mass (ESI-MS, *i*PrOH:H_2O):

calculated for $C_{14}H_{16}ClN_8O_4$ $[M+H]^+$: 395.0982, found 395.0982.

2.7.5 Preparation of the N^6-substituted adenosine analogues

General procedure for the "one pot" N^6-substitution/deprotection

An amount of the appropriate chloropurine and the appropriate amine salt (or ammonia in the case of **25**) (1.5 eq.), were dissolved in EtOH (15 mL/mmol chloropurine) containing Et_3N (1.25 eq.). The reaction mixture was refluxed overnight and evaporated to dryness. The residue was dissolved in 7 N NH_3 in MeOH (ca. 30 mL), stirred for 24 h at room temperature and evaporated in vacuo. The target compounds were purified by precipitation from MeOH and subsequent filtration in the case of **25**-**28**, by chromatography on a silica gel column (elution with a suitable mixture of CH_2Cl_2-MeOH) to furnish **35**-**37**, **41** and **42** as pure white solids.

9-(3-*C*-Azidomethyl-3-deoxy-β-D-ribofuranosyl)-adenine (25)

300 mg (0.62 mmol) of **21** yielded 80 mg (42 %) of **25**.

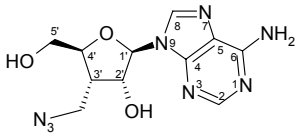

Molecular formula: $C_{11}H_{14}N_8O_3$

Molecular weight: 306.29

^{1}H-NMR (300 MHz, DMSO-d_6):

δ 2.58-2.67 (m, 1H, H-3'), 3.44 (dd, 1H, *J* = 5.7 Hz and -12.4 Hz, 3'-CH_b), 3.53 (ddd, 1H, *J* = 3.8 Hz and 5.9 Hz and -12.2 Hz, H-5B'), 3.65 (dd, 1H, *J* = 8.2 Hz, 3'-CH_a), 3.73 (ddd, 1H, *J* = 3.0 Hz and 5.1 Hz, H-5A'), 3.99 (dt, 1H, *J* = 3.2 Hz and 8.6 Hz, H-4'), 4.54-4.58 (m, 1H, H-2'), 5.22 (t, 1H, *J* = 5.5 Hz, 5'-OH), 5.91 (d, 1H, *J* = 2.1 Hz, H-1'), 6.04 (d, 1H, *J* = 4.6 Hz, 2'-OH), 7.29 (s, 2H, 6-NH_2), 8.13 and 8.39 (2 x s, 2H, H-2 and H-8).

Exact mass (ESI-MS, *i*PrOH:H_2O):

calculated for $C_{11}H_{15}N_8O_3$ $[M+H]^+$: 307.1267, found 307.1270.

Elemental analysis ($C_{11}H_{14}N_8O_3$.1/4 H_2O) C,H,N.

9-(3-*C*-Azidomethyl-3-deoxy-β-D-ribofuranosyl)-N^6-methyladenine (26)

400 mg (0.82 mmol) of **21** yielded 180 mg (68 %) of **26**.

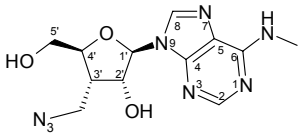

Molecular formula: $C_{12}H_{16}N_8O_3$

Molecular weight: 320.31

^{1}H-NMR (300 MHz, DMSO-d_6):

δ 2.58-2.68 (m, 1H, H-3'), 2.93 (br s, 3H, N(6)-CH_3), 3.44 (dd, 1H, *J* = 5.6 Hz and -12.31 Hz, 3'-CH_b), 3.53 (ddd, 1H, *J* = 3.7 Hz, 5.7 Hz and -12.2 Hz, H-5B'), 3.64 (dd, 1H, *J* = 7.9 Hz, 3'-CH_a), 3.73 (ddd, 1H, *J* = 2.9 Hz and 5.3 Hz, H-5A'), 3.99 (dt, 1H, *J* = 3.2 Hz and 8.8 Hz, H-4'), 4.55 (dt, 1H, *J* = 2.1 Hz and 5.2 Hz, H-2'), 5.23 (t, 1H, *J* = 5.4 Hz, 5'-OH), 5.92 (d, 1H, *J* = 2.3 Hz, H-1'), 6.05 (d, 1H, *J* = 5.0 Hz, 2'-OH), 7.78 (s, 1H, N(6)-H), 8.22 and 8.39 (2 x s, 2H, H-2 and H-8).

Exact mass (ESI-MS, *i*PrOH:H_2O):

calculated for $C_{12}H_{17}N_8O_3$ $[M+H]^+$: 321.1423, found 321.1429.

Elemental analysis ($C_{12}H_{16}N_8O_3$.2/3 H_2O) C,H,N.

9-(3-*C*-Azidomethyl-3-deoxy-β-D-ribofuranosyl)-N^6-(3-iodobenzyl)adenine (27)

340 mg (0.69 mmol) of **21** yielded 227 mg (62 %) of **27**.

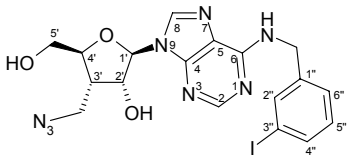

Molecular formula: $C_{18}H_{19}IN_8O_3$

Molecular weight: 522.31

^{1}H-NMR (300 MHz, DMSO-d_6):

δ 2.59-2.68 (m, 1H, H-3'), 3.44 (dd, 1H, *J* = 5.6 Hz and -12.3 Hz, 3'-CH_b), 3.54 (ddd, 1H, *J* = 3.7 Hz, 5.6 Hz and -12.3 Hz, H-5B'), 3.64 (dd, 1H, *J* = 8.2 Hz, 3'-CH_a), 3.73 (ddd, 1H, *J* = 2.9 Hz and 5.3 Hz, H-5A'), 4.00 (dt, 1H, *J* = 3.2 Hz and 8.6 Hz, H-4'), 4.55-4.59 (m, 1H, H-2'), 4.64 (br s, 2H, CH_2-Ar), 5.20 (t, 1H, *J* = 5.6 Hz, 5'-OH), 5.93 (d, 1H, *J* = 2.1 Hz, H-1'), 6.05 (d, 1H, *J* = 5.0 Hz, 2'-OH), 7.05 (t, 1H, *J* = 7.8 Hz, H-5''), 7.34 (d, 1H, *J* = 7.9 Hz, H-6''), 7.56 (d, 1H, *J* = 8.2 Hz, H-4''), 7.70 (s, 1H, H-2"), 8.20 and 8.44 (2 x s, 2H, H-2 and H-8), 8.46 (br s, 1H, N(6)-H).

Exact mass (ESI-MS, *i*PrOH:H_2O):

calculated for $C_{18}H_{20}IN_8O_3$ $[M+H]^+$: 523.0704, found 523.0698.

Elemental analysis ($C_{18}H_{19}IN_8O_3$) C,H,N.

9-(3-*C*-Azidomethyl-3-deoxy-β-D-ribofuranosyl)-N^6-(5-chloro-2-methoxybenzyl)-adenine (28)

300 mg (0.62 mmol) of **21** yielded 100 mg (35 %) of **28**.

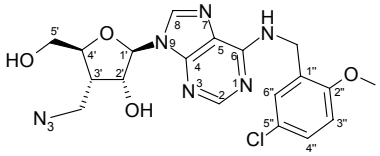

Molecular formula: $C_{19}H_{21}ClN_8O_4$

Molecular weight: 460.88

^{1}H-NMR (300 MHz, DMSO-d_6):

δ 2.61-2.70 (m, 1H, H-3'), 3.45 (dd, 1H, *J* = 5.7 Hz and -12.3 Hz, 3'-CH_b), 3.55 (ddd, 1H, *J* = 3.7 Hz, 5.4 Hz and -12.2 Hz, H-5B'), 3.65 (dd, 1H, *J* = 8.1 Hz, 3'-CH_a), 3.75 (ddd, 1H, *J* = 2.9 Hz and 5.0 Hz, H-5A'), 3.83 (s, 3H, Ar-OCH_3), 4.01 (dt, 1H, *J* = 3.2 Hz and 8.7 Hz, H-4'), 4.63 (m, 3H, H-2' and CH_2-Ar), 5.16 (t, 1H, *J* = 5.4 Hz, 5'-OH), 5.95 (d, 1H, *J* = 2.1 Hz, H-1'), 6.01 (d, 1H, *J* = 5.0 Hz, 2'-OH), 7.01 (d, 1H, *J* = 8.8 Hz,

H-3''), 7.08 (br s, 1H, H-6''), 7.24 (dd, 1H, *J* = 2.6 and 8.8 Hz, H-4''), 8.19 (br s, 2H, H-2 and N(6)-H), 8.44 (s, 1H, H-8).

Exact mass (ESI-MS, *i*PrOH:H_2O):

calculated for $C_{19}H_{22}ClN_8O_4$ $[M+H]^+$: 461.1452, found 461.1460.

Elemental analysis ($C_{19}H_{21}ClN_8O_4$) C,H,N.

9-[3-Azido-3-deoxy-5-(methylcarbamoyl)-β-D-ribofuranosyl]-*N*^{6}-(3-iodobenzyl)adenine (35)

300 mg (0.79 mmol) of **10** yielded 250 mg (60 %) of **35**.

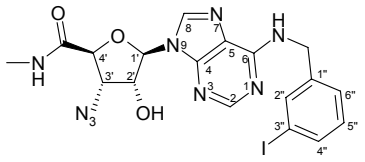

Molecular formula: $C_{18}H_{18}IN_9O_3$

Molecular weight: 535.31

^{1}H-NMR (300 MHz, DMSO-d_6):

δ 2.68 (d, 3H, *J* = 4.4 Hz, CH_3-N), 4.33 (d, 1H, *J* = 3.2 Hz, H-4'), 4.48 (dd, 1H, *J* = 3.2 Hz and 5.3 Hz, H-3'), 4.66 (br s, 2H, CH_2-Ar), 4.96 (q, 1H, *J* = 5.4 Hz and 10.9 Hz, H-2'), 5.99 (d, 1H, *J* = 6.5 Hz, H-1'), 6.28 (d, 1H, *J* = 5.3 Hz, 2'-OH), 7.09 (t, 1H, *J* = 7.8 Hz, H-5''), 7.35 (d, 1H, *J* = 7.9 Hz, H-6''), 7.57 (d, 1H, *J* = 8.2 Hz, H-4''), 7.71 (s, 1H, H-2''), 8.27 and 8.45 (2 x s, 2H, H-2 and H-8), 8.53 (br s, 1H, N(6)-H), 8.62 (d, 1H, *J* = 4.7 Hz, NH).

Exact mass (ESI-MS, *i*PrOH:H_2O):

calculated for $C_{18}H_{19}IN_9O_3$ $[M+H]^+$: 536.0657, found 536.0658.

Elemental analysis ($C_{18}H_{18}IN_9O_3$.3/2 H_2O) C,H,N.

9-[3-*C*-Azidomethyl-3-deoxy-5-(methylcarbamoyl)-β-D-ribofuranosyl]-*N*^{6}-(3-iodobenzyl)adenine (36)

300 mg (0.75 mmol) of **24** yielded 360 mg (73 %) of **36**.

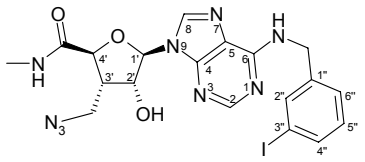

Molecular formula: $C_{19}H_{20}IN_9O_3$

Molecular weight: 549.33

^{1}H-NMR (300 MHz, DMSO-d_6):

δ 2.63 (d, 3H, *J* = 4.4 Hz, CH_3-N), 2.75-2.84 (m, 1H, H-3'), 3.50 (dd, 1H, *J* = 5.9 Hz and -12.3 Hz, 3'-CH_b), 3.71 (dd, 1H, *J* = 7.9 Hz, 3'-CH_a), 4.33 (d, 1H, *J* = 8.5 Hz, H-4'), 4.63 (m, 3H, H-2' and CH_2-Ar), 6.03 (d, 1H, *J* = 2.1 Hz, H-1'), 6.15 (d, 1H, *J* = 4.7 Hz, 2'-OH), 7.09 (t, 1H, *J* = 7.8 Hz, H-5''), 7.35 (d, 1H, *J* = 7.6 Hz, H-6''), 7.57 (d, 1H, *J* = 7.9 Hz, H-4''), 7.71 (s, 1H, H-2''), 8.24 (m, 2H, H-2 and NH), 8.43 (br s, 1H, N(6)-H), 8.55 (s, 1H, H-8).

Exact mass (ESI-MS, *i*PrOH:H_2O):

calculated for $C_{19}H_{21}IN_9O_3$ $[M+H]^+$: 550.0813, found 550.0803.

Elemental analysis ($C_{19}H_{20}IN_9O_3$.3/2 H_2O) C,H,N.

2-Chloro-9-[3-azido-3-deoxy-5-(methylcarbamoyl)-β-D-ribofuranosyl]-*N*^{6}-(3-iodobenzyl)adenine (37)

200 mg (0.48 mmol) of **11** yielded 210 mg (77 %) of **37**.

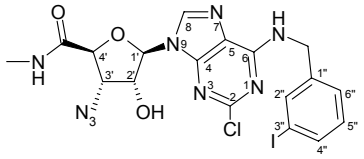

Molecular formula: $C_{18}H_{17}ClIN_9O_3$

Molecular weight: 569.75

^{1}H-NMR (300 MHz, DMSO-d_6):

δ 2.69 (d, 3H, *J* = 4.1 Hz, CH_3-N), 4.35 (d, 1H, *J* = 2.9 Hz, H-4'), 4.47 (t, 1H, *J* = 4.1 Hz, H-3'), 4.60 (brs, 2H, CH_2-Ar), 4.92 (app d, 1H, *J* = 4.9 Hz, H-2'), 5.92 (d, 1H, *J* = 6.2 Hz, H-1'), 6.31 (d, 1H, *J* = 4.7 Hz, 2'-OH), 7.12 (t, 1H, *J* = 7.8 Hz, H-5''), 7.35 (d, 1H, *J* = 7.3 Hz, H-6''), 7.59 (d, 1H, *J* = 7.9 Hz, H-4''), 7.74 (s, 1H, H-2''), 8.25 (d, 1H, *J* = 4.1 Hz, NH), 8.49 (s, 1H, H-8), 8.99 (brs, 1H, N(6)-H).

Exact mass (ESI-MS, *i*PrOH:H_2O):

calculated for $C_{18}H_{17}ClIN_9O_3Na$ $[M+Na]^+$: 592.0087, found 592.0092.

Elemental analysis ($C_{18}H_{17}ClIN_9O_3$.1/2 H_2O) C,H,N.

9-[3-Azido-3-deoxy-5-(methylcarbamoyl)-β-D-ribofuranosyl]-*N*^{6}-(5-chloro-2-methoxybenzyl)adenine (41)

300 mg (0.79 mmol) of **10** yielded 251 mg (67 %) of **41**.

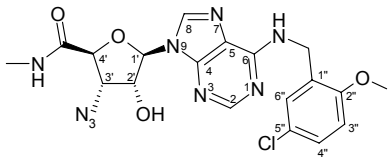

Molecular formula: $C_{19}H_{20}ClN_9O_4$

Molecular weight: 473.88

^{1}H-NMR (300 MHz, DMSO-d_6):

δ 2.68 (d, 3H, *J* = 4.7 Hz, CH_3-N), 3.83 (s, 3H, Ar-OCH_3), 4.34 (d, 1H, *J* = 3.2 Hz, H-4'), 4.49 (dd, 1H, *J* = 3.2 Hz and 5.3 Hz, H-3'), 4.65 (br s, 2H, CH_2-Ar), 4.97 (q, 1H, *J* = 5.6 Hz and 11.1 Hz, H-2'), 6.00 (d, 1H, *J* = 6.5 Hz, H-1'), 6.29 (d, 1H, *J* = 5.3 Hz, 2'-OH), 7.00 (d, 1H, *J* = 9.08 Hz, H-3''), 7.08 (br s, 1H, H-6''), 7.24 (dd, 1H, *J* = 2.8 Hz and 8.6 Hz, H-4''), 8.25 (s, 1H, H-2), 8.35 (br s, 1H, N(6)-H), 8.47 (s, 1H, H-8), 8.62 (d, 1H, *J* = 4.7 Hz, NH).

Exact mass (ESI-MS, *i*PrOH:H_2O):
calculated for $C_{19}H_{21}ClN_9O_4$ $[M+H]^+$: 474.1404, found 474.1400.

Elemental analysis ($C_{19}H_{20}ClN_9O_4$.1/2 H_2O) C,H,N.

9-[3-Azidomethyl-3-deoxy-5-(methylcarbamoyl)-β-D-ribofuranosyl]-*N*^{6}-(5-chloro-2-methoxybenzyl)adenine (42)

300 mg (0.75 mmol) of **24** yielded 300 mg (82 %) of **42**.

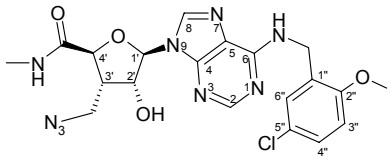

Molecular formula: $C_{20}H_{22}ClN_9O_4$

Molecular weight: 487.91

^{1}H-NMR (300 MHz, DMSO-d_6):

δ 2.63 (d, 3H, *J* = 4.4 Hz, CH_3-N), 2.76-2.85 (m, 1H, H-3'), 3.50 (dd, 1H, *J* = 5.9 Hz and -12.4 Hz, 3'-CH_b), 3.71 (dd, 1H, *J* = 7.8 Hz, 3'-CH_a), 3.83 (s, 3H, Ar-OCH_3), 4.32 (d, 1H, *J* = 8.8 Hz, H-4'), 4.60 (br s, 3H, CH_2-Ar and H-2'), 6.04 (s, 1H, H-1'), 6.21 (d, 1H, *J* = 4.7 Hz, 2'-OH), 7.00 (d, 1H, *J* = 8.8 Hz, H-3''), 7.05 (br s, 1H, H-6''), 7.24 (dd, 1H, *J* = 2.6 Hz and 8.5 Hz, H-4''), 8.21 (s, 1H, H-2), 8.30 (d, 1H, *J* = 4.7 Hz, NH), 8.36 (br s, 1H, N(6)-H), 8.60 (s, 1H, H-8).

Exact mass (ESI-MS, *i*PrOH:H_2O):
calculated for $C_{20}H_{23}ClN_9O_4$ $[M+H]^+$: 488.15661, found 488.1559.

Elemental analysis ($C_{20}H_{22}ClN_9O_4$.1/2 H_2O) C,H,N.

General procedure for the synthesis of the amino modified adenosine analogues from their azido precursors

The azido nucleoside was dissolved in dry pyridine (8 mL/mmol) and PhP_3 (1.6 eq.) was added to the solution. After stirring at room temperature for 1.5 h, concentrated NH_4OH (3 mL/mmol) was added. The reaction mixture was stirred for another 2 h, evaporated to dryness and purified by silica gel chromatography (CH_2Cl_2-MeOH).

9-(3-*C*-Aminomethyl-3-deoxy-β-D-ribofuranosyl)-adenine (29)

60 mg (0.20 mmol) of **25** furnished 35 mg (64 %) of **29** as a white solid.

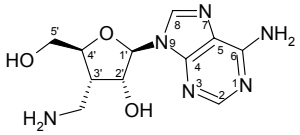

Molecular formula: $C_{11}H_{16}N_6O_3$

Molecular weight: 280.29

^{1}H-NMR (300 MHz, DMSO-d_6):

δ 2.31-2.40 (m, 1H, H-3'), 2.65 (dd, 1H, *J* = 6.2 Hz and -12.6 Hz, 3'-CH_b), 2.89 (dd, 1H, *J* = 7.3 Hz, 3'-CH_a), 3.56 (dd, 1H, *J* = 3.2 Hz and -11.9 Hz, H-5B'), 3.68 (dd, 1H, *J* = 4.0 Hz, H-5A'), 3.98 (dt, 1H, *J* = 3.7 Hz and 9.4 Hz, H-4'), 4.50 (dd, 1H, *J* = 1.5 Hz and 5.3 Hz, H-2'), 5.88 (d, 1H, *J* = 1.5 Hz, H-1'), 7.27 (s, 2H, 6-NH_2), 8.12 and 8.36 (2 x s, 2H, H-2 and H-8).

Exact mass (ESI-MS, *i*PrOH:H_2O):

calculated for $C_{11}H_{17}N_6O_3$ $[M+H]^+$: 281.1362, found 281.1370.

Elemental analysis ($C_{11}H_{16}N_6O_3$) C,H,N.

9-(3-*C*-Aminomethyl-3-deoxy-β-D-ribofuranosyl)-N^6-methyladenine (30)

100 mg (0.31 mmol) of **26** furnished 64 mg (70 %) of **30** as a white solid.

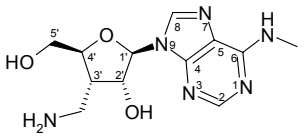

Molecular formula: $C_{12}H_{18}N_6O_3$

Molecular weight: 294.32

^{1}H-NMR (300 MHz, DMSO-d_6):

δ 2.26-2.35 (m, 1H, H-3'), 2.62 (dd, 1H, *J* = 6.5 Hz and -12.6 Hz, 3'-CH_b), 2.87 (dd, 1H, *J* = 7.0 Hz, 3'-CH_a), 2.93 (br s, 3H, N(6)-CH_3), 3.56 (dd, 1H, *J* = 3.5 Hz and -11.9

Hz, H-5B'), 3.67 (dd, 1H, *J* = 4.3 Hz, H-5A'), 3.99 (dt, 1H, *J* = 3.8 Hz and 9.1 Hz, H-4'), 4.50 (dd, 1H, *J* = 1.6 Hz and 5.1 Hz, H-2'), 5.88 (d, 1H, *J* = 1.8 Hz, H-1'), 7.75 (s, 1H, N(6)-H), 8.21 and 8.34 (2 x s, 2H, H-2 and H-8).

Exact mass (ESI-MS, *i*PrOH:H_2O):

calculated for $C_{12}H_{19}N_6O_3$ $[M+H]^+$: 295.1518, found 295.1513.

Elemental analysis ($C_{12}H_{18}N_6O_3.3/2\ H_2O$) C,H,N.

9-(3-*C*-Aminomethyl-3-deoxy-β-D-ribofuranosyl)-N^6-(3-iodobenzyl)adenine (31)

200 mg (0.38 mmol) of **27** furnished 131 mg (69 %) of **31** as a white solid.

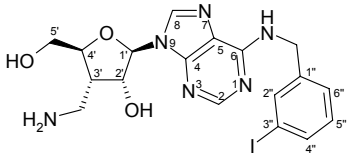

Molecular formula: $C_{18}H_{21}IN_6O_3$

Molecular weight: 496.31

^{1}H-NMR (300 MHz, DMSO-d_6):

δ 2.26-2.35 (m, 1H, H-3'), 2.62 (dd, 1H, *J* = 6.3 Hz and -12.5 Hz, 3'-CH_b), 2.86 (dd, 1H, *J* = 6.7 Hz, 3'-CH_a), 3.56 (dd, 1H, *J* = 3.4 Hz and -12.0 Hz, H-5B'), 3.68 (dd, 1H, *J* = 4.1 Hz, H-5A'), 3.99 (dt, 1H, *J* = 3.8 Hz and 9.1 Hz, H-4'), 4.51 (d, 1H, *J* = 4.98 Hz, H-2'), 4.63 (br s, 2H, CH_2-Ar), 5.89 (d, 1H, *J* = 1.5 Hz, H-1'), 7.09 (t, 1H, *J* = 7.6 Hz, H-5''), 7.33 (d, 1H, *J* = 7.9 Hz, H-6''), 7.56 (d, 1H, *J* = 7.3 Hz, H-4''), 7.70 (s, 1H, H-2''), 8.19 and 8.40 (2 x s, 2H, H-2 and H-8), 8.44 (br s, 1H, N(6)-H).

Exact mass (ESI-MS, *i*PrOH:H_2O):

calculated for $C_{18}H_{22}IN_6O_3$ $[M+H]^+$: 497.0799, found 497.0793.

Elemental analysis ($C_{18}H_{21}IN_6O_3$) C,H,N.

9-(3-*C*-Aminomethyl-3-deoxy-β-D-ribofuranosyl)-N^6-(5-chloro-2-methoxybenzyl)-adenine (32)

90 mg (0.17 mmol) of **28** furnished 54 mg (64 %) of **32** as a white solid.

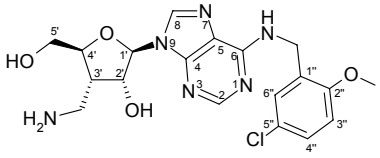

Molecular formula: $C_{19}H_{23}ClN_6O_4$

Molecular weight: 434.89

^{1}H-NMR (300 MHz, DMSO-d_6):

δ 2.29-2.38 (m, 1H, H-3'), 2.65 (dd, 1H, J = 6.3 Hz and -12.5 Hz, 3'-CH_b), 2.89 (dd, 1H, J = 7.0 Hz, 3'-CH_a), 3.57 (dd, 1H, J = 3.5 Hz and -11.9 Hz, H-5B'), 3.69 (dd, 1H, J = 4.1 Hz, H-5A'), 3.83 (s, 3H, Ar-OCH_3), 4.01 (dt, 1H, J = 3.9 Hz and 9.0 Hz, H-4'), 4.55 (dd, 1H, J = 1.2 Hz and 5.0 Hz, H-2'), 4.65 (br s, 2H, CH_2-Ar), 5.91 (d, 1H, J = 1.5 Hz, H-1'), 7.00 (d, 1H, J = 8.8 Hz, H-3''), 7.07 (d, 1H, J = 2.3 Hz, H-6''), 7.24 (dd, 1H, J = 2.6 Hz and 8.8 Hz, H-4''), 8.18 (br s, 2H, H-2 and N(6)-H), 8.40 (s, 1H, H-8).

Exact mass (ESI-MS, *i*PrOH:H_2O):

calculated for $C_{19}H_{24}ClN_6O_4$ $[M+H]^+$: 435.1547, found 435.1546.

Elemental analysis ($C_{19}H_{23}ClN_6O_4.1/4\ H_2O$) C,H,N.

9-[3-Amino-3-deoxy-5-(methylcarbamoyl)-β-D-ribofuranosyl]-*N*^{6}-(3-iodobenzyl)-adenine (38)

176 mg (0.33 mmol) of **35** furnished 30 mg (18 %) of **38** as a white solid.

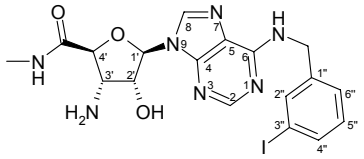

Molecular formula: $C_{18}H_{20}IN_7O_3$

Molecular weight: 509.31

^{1}H-NMR (300 MHz, DMSO-d_6):

δ 2.67 (d, 3H, J = 4.4 Hz, CH_3-N), 3.56 (t, 1H, J = 5.4 Hz, H-3'), 4.11 (d, 1H, J = 5.6 Hz, H-4'), 4.36 (t, 1H, J = 4.6 Hz, H-2'), 4.65 (br s, 2H, CH_2-Ar), 6.01 (d, 1H, J = 3.8 Hz, H-1'), 7.09 (t, 1H, J = 7.8 Hz, H-5''), 7.35 (d, 1H, J = 7.9 Hz, H-6''), 7.56 (d, 1H, J = 7.6 Hz, H-4''), 7.71 (s, 1H, H-2''), 8.24 (s, 1H, H-2), 8.44 (m, 2H, NH and N(6)-H), 8.55 (s, 1H, H-8).

Exact mass (ESI-MS, *i*PrOH:H_2O):

calculated for $C_{18}H_{21}IN_7O_3$ $[M+H]^+$: 510.0752, found 510.0757.

Elemental analysis ($C_{18}H_{20}IN_7O_3.1/2\ H_2O$) C,H,N.

9-[3-*C*-Aminomethyl-3-deoxy-5-(methylcarbamoyl)-β-D-ribofuranosyl]-*N*^{6}-(3-iodobenzyl)adenine (39)

100 mg (0.18 mmol) of **36** furnished 45 mg (48 %) of **39** as a white solid.

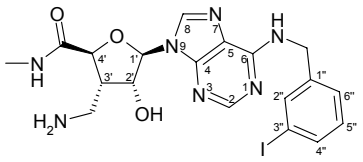

Molecular formula: $C_{19}H_{22}IN_7O_3$

Molecular weight: 523.34

^{1}H-NMR (300 MHz, DMSO-d_6):

δ 2.41-2.47 (m, 1H, H-3'), 2.64 (d, 3H, *J* = 4.7 Hz, CH_3-N), 2.76 (dd, 1H, *J* = 5.3 Hz and -12.3 Hz, 3'-CH_b), 2.90 (dd, 1H, *J* = 7.6 Hz, 3'-CH_a), 4.34 (d, 1H, *J* = 8.8 Hz, H-4'), 4.55 (dd, 1H, *J* = 2.1 Hz and 5.3 Hz, H-2'), 4.66 (br s, 2H, CH_2-Ar), 6.00 (d, 1H, *J* = 2.4 Hz, H-1'), 7.09 (t, 1H, *J* = 7.8 Hz, H-5''), 7.35 (d, 1H, *J* = 7.9 Hz, H-6''), 7.56 (d, 1H, *J* = 7.6 Hz, H-4''), 7.71 (s, 1H, H-2''), 8.22 (s, 1H, H-2), 8.29 (d, 1H, *J* = 4.7 Hz, NH), 8.42 (br s, 1H, N(6)-H), 8.62 (s, 1H, H-8).

Exact mass (ESI-MS, *i*PrOH:H_2O):

calculated for $C_{19}H_{23}IN_7O_3$ $[M+H]^+$: 524.0908, found 524.0912.

Elemental analysis ($C_{19}H_{22}IN_7O_3$.3/4 H_2O) C,H,N.

2-Chloro-9-[3-amino-3-deoxy-5-(methylcarbamoyl)-β-D-ribofuranosyl]-*N*^{6}-(3-iodobenzyl)adenine (40)

200 mg (0.35 mmol) of **37** furnished 140 mg (74 %) of **40** as a white solid.

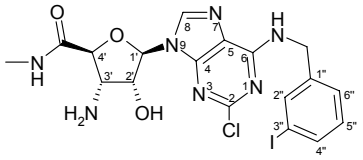

Molecular formula: $C_{18}H_{19}ClIN_7O_3$

Molecular weight: 543.75

^{1}H-NMR (300 MHz, DMSO-d_6):

δ 2.67 (d, 3H, *J* = 4.7 Hz, CH_3-N), 3.54 (t, 1H, *J* = 5.6 Hz, H-3'), 4.11 (d, 1H, *J* = 5.9 Hz, H-4'), 4.31 (t, 1H, *J* = 4.1 Hz, H-2'), 4.59 (brs, 2H, CH_2-Ar), 5.95 (d, 1H, *J* = 3.5 Hz, H-1'), 7.11 (t, 1H, *J* = 7.8 Hz, H-5''), 7.35 (d, 1H, *J* = 7.6 Hz, H-6''), 7.59 (d, 1H, *J* = 7.6 Hz, H-4''), 7.73 (s, 1H, H-2''), 8.15 (d, 1H, *J* = 4.1 Hz, NH), 8.61 (s, 1H, H-8), 8.93 (brs, 1H, N(6)-H).

Exact mass (ESI-MS, *i*PrOH:H_2O):

calculated for $C_{18}H_{20}ClIN_7O_3$ $[M+H]^+$: 544.0362, found 544.0366.

Elemental analysis ($C_{18}H_{19}ClIN_7O_3$) C,H,N.

9-[3-Amino-3-deoxy-5-(methylcarbamoyl)-β-D-ribofuranosyl]-*N*^{6}-(5-chloro-2-methoxybenzyl)adenine (43)

176 mg (0.33 mmol) of **41** furnished 29 mg (20 %) of **43** as a white solid.

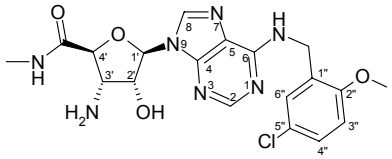

Molecular formula: $C_{19}H_{22}ClN_7O_4$

Molecular weight: 447.88

^{1}H-NMR (300 MHz, DMSO-d_6):

δ 2.67 (d, 3H, *J* = 4.7 Hz, CH_3-N), 3.57 (t, 1H, *J* = 5.4 Hz, H-3'), 3.83 (s, 3H, Ar-OCH_3), 4.12 (d, 1H, *J* = 5.9 Hz, H-4'), 4.38 (t, 1H, *J* = 4.5 Hz, H-2'), 4.65 (br s, 2H, CH_2-Ar), 6.02 (d, 1H, *J* = 4.1 Hz, H-1'), 7.00 (d, 1H, *J* = 8.8 Hz, H-3''), 7.08 (br s, 1H, H-6''), 7.20 (dd, 1H, *J* = 2.6 Hz and 8.8 Hz, H-4''), 8.23 (s, 1H, H-2), 8.29 (br s, 1H, N(6)-H), 8.44 (d, 1H, *J* = 5.0 Hz, NH), 8.57 (s, 1H, H-8).

Exact mass (ESI-MS, *i*PrOH:H_2O):

calculated for $C_{19}H_{23}ClN_7O_4$ $[M+H]^+$: 448.1499, found 448.1483.

Elemental analysis ($C_{19}H_{22}ClN_7O_4$.3/2 H_2O) C,H,N.

9-[3-Aminomethyl-3-deoxy-5-(methylcarbamoyl)-β-D-ribofuranosyl]-*N*^{6}-(5-chloro-2-methoxybenzyl)adenine (44)

150 mg (0.31 mmol) of **42** furnished 100 mg (70 %) of **44** as a white solid.

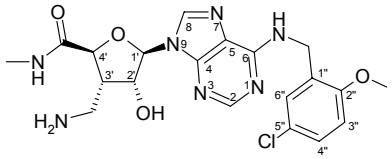

Molecular formula: $C_{20}H_{24}ClN_7O_4$

Molecular weight: 461.91

^{1}H-NMR (300 MHz, DMSO-d_6):

δ 2.40-2.48 (m, 1H, H-3'), 2.64 (d, 3H, *J* = 4.7 Hz, CH_3-N), 2.76 (dd, 1H, *J* = 5.1 Hz and -12.8 Hz, 3'-CH_b), 2.90 (dd, 1H, *J* = 7.9 Hz, 3'-CH_a), 3.83 (s, 3H, Ar-OCH_3), 4.34 (d, 1H, *J* = 9.1 Hz, H-4'), 4.55 (dd, 1H, *J* = 1.6 Hz and 5.1 Hz, H-2'), 4.62 (br s, 2H, CH_2-Ar), 6.01 (d, 1H, *J* = 1.8 Hz, H-1'), 7.00 (d, 1H, *J* = 8.8 Hz, H-3''), 7.04 (s, 1H, H-6''), 7.24 (dd, 1H, *J* = 2.6 Hz and 8.8 Hz, H-4''), 8.20 (s, 1H, H-2), 8.35 (br d, 2H, *J* = 4.7 Hz, NH and N(6)-H), 8.68 (s, 1H, H-8).

Exact mass (ESI-MS, *i*PrOH:H_2O):

calculated for $C_{20}H_{25}ClN_7O_4$ $[M+H]^+$: 462.1652, found 462.1657.

Elemental analysis ($C_{20}H_{24}ClN_7O_4.3/2H_2O$) C,H,N.

Procedure for the amidation of 31 and 32

To a solution of the appropriate amine in THF (10 mL/mmol) were added 50 % aqueous NaOAc solution (10 mL/mmol) and acetyl chloride (1.0 eq.). After completion of the reaction (6 h), THF and brine were added. The organic phase was separated, washed with water, dried over $MgSO_4$ and concentrated in vacuo. Precipitation from MeOH and subsequent filtration furnished the product as a white solid.

9-(3-Acetamidomethyl-3-deoxy-β-D-ribofuranosyl)-*N*^{6}-(3-iodobenzyl)adenine (33)

70 mg (0.14 mmol) of **31** yielded 48 mg (63 %) of **33**.

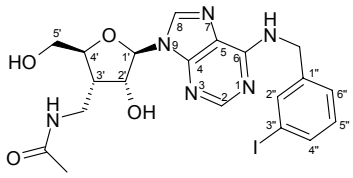

Molecular formula: $C_{20}H_{23}IN_6O_4$

Molecular weight: 538.35

^{1}H-NMR (300 MHz, DMSO-d_6):

δ 1.77 (s, 3H, CH_3), 2.46 (m, 1H, H-3'), 3.08-3.16 (m, 1H, 3'-CH_b), 3.24-3.30 (m, 1H, 3'-CH_a), 3.54 (ddd, 1H, *J* = 3.4 Hz, 5.3 Hz and -12.5 Hz, H-5B'), 3.77 (ddd, 1H, *J* = 2.6 Hz and 5.0 Hz, H-5A'), 3.97 (dt, 1H, *J* = 2.8 Hz and 9.4 Hz, H-4'), 4.41 (t, 1H, *J* = 4.0 Hz, H-2'), 4.63 (br s, 2H, CH_2-Ar), 5.22 (t, 1H, *J* = 5.3 Hz, 5'-OH), 5.85 (d, 1H, *J* = 4.4 Hz, H-1'), 5.93 (d, 1H, *J* = 1.2 Hz, 2'-OH), 7.09 (t, 1H, *J* = 7.8 Hz, H-5''), 7.34 (d, 1H, *J* = 7.6 Hz, H-6''), 7.56 (d, 1H, *J* = 7.9 Hz, H-4''), 7.70 (s, 1H, H-2''), 7.89 (t, 1H, *J* = 5.4 Hz, 3'-C-*N*H), 8.20 (s, 1H, H-2), 8.47 (2s, 2H, H-8 and N(6)-H).

Exact mass (ESI-MS, *i*PrOH:H_2O):

calculated for $C_{20}H_{24}IN_6O_4$ $[M+H]^+$: 539.0905, found 539.0890.

Elemental analysis ($C_{20}H_{23}IN_6O_4.3/2$ H_2O) C,H,N.

9-(3-Acetamidomethyl-3-deoxy-β-D-ribofuranosyl)-N^6-(5-chloro-2-methoxy-benzyl)adenine (34)

10 mg (0.023 mmol) of **32** yielded 6.6 mg (60 %) of **34**.

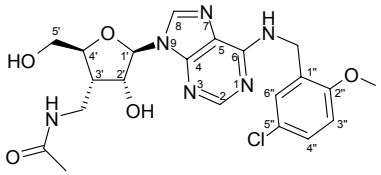

Molecular formula: $C_{21}H_{25}ClN_6O_5$

Molecular weight: 476.92

^{1}H-NMR (300 MHz, DMSO-d_6):

δ 1.79 (s, 3H, CH_3), 3.10-3.19 (m, 1H, H-3'), 3.27-3.36 (m, 1H, 3'-CH_b), 3.51-3.60 (m, 1H, 3'-CH_a), 3.77-3.84 (m, 5H, H-5B', H-5A' and Ar-OCH_3), 4.00 (m, 1H, H-4'), 4.45 (app s, 1H, H-2'), 4.65 (brs, 2H, CH_2-Ar), 5.22 (t, 1H, *J* = 5.1 Hz, 5'-OH), 5.87 (d, 1H, *J* = 4.4 Hz, H-1'), 5.95 (d, 1H, *J* = 1.5 Hz, 2'-OH), 7.02 (d, 1H, *J* = 8.8 Hz, H-3''), 7.07 (s, 1H, H-6''), 7.25 (dd, 1H, *J* = 2.8 Hz and 8.7 Hz, H-4''), 7.90 (t, 1H, *J* = 5.3 Hz, 3'-*C*-*N*H), 8.20 (s, 1H, H-2), 8.26 (brs, 1H, N(6)-H), 8.49 (s, 1H, H-8).

Exact mass (ESI-MS, *i*PrOH:H_2O):

calculated for $C_{21}H_{26}ClN_6O_5$ $[M+H]^+$: 477.1653, found 477.1641.

Elemental analysis ($C_{21}H_{25}ClN_6O_5.1/2H_2O$) C,H,N.

2.7.6 Synthesis of the thymidine analogues modified at the 2'- and 3'-position

1-(3-Azido-3-deoxy-β-D-ribofuranosyl)thymine (45)

A mixture of thymine (838 mg, 6.7 mmol) in HMDS (120 mL), TMSCl (0.85 mL) and dry pyridine (12 mL) was refluxed overnight. After evaporation in vacuo, **4** (2.1 g, 5.5 mmol) in dry 1,2-dichloroethane (50 mL) and TMSOTf (1.2 mL, 6.7 mmol) were added to the residue. After stirring for 5 h at rt, CH_2Cl_2 (50 mL) and cooled 7 % $NaHCO_3$ solution (100 mL) were added to the reaction mixture. The organic layer was separated, washed twice with H_2O (100 mL), dried with $MgSO_4$, filtered and evaporated to dryness. The residue was dissolved in 0.15N $NaOCH_3$ in CH_3OH (100 mL), stirred for 1 h, and neutralised with a H_2O/HOAc (9:1) solution. The mixture was evaporated in vacuo, purified by column chromatography (CH_2Cl_2/MeOH, 95/5) and precipitated from CH_3OH to yield 1.52 g (80 %) of the title compound.

	calculated %				found %		
Compound	C	H	N		C	H	N
25	42.51	4.70	36.05		42.86	4.60	35.84
26	43.37	5.26	33.72		43.62	4.99	33.55
27	41.39	3.67	21.45		41.40	4.00	21.11
28	49.52	4.59	24.31		49.60	4.73	24.11
29	47.14	5.75	29.98		47.05	5.88	29.64
30	44.85	6.59	26.15		44.95	6.58	26.35
31	43.56	4.26	16.93		43.90	4.58	16.60
32	51.94	5.39	19.13		52.07	5.31	19.13
33	42.49	4.64	14.86		42.26	4.42	14.53
34	51.91	5.39	17.29		51.78	5.03	17.11
35	***38.45***	3.76	22.42		***38.94***	3.51	22.11
36	39.60	4.02	21.87		39.68	3.87	21.78
37	37.36	3.13	21.78		37.62	2.94	21.56
38	41.71	4.08	18.92		41.82	4.25	18.59
39	42.51	4.41	18.26		42.83	4.34	17.90
40	39.76	3.52	18.03		39.47	3.34	17.66
41	47.26	4.38	26.11		46.94	4.09	26.44
42	48.34	4.67	25.37		48.52	4.44	29.97
43	48.05	5.31	20.65		48.27	5.18	20.73
44	49.13	5.57	20.05		48.86	5.19	19.90

Table 2.2 Elemental analysis of final products **25**-**44**.

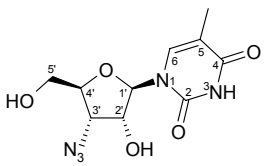

Molecular formula: $C_{10}H_{13}N_5O_5$

Molecular weight: 283.24

^{1}H-NMR (300 MHz, DMSO-d_6)

δ = 1.77 (d, 3H, *J* = 1.2 Hz, 5-CH_3), 3.54 (dd, 1H, *J* = 3.2 Hz and -12.3 Hz, H-5B'), 3.63 (d, 1H, *J* = 3.0 Hz, H-5A'), 3.84 (q, 1H, *J* = 3.3 Hz and 7.8 Hz, H-4'), 4.06 (app t, 1H, *J* = 5.1 Hz, H-3'), 4.40 (t, 1H, *J* = 5.7 Hz, H-2'), 5.29 (br s, 1H, 5'-OH), 5.74 (d,

1H, *J* = 5.7 Hz, H-1'), 6.13 (br s, 1H, 2'-OH), 7.69 (d, 1H, *J* = 1.2 Hz, H-6), 11.35 (br s, 1 H, N(3)-H).

^{13}C-NMR (75 MHz, DMSO-d_6)

δ 12.85, 61.50, 61.81, 74.37, 82.44, 88.27, 110.16, 136.77, 151.41, 164.34.

Exact mass (ESI-MS, *i*PrOH:H_2O):

calculated for $C_{10}H_{13}N_5O_5Na$ $[M+Na]^+$ 306.0814; found 306.0798.

_O_-2,2'-Anhydro-1-(3-azido-3-deoxy-5-_O_-trityl-β-D-arabinofuranosyl)thymine (47)

45 (1.43 g, 5.1 mmol) and trityl chloride (1.55 g, 5.6 mmol) were dissolved in dry pyridine (15 mL). The reaction mixture was heated at 65 °C for 7 hours, stirred overnight at room temperature and evaporated to dryness. The residue was dissolved in CH_2Cl_2 (150 mL) and washed subsequently with 7 % $NaHCO_3$ solution (150 mL) and water (150 mL). The organic layer was dried over $MgSO_4$, filtered and evaporated to dryness. The residue was chromatographed on a silica gel column prepared in CH_2Cl_2/MeOH (99/1) and eluted with CH_2Cl_2/MeOH (97/3) to give 2.46 g (93 %) of 1-(3-Azido-3-deoxy-5-*O*-trityl-β-D-ribofuranosyl)thymine.

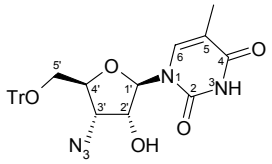

Molecular formula: $C_{29}H_{27}N_5O_5$

Molecular weight: 525.57

^{1}H-NMR (300 MHz, DMSO-d_6)

δ = 1.42 (d, 3H, *J* = 0.9 Hz, 5-CH_3), 3.19 (dd, 1H, *J* = 2.9 Hz and -11.0 Hz, H-5B'), 3.29 (dd, 1H, *J* = 3.8 Hz, H-5A'), 3.97 (m, 1H, H-4'), 4.30 (q, 1H, *J* = 5.4 Hz and 10.8 Hz, H-3'), 4.57 (q, 1H, *J* = 5.0 Hz and 10.1 Hz, H-2'), 5.76 (d, 1H, *J* = 5.4 Hz, H-1'), 6.24 (d, 1H, *J* = 4.8 Hz, 2'-OH), 7.21-7.40 (m, 15H, trityl), 7.46 (d, 1H, *J* = 1.2 Hz, H-6), 11.40 (s, 1H, N^3-H).

Exact mass (ESI-MS, *i*PrOH:H_2O):

calculated for $C_{29}H_{27}N_5O_5Na$ $[M+Na]^+$ 548.1910; found 548.1910.

Trifluoromethanesulfonyl chloride (1.0 mL, 9.36 mmol) was added to a cooled solution of 1-(3-Azido-3-deoxy-5-*O*-trityl-β-D-ribofuranosyl)thymine (2.46 g, 4.68 mmol) and DMAP (2.30 g, 18.7 mmol) in dry CH_2Cl_2 (50 mL). After 2 hours the

reaction was quenched with water (15 mL) and extracted. The organic layer was washed with a 7 % $NaHCO_3$ solution, dried over $MgSO_4$, filtered and evaporated to dryness to give a white semi-solid that was purified on a silica gel column (CH_2Cl_2/MeOH, 97/3) to give 1.91 g (81 %) of **47**.

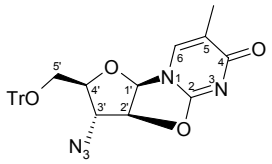

Molecular formula: $C_{29}H_{25}N_5O_4$

Molecular weight: 507.55

^{1}H-NMR (300 MHz, DMSO-d_6)

δ = 1.79 (d, 3H, *J* = 0.9 Hz, 5-CH_3), 2.77 (dd, 1H, *J* = 7.6 Hz and -10.6 Hz, H-5B'), 3.04 (dd, 1H, *J* = 4.1 Hz, H-5A'), 4.38 (m, 1H, H-4'), 4.60 (dd, 1H, *J* = 1.8 Hz and 3.2 Hz, H-3'), 5.43 (dd, 1H, *J* = 1.6 Hz and 5.7 Hz, H-2'), 6.31 (d, 1H, *J* = 5.7 Hz, H-1'), 7.20-7.28 (m, 15H, trityl), 7.82 (d, 1H, *J* = 1.2 Hz, H-6).

Exact mass (ESI-MS, *i*PrOH:H_2O):

calculated for $C_{29}H_{26}N_5O_4$ $[M+H]^+$ 508.1984; found 508.1982.

1-(3-Azido-3-deoxy-5-*O*-trityl-β-D-arabinofuranosyl)thymine (48)

A mixture of **47** (1.91 g, 3.76 mmol), 1N NaOH (10 mL) and 50 % EtOH (100 mL) was stirred at room temperature for 4 hours. The solution was neutralised with an acetic acid/EtOH mixture (1:1, v/v) to pH~7. The resulting white solid was collected by filtration and washed with water. The solid was then dissolved in CH_2Cl_2, extracted with water, dried over $MgSO_4$, filtered and evaporated to dyness to produce 1.74 g (88 %) of **48** as a white solid.

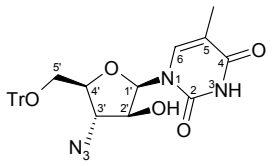

Molecular formula: $C_{29}H_{27}N_5O_5$

Molecular weight: 525.57

^{1}H-NMR (300 MHz, DMSO-d_6)

δ = 1.59 (d, 3H, *J* = 0.6 Hz, 5-CH_3), 3.28 (dd, 2H, *J* = 4.1 Hz and -11.1 Hz, H-5B' and H-5A'), 3.80 (app quinted, 1H, *J* = 4.1 Hz and 8.2 Hz, H-4'), 4.15 (t, 1H, *J* = 7.5 Hz,

H-3'), 4.34 (m, 1H, H-2'), 6.07 (d, 1H, *J* = 6.2 Hz, H-1'), 6.10 (d, 1H, *J* = 5.6 Hz, 2'-OH), 7.24-7.40 (m, 15H, trityl), 7.38 (d, 1H, *J* = 0.6 Hz, H-6), 11.34 (s, 1H, N^3-H).

Exact mass (ESI-MS, *i*PrOH:H_2O):

calculated for $C_{29}H_{27}N_5O_5Na$ $[M+Na]^+$ 548.1910; found 548.1906.

1-(3-Azido-3-deoxy-β-D-arabinofuranosyl)thymine (49)

A suspension of compound **48** (0.5 g, 0.95 mmol) in 80 % HOAc (10 mL) was heated at 90 °C with stirring for 25 min. The solution was evaporated in vacuo to give a residue that was chromatographed on a silica gel column (CH_2Cl_2/MeOH, 95/5) to afford 0.2 g (79 %) of **49**.

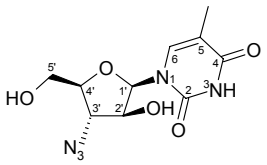

Molecular formula: $C_{10}H_{13}N_5O_5$

Molecular weight: 283.24

^{1}H-NMR (300 MHz, DMSO-d_6)

δ = 1.74 (s, 3H, *J* = 1.2 Hz, 5-CH_3), 3.62 (m, 3H, H-4', H-5B' and H-5A'), 4.00 (t, 1H, *J* = 7.5 Hz, H-3'), 4.32 (t, 1H, *J* = 6.6 Hz, H-2'), 5.29 (br s, 1H, 5'-OH), 5.99 (d, 1H, *J* = 6.2 Hz, H-1'), 6.07 (d, 1H, *J* = 0.6 Hz, 2'-OH), 7.58 (d, 1H, *J* = 1.2 Hz, H-6), 11.27 (s, 1H, N^3-H).

^{13}C-NMR (75 MHz, DMSO-d_6)

δ 12.84, 60.20, 64.84, 74.80, 80.26, 83.78, 108.70, 138.29, 151.14, 164.503.

Exact mass (ESI-MS, *i*PrOH:H_2O):

calculated for $C_{10}H_{13}N_5O_5Na$ $[M+Na]^+$ 306.0814; found 306.0810.

1-(3-Azido-2-chloro-2,3-dideoxy-β-D-ribofuranosyl)thymine (51)

47 (310 mg, 0.61 mmol) was transferred into a sealable glass vial and 4 M HCl in dioxane (20 mL) was added. The vial was firmly sealed and temperature was raised to 75-80 °C for 24 hours. After cooling to room temperature the reaction mixture was evaporated in vacuo and purified on a silica gel column CH_2Cl_2/MeOH (98/2) to give 170 mg (92 %) of **51**.

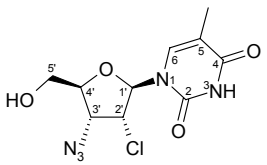

Molecular formula: $C_{10}H_{12}ClN_5O_4$

Molecular weight: 301.69

^{1}H-NMR (300 MHz, DMSO-d_6)

δ = 1.75 (d, 3H, J = 1.2 Hz, 5-CH_3), 3.61 (ddd, 1H, J = 3.0 Hz, 5.0 Hz and -12.6 Hz, H-5B'), 3.75 (ddd, 1H, J = 3.1 Hz and 5.3 Hz, H-5A'), 3.99 (app quinted, 1H, J = 2.9 Hz, 3.13 Hz and 6.0 Hz, H-4'), 4.57 (t, 1H, J = 5.7 Hz, H-3'), 4.92 (t, 1H, J = 5.1 Hz, H-2'), 5.47 (t, 1H, J = 4.7 Hz, 5'-OH), 5.93 (d, 1H, J = 4.7 Hz, H-1'), 7.80 (d, 1H, J = 1.2 Hz, H-6), 11.46 (s, 1H, N^3-H).

^{13}C-NMR (75 MHz, DMSO-d_6)

δ 12.92, 60.37, 61.10, 61.90, 83.12, 89.02, 110.23, 135.89, 151.17, 164.29.

Exact mass (ESI-MS, *i*PrOH:H_2O):

calculated for $C_{10}H_{13}ClN_5O_4$ $[M+H]^+$ 302.0655; found 302.0658.

1-(3-Azido-2,3-dideoxy-2-fluoro-β-D-ribofuranosyl)thymine (53)

To a solution of **48** (1.59 g, 3.0 mmol) in toluene (30 mL) and pyridine (3 mL), DAST (1.5 mL, 11.3 mmol) was added and stirred at room temperature for 2 h before heating the reaction mixture to 50 °C. After 5 hours EtOAc (170 mL) was added and the organic layer washed successively with 7 % $NaHCO_3$ (200 mL) and H_2O (200 mL), dried over $MgSO_4$, filtered and concentrated in vacuo. The residue was purified on a silica gel column prepared in $CHCl_3$ and eluated with $CHCl_3$/MeOH, 99/1 to give 1.45 g (90 %) of 1-(3-Azido-2,3-dideoxy-2-fluoro-5-*O*-trityl-β-D-ribofuranosyl)thymine.

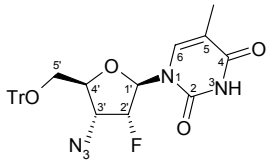

Molecular formula: $C_{29}H_{26}FN_5O_4$

Molecular weight: 527.56

^{1}H-NMR (300 MHz, DMSO-d_6)

δ = 1.52 (d, 3H, J = 0.9 Hz, 5-CH_3), 3.24 (dd, 1H, J = 4.1 Hz and -11.1 Hz, H-5B'), 3.35 (dd, 1H, J = 2.4 Hz, H-5A'), 4.12 (m, 1H, H-4'), 4.56 (ddd, 1H, J = 4.7 Hz, 9.5 Hz and $J_{3',F}$ = 24.5 Hz, H-3'), 5.53 (dd, 1H, J = 4.8 Hz and $J_{2',F}$ = 52.9 Hz, H-2'), 5.91 (dd,

1H, J = 1.1 Hz and $J_{1',F}$ = 21.6 Hz, H-1'), 7.24-7.40 (m, 15H, trityl), 7.51 (d, 1H, J = 1.2 Hz, H-6), 11.51 (br s, 1H, N^3-H).

Exact mass (ESI-MS, *i*PrOH:H_2O):

calculated for $C_{29}H_{26}FN_5O_4Na$ $[M+Na]^+$ 550.1866; found 550.1862.

1-(3-Azido-2,3-dideoxy-2-fluoro-5-*O*-trityl-β-D-ribofuranosyl)thymine (1.45 g, 2.75 mmol) was detritylated to give 0.52 g (64 %) of **53** using the same procedure as described for **49**.

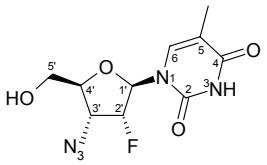

Molecular formula: $C_{10}H_{12}FN_5O_4$

Molecular weight: 285.24

^{1}H-NMR (300 MHz, DMSO-d_6)

δ = 1.74 (d, 3H, J = 1.2 Hz, 5-CH_3), 3.60 (dd, 1H, J = 2.9 Hz and -12.6 Hz, H-5B'), 3.79 (dd, 1H, J = 2.6 Hz, H-5A'), 3.98 (dt, 1H, J = 2.6 Hz and 8.8 Hz, H-4'), 4.30 (ddd, 1H, J = 4.6 Hz, 8.9 Hz and $J_{3',F}$ = 23.5 Hz, H-3'), 5.42 (ddd, 1H, J = 1.5 Hz, 4.5 Hz and $J_{2',F}$ = 52.9 Hz, H-2'), 5.43 (br s, 1H, 5'-OH), 5.90 (dd, 1H, J = 1.6 Hz and $J_{1',F}$ = 19.2 Hz, H-1'), 7.74 (d, 1H, J = 1.2 Hz, H-6), 11.44 (br s, 1H, N^3-H).

^{13}C-NMR (75 MHz, DMSO-d_6)

δ 12.76, 58.67 (J = 15.3 Hz), 59.76, 81.65, 88.38 (J = 34.8 Hz), 94.68 (J = 186.3 Hz), 110.10, 136.89, 150.84, 164.51.

Exact mass (ESI-MS, *i*PrOH:H_2O):

calculated for $C_{10}H_{12}FN_5O_4Na$ $[M+Na]^+$ 308.0771; found 308.0759.

General procedure for the synthesis of the 3'-amine modified thymidine nucleosides from their 3'-azide precursors

The 3'-azido modified nucleoside (1 mmol) was dissolved in dry pyridine (8 mL) and PhP_3 (1.6 mmol) was added to the solution. After stirring at rt for 1.5 h, concentrated NH_4OH (3 mL) was added. The reaction mixture was stirred for another 2 h, evaporated to dryness and purified by silica gel chromatography using a suitable mixture of CH_2Cl_2/MeOH.

1-(3-Amino-3-deoxy-β-D-ribofuranosyl)thymine (46)

500 mg (1.77 mmol) of **45** yielded 320 mg (71 %) of **46** as a white solid.

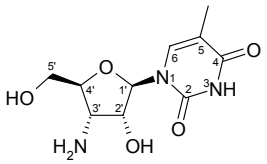

Molecular formula: $C_{10}H_{15}N_3O_5$

Molecular weight: 257.10

^{1}H-NMR (300 MHz, DMSO-d_6)

δ = 1.75 (s, 3H, 5-CH_3), 3.21 (dd, 1H, *J* = 5.4 Hz and 7.7 Hz, H-3'), 3.60 (m, 2H, H-4' and H-5B'), 3.74 (app d, 1H, *J* = -11.2 Hz, H-5A'), 3.86 (dd, 1H, *J* = 2.4 Hz and 5.3 Hz, H-2'), 5.11 (br s, 1H, 5'-OH), 5.69 (d, 1H, *J* = 2.4 Hz, H-1'), 7.61 (s, 1H, H-6).

^{13}C-NMR (75 MHz, DMSO-d_6)

δ 12.85, 52.42, 60.74, 75.39, 85.55, 90.12, 109.29, 137.16, 151.13, 164.48.

Exact mass (ESI-MS, *i*PrOH:H_2O):

calculated for $C_{10}H_{16}N_3O_5Na$ $[M+H]^+$ 258.1089; found 258.1095.

1-(3-Amino-3-deoxy-β-D-arabinofuranosyl)thymine (50)

120 mg (0.42 mmol) of **49** yielded 60 mg (54 %) of **50** as a white solid.

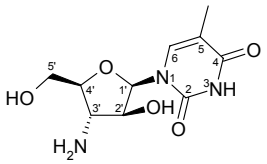

Molecular formula: $C_{10}H_{15}N_3O_5$

Molecular weight: 257.25

^{1}H-NMR (300 MHz, DMSO-d_6)

δ = 1.73 (d, 3H, *J* = 1.2 Hz, 5-CH_3), 3.05 (t, 1H, *J* = 6.2 Hz, H-3'), 3.50 (m, 1H, H-4'), 3.61 (app t, 2H, *J* = 15.8 Hz, 2H, H-5B' and H-5A'), 3.90 (br q, 1H, *J* = 5.0 Hz and 9.7 Hz, H-2'), 5.04 (s, 1H, 5'-OH), 5.42 (d, 1H, *J* = 4.4 Hz, 2'-OH), 5.98 (d, 1H, *J* = 5.6 Hz, H-1'), 7.60 (d, 1H, *J* = 1.2 Hz, H-6).

^{13}C-NMR (75 MHz, DMSO-d_6)

δ 12.88, 57.83, 60.99, 77.41, 84.54, 84.66, 107.97, 138.82, 151.15, 164.59.

Exact mass (ESI-MS, *i*PrOH:H_2O):

calculated for $C_{10}H_{16}N_3O_5$ $[M+H]^+$ 258.1089; found 258.1084.

1-(3-Amino-2-chloro-2,3-dideoxy-β-D-ribofuranosyl)thymine (52).

90 mg (0.30 mmol) of **51** yielded 24 mg (30 %) of **52** as a white solid.

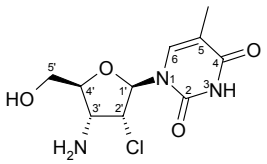

Molecular formula: $C_{10}H_{14}ClN_3O_4$

Molecular weight: 275.69

^{1}H-NMR (300 MHz, DMSO-d_6)

δ = 1.73 (d, 3H, *J* = 0.9 Hz, 5-CH_3), 1.85 (br s, 2H, 3'-NH_2), 3.50 (dd, 1H, *J* = 5.3 Hz and 7.9 Hz, H-3'), 3.62 (ddd, 1H, *J* = 2.6 Hz, 4.7 Hz and -12.2 Hz, H-5B'), 3.75 (m, 2H, H-4' and H-5A'), 4.53 (dd, 1H, *J* = 2.4 Hz and 5.3 Hz, H-2'), 5.26 (t, 1H, *J* = 5.0 Hz, 5'-OH), 5.94 (d, 1H, *J* = 2.6 Hz, H-1'), 7.99 (d, 1H, *J* = 1.5 Hz, H-6), 11.35 (s, 1H, N^3-H).

^{13}C-NMR (75 MHz, DMSO-d_6)

δ 12.91, 52.06, 59.97, 84.69, 89.64, 91.10, 109.64, 136.22, 151.09, 164.42.

Exact mass (ESI-MS, *i*PrOH:H_2O):

calculated for $C_{10}H_{15}ClN_3O_4$ $[M+H]^+$ 276.0750; found 276.0765.

1-(3-Amino-2,3-dideoxy-2-fluoro-β-D-ribofuranosyl)thymine (54).

120 mg, 0.42 mmol of **53** yielded 60 mg (55 %) of **54** as a white solid.

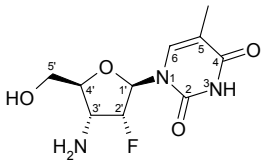

Molecular formula: $C_{10}H_{14}FN_3O_4$

Molecular weight: 259.24

^{1}H-NMR (300 MHz, DMSO-d_6)

δ = 1.72 (d, 3H, *J* = 1.2 Hz, 5-CH_3), 3.32 (ddd, 1H, *J* = 4.3 Hz, 9.7 Hz and $J_{3',F}$ = 28.6 Hz, H-3'), 3.61 (m, 2H, H-4' and H-5B'), 3.78 (dd, 1H, *J* = 1.76 Hz and -12.3 Hz, H-5A'), 4.87 (dd, 1H, *J* = 4.1 Hz and $J_{2',F}$ = 53.1 Hz, H-2'), 5.19 (br s, 1H, 5'-OH), 5.83 (d, 1H, $J_{1',F}$ = 18.2 Hz, H-1'), 7.86 (d, 1H, *J* = 1.2 Hz, H-6).

^{13}C-NMR (75 MHz, DMSO-d_6)

δ 12.82, 51.73 (*J* = 18.1 Hz), 59.54, 84.83, 88.30 (*J* = 35.7 Hz), 96.72 (*J* = 180.5 Hz), 109.54, 136.80, 150.79, 164.52.

Exact mass (ESI-MS, *i*PrOH:H_2O):
calculated for $C_{10}H_{15}FN_3O_4$ $[M+H]^+$ 260.1046; found 260.1053.

2.8 References

[1] Ozols, A. M.; Azhayev, A. V.; Dyatkina, N. B.; Krayevski, A. A. *Synthesis*. **1980**, *7*, 557.

[2] Vorbrüggen, H.; Krolikiewicz, K.; Bennua, B. *Chem. Ber.* **1981**, *114*, 1234.

[3] (i) Kim, H. O.; Ji, X.-D.; Siddiqi, S. M.; Olah, M. E.; Stiles, G. L.; Jacobson, K. A. *J. Med. Chem.* **1994**, *37*, 3614. (ii) Jacobson, K. A.; Siddiqi, S. M.; Olah, M. E.; Ji, X.-D.; Melman, N.; Bellamkonda, K.; Meshulam, Y.; Stiles, G. L.; Kim, H. O. *J. Med. Chem.* **1995**, *38*, 1720.

[4] (i) Botta, O.; Moyroud, E.; Lobato, C.; Strazewski, P. *Tetrahedron* **1998**, *54*, 13529. (ii) McDevitt, J. P.; Lansbury, P. T. *J. Am. Chem. Soc.* **1996**, *118*, 3818.

[5] Dauban, P.; Chiaroni, A.; Riche, C.; Dodd, R. H. *J. Org. Chem.* **1996**, *61*, 2488.

[6] DeNinno, M. P.; Masumane, H.; Chenard, L. K.; DiRico, K. J.; Eller, C.; Etienne, J. B.; Tickner, J. E.; Kennedy, S. P.; Knight, D. R.; Kong, J.; Oleynek, J. J.; Tracey, W. R.; Hill, R. J. *J. Med. Chem.* **2003**, *46*, 353.

[7] Van Tilburg, E. W.; Van Der Klein, P. A. M.; Von Frijtag Drabbe Künzel, J.; De Groote, M.; Stannek, C.; Lorenzen, A.; IJzerman, A. P. *J. Med. Chem.* **2001**, *44*, 2966.

[8] Parr, I. B.; Horenstein, B. A. *J. Org. Chem.* **1997**, *62*, 7489.

[9] Lin, T.-S.; Zhu, J.-L.; Dutschman, G. E.; Cheng, Y.-C.; Prusoff, W. H. *J. Med. Chem.* **1993**, *36*, 353.

[10] (i) Filichev, V. V.; Brandt, M.; Pedersen, E. B. *Carbohydrate Res.* **2001**, *333*, 115. (ii)Van Rompaey, P.; Jacobson, K. A.; Gao, Z.-G.; Chen, A.; Barak, D.; Kim, S.-A.; Lee, K.; Link, A.; Liang, B. T.; Herdewijn, P.; Van Calenbergh, S. *Collection Symposium Series* **2002**, *5*, 267.

[11] Yu, G.; Mason, H. J.; Wu, X.; Endo, M.; Douglas, J.; Macor, J. E. *Tetrahedron Lett.* **2001**, *42*, 3247–3249.

[12] Gryaznov, S. M.; Winter, H. *Nucleic Acids Res.* **1998**, *26*, 4160.

[13] Aoyama, Y.; Sekine, T.; Iwamoto, Y.; Kawashima, E.; Ishido, Y. *Nucleosides Nucleotides* **1996**, *15*, 733.

[14]. Lin, T.-S. ; Yang, J.-H.; Liu, M.-C.; Shen, Z.-Y.; Cheng, Y.-C.; Prusoff, W. H.; Birnbaum, G. I.; Giziewicz, J.; Ghazzouli, I.; Brankovan, V.; Feng, J.-S.; Hsiung, G.-D. *J. Med. Chem.* **1991**, *34*, 693.

[15] (i) Papchikhin, A. V.; Purygin, P. P.; Azhaev, A. V.; Kraevskii, A. A.; Kutateladze, T. V.; Chidzhavadze, Z. G.; Bibilashvilli, R. Sh. *S. Bioorg. Khim.* **1985**, *11*, 1367. (ii) Webb, T. R.; Mitsuya, H.; Broder, S. *J. Med. Chem.* **1988**, *31*, 1475.

[16] Codington, J. F.; Doerr, I. L.; Fox, J. J. *J. Org. Chem.* **1964**, *29*, 558.

[17] Middleton, W. J. *J. Org. Chem.* **1975**, *40*, 574.

[18] (i) Herdewijn, P.; Van Aerschot, A. *Bull. Soc. Chim. Belg* **1989**, *12*, 937. (ii) Huang, J.-T.; Chen, L.-C.; Wang, L.; Kim, M.-H.; Warshaw, J. A.; Armstrong, D.; Zhu, Q.-H.; Chou, T.-C.; Watanabe, K. A.; Matulic-Adamic, J.; Su, T.-L.; Fox, J. J.; Polsky, B.; Baron, P. A.; Gold, J. W. M.; Hardy, W. D.; Zuckerman, E. *J. Med. Chem.* **1991**, *34*, 1640-1646.

[19] Terent'ev, L. L.; Terent'eva, N. A.; Rasskazov, V. A.; Aleksandrova, L. A.; Viktorova, L. S.; Kraevskii, A. A. *Biokhimiya* (*Moscow*) **1985**, *50*, 1024.

PART II
BIOLOGICAL EVALUATION OF THE MODIFIED ADENOSINE ANALOGUES

Biological results in this part were published in:

Bioorg. Med. Chem. **2004**, *Accepted*.

J. Med. Chem. **2003**, *46*, 4847.

J. Med. Chem. **2001**, *44*, 4125.

Chapter 3

GENERAL BACKGROUND

3.1 Adenosine receptors and G-protein coupled receptors

Integral membrane G-protein coupled receptors (GPCRs or 7TM), a small subset of the human genome (2–3%),[1] constitute about 50% of the drug targets that are of interest to the pharmaceutical industry.[2] GPCRs are involved in the regulation of a wide range of body functions and hence used for treatment of diseases such as hypertension, cardiac dysfunction, depression, pain and schizophrenia.[3]

The GPCR superfamily can be subdivided into six classes, that share significant sequence similarity (see also Figure 3.1):[3]

- Class A, the rhodopsin/adrenergic receptors, consists of the majority of GPCRs identified to date. These GPCRs are activated by various ligands such as photons, odorants, hormones, neurotransmitters (ranging from small biogenic amines to peptides) and complex glycoproteins. Both structurally and functionally they are the best studied GPCRs.
- Class B, the secretin/vasointestinal peptide (VIP) receptors, binds neuropeptides and peptide hormones.
- Class C, the metabotropic glutamate receptor family, comprises at least six closely related subtypes of receptors that bind glutamate, the major excitatory neurotransmitter in the central nervous system.
- Three additional GPCR classes are: the fungal pheromone P and a-factor (STE2/MAM2) family (class D), the fungal pheromone A and M factor (STE3/MAP3) receptors (class E), and the cyclic adenosine monophosphate (cAMP) receptors of Dictyostelium (class F).

Biophysically, GPCRs are characterized by their seven transmembranal (7TM) hydrophobic regions (each 20-25 amino acids in length). Seen from the top of the membrane, the 7TM domains form a barrel shape, perpendicularly oriented in a counter clockwise manner to the plane of the membrane. All GPCRs have an

extracellular N-terminal region (from <10 to >100 amino acids) and an intracellular C-terminal region. Intra- and extracellular loops (ILs and ELs) are 10-40 amino acids long, although the third intracellular loop (EL3) and C-terminal loop sequence can have over 150 residues. The overall size of GPCRs can vary significantly from <300 to >1100 amino acids.[3]

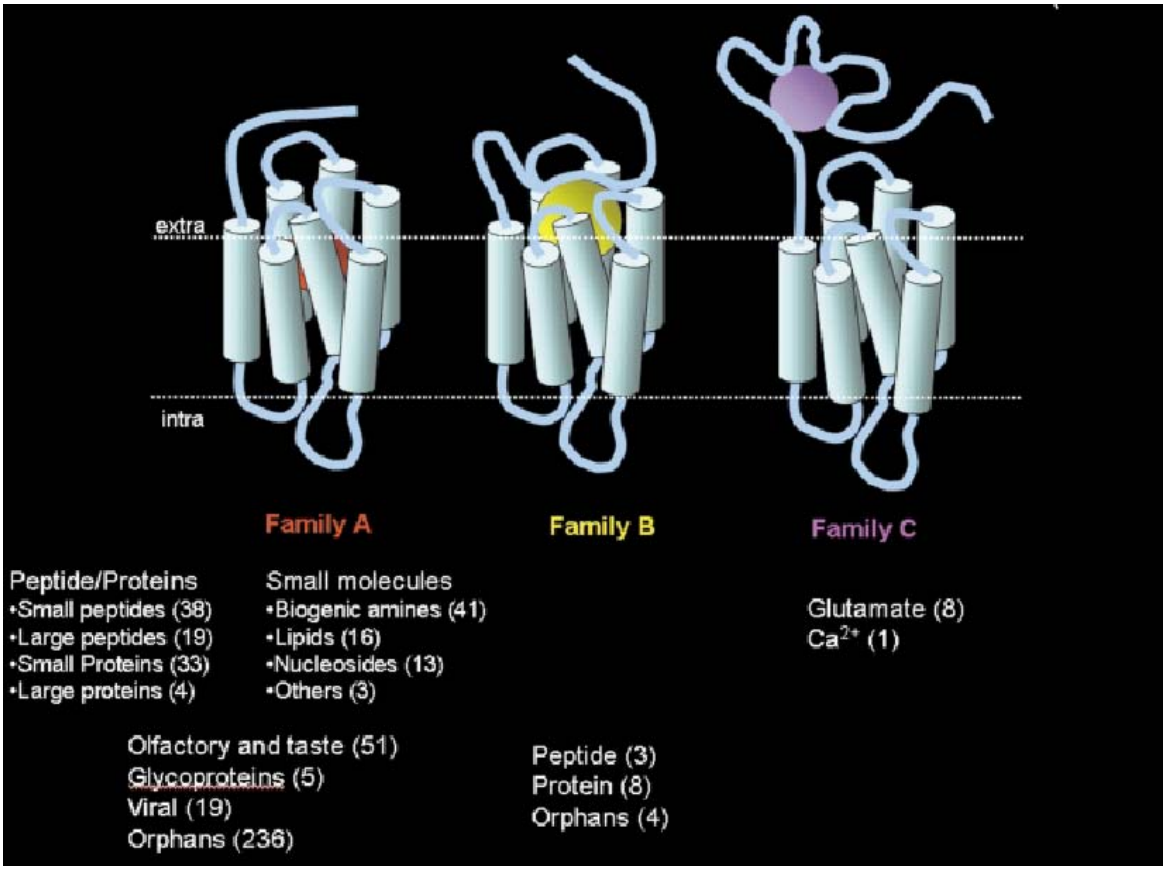

Figure 3.1 The "world of human GPCRs". A distribution of the 508 human GPCRs that have been discovered so far, grouped according to the type of natural ligand that binds to them. Orphan receptors are receptors of yet unknown function.[3]

In the GPCR superfamily the most conserved residues are located within the TM domains, making up the essential determinants of the receptors structure and function.[4] However, the exact 3D structure of most GPCRs is still unknown, due to the technical difficulties regarding X-ray crystallography and NMR experiments on GPCRs. In fact, the recently published X-ray structure of rhodopsin[5] is the only 3D structure of a GPCR available. Before the publication of the rhodopsin X-ray structure, the low-resolution cryo-electron microscopic structure of rhodopsin[6] and the X-ray structure of bacteriorhodopsin[7] (a proton pump and not a GPCR) were the only major advancements in GPCR structural information.

For most GPCRs, rhodopsin[6] is used as a template for homology modeling techniques.[8] With homology modeling the 3D structure of an unknown protein can be created, based on the known structure(s) of related protein(s). The accuracy of the prediction relies on the number of structures that serve as a template and their homology to the protein of interest (typically >35% sequence identity).[9-11] This method has proven successful in modeling globular proteins, like kinase enzymes. However, applying homology modeling to GPCRs is hampered by the low sequence identity between most GPCRs and rhodopsin (or bacteriorhodopsin). Differences between rhodopsin and bacteriorhodopsin, and their use as GPCR (modeling) templates are much debated in recent critical reviews.[8]

In this thesis (Chapters 4-6) we focus on adenosine receptors (AR), a subfamily of class A GPCRs to which also rhodopsin belongs (see above). Since the discovery of the hypotensive and bradycardiac effects of adenosine, ARs have become an interesting field of research.[12] Today, four adenosine receptor subtypes (A_1, A_{2A}, A_{2B} and A_3) are known. As shown in Figure 3.2, AR subtypes can be differentiated according to their preferred mechanism of signal transduction: A_1AR and A_3AR interact with G_i heterotrimeric G-proteins, whereas A_{2A}AR and A_{2B}AR couple with G_s, resulting respectively in the inhibition (for A_1AR and A_3AR) and stimulation (for A_{2A}AR and A_{2B}AR) of adenylate cyclase. A_{2B}AR and A_3AR can, in addition, also activate phospholipase C by activation of G_q.[12,13]

The A_3AR is the most recently identified AR subtype (Chapter 4).[12,14] A_3AR ligands are potentially interesting therapeutic agents for the treatment of ischemic and inflammatory diseases.[14] Ligand-binding sites of A_1AR, A_{2A}AR, and A_{2B}AR were (previously) experimentally characterized by site-directed mutagenesis (SDM).[15-19] For the TM region of the human A_3AR an (improved) model was build,[20-22] based on the high resolution crystal structure of bovine rhodopsin[5] (Figure 3.3). However, the molecular basis for ligand recognition in the A_3AR, remained unclear. Creation of the A_3 "neoceptor" by Dr. Kenneth A. Jacobson and co-workers,[23] provided new insights into the molecular recognition in the adenosine receptors.

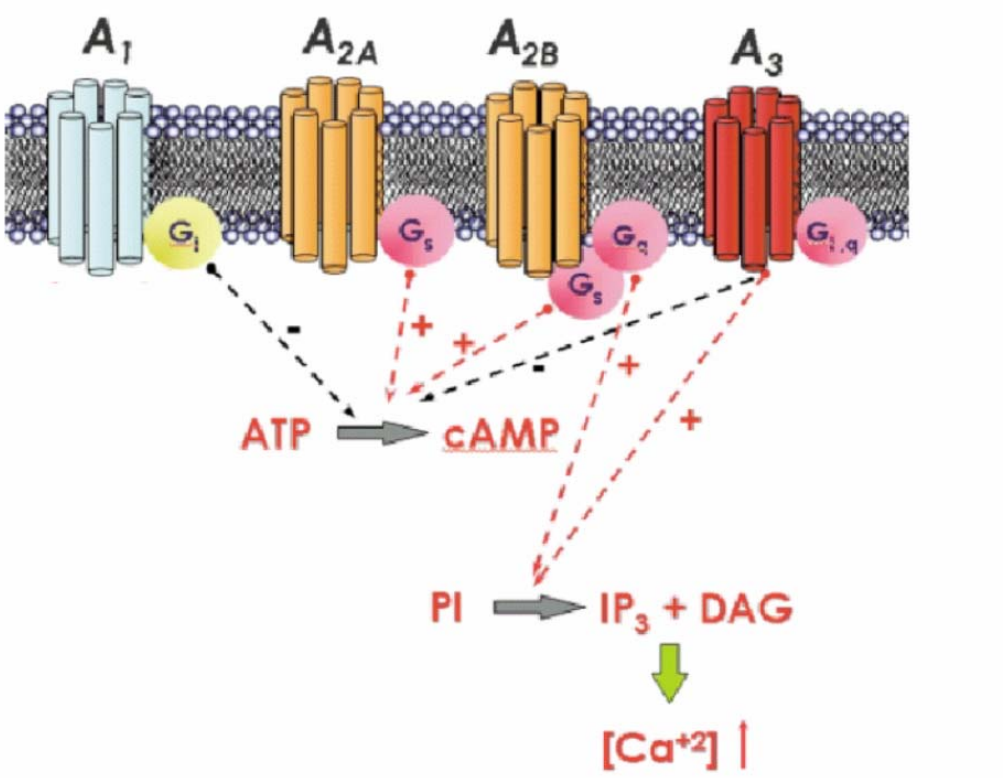

Figure 3.2 Signal transduction pathways associated with activation of the human adenosine receptors.[3]

To further investigate the ligand-A_3AR interactions, SDM was used to study the role of a number of residues in TM domains 3,6 and EL2, predicted (by previous molecular modeling)[24] to be involved in the ligand recognition. These SDM studies showed Trp243 in the A_3AR to be critical for receptor activation, but not for agonist binding, a finding that further refined the rhodopsin-based model of ligand-A_3AR interactions.[25]

Note on the residue indexing in this work

To facilitate comparison of aligned residues in related GPCRs, residues are supplemented with an index, according to the van Rhee-convention.[32] The most conserved residue in a TM region X is given the index number (X.50). Residues within the given TM are then indexed relative to the "50" position. Note that the "50" position is not necessarily the residue in the middle of the TM region. For example, in the hA_3AR His272 has the index (7.43) as it is located in TM7, seven residues apart from the conserved Pro279 (7.50).

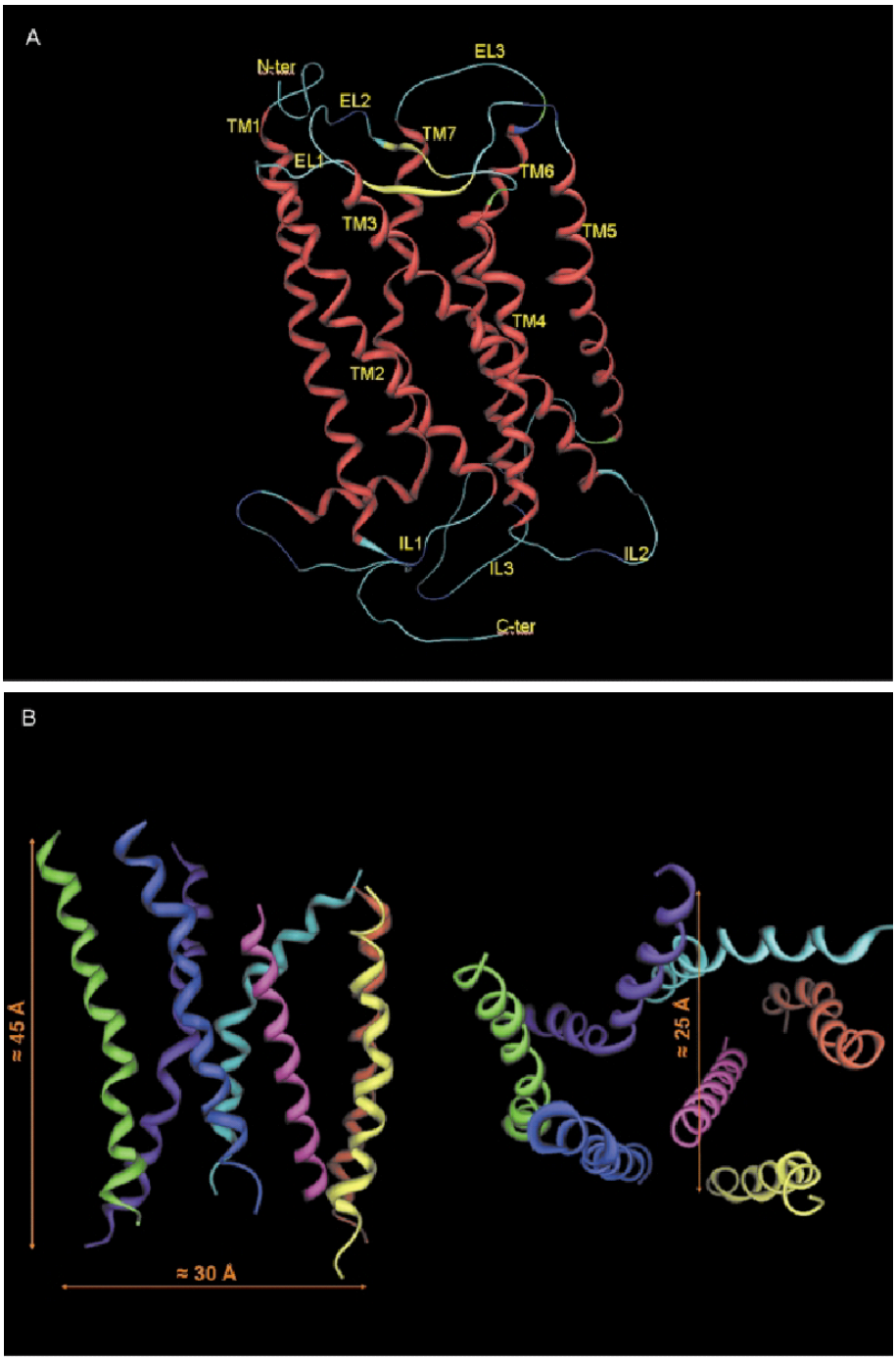

Figure 3.3 A Stereoview of the complete topology of human A_3AR obtained by a homology modeling approach. **B** Stereoview of the human A_3AR transmembrane helical bundle model viewed perpendicular to the helical axes (**left**) and along the helical axes from the extracellular end (**right**).[3]

3.2 Chemical genetics: situating the "neoceptor-neoligand" concept

The approximately 40,000 genes in the human genome[1] represent a great challenge in "post-genomic" drug discovery. Logically there is much interest in the development

of technologies that can (functionally) validate potential drug targets and/or yield pharmacological information about their mechanism of action.

The power of genetic approaches for the study of target function is their high specificity, i.e. the ability to affect a single protein in a whole organism (hence the popularity of knockout mice for target validation). However, genetics has its drawbacks:[26]

- Genetic approaches affect the entire protein target, which makes it difficult to determine the difference between effects resulting from the loss of the entire protein (i.e. as a functional scaffold of the cell) and effects resulting from the loss of the proteins intrinsic activity (i.e. signal transduction, enzyme activity, ...).
- Difficult temporal control. Both gene knockouts and RNA-based approaches (antisense and RNAi) modulate protein levels rather slowly, which can be problematic for the study of processes such as signal transduction that have millisecond time scales.
- Gene knockouts often result in a lethal phenotype.

Chemical approaches, on the other hand, also have advantages and disadvantages. Small molecules influence protein function in a (pharmacologically) controllable way, but in most cases suffer from a lack of specificity. When using a purely chemical approach, it is often difficult to determine the true action of small molecules on an individual target, as “off-target” effects can contribute to toxicity or even positive biological effects.[26]

So, where genetics offer target specificity, chemistry offers temporal control over the proteins targeted. Experimental systems that incorporate the advantages of both approaches, are expected to represent powerful tools for target validation (in drug discovery) and protein functional studies.

3.2.1 Orthogonal chemical genetics

Recently several studies have shown the advantages of combining (orthogonal) chemistry and genetics (Figure 3.4).[27] These experiments are all based on the same "lock-and-key" design approach:

- Step 1; a (small) molecule that binds to the protein of interest, i.e. the "key", is synthetically modified to eliminate its ability to bind to its wild-type target. This designed compound is said to be "orthogonal" when it can no longer interact with its natural (protein) target or, ideally, with any other target in the cell (Figure 3.4**A**).
- Step 2; the (protein) target of interest, i.e. the "lock", is engineered to accept the orthogonal compound (Figure 3.4**A**). However, it is crucial that the mutation in the protein only affects the binding of the orthogonal compound, but does not alter the function of the protein in any other way. On the other hand, when the engineered lock no longer accepts the natural ligand, the target protein itself becomes orthogonal (Figure 3.4**B** and 3.4**C**).

Since the pioneering work of Hwang and Miller[28] numerous ligand-receptor, protein-protein interaction and enzymatic systems have been studied using orthogonal chemical genetic techniques.[26,27,29]

3.2.2 Receptors activated solely by synthetic ligands (RASSL)

GPCRs control many physiological processes and therefore constitute an important class of therapeutically interesting targets (see above).[2] Although, many (specific) ligands for these receptors are known, the (chemical) control of GPCRs is complicated by the presence of endogenous ligands, that can activate or inhibit signalling events. To simplify the study of individual GPCRs, Conklin and co-workers[30] started to use engineered receptors that respond only to synthetic ligands (RASSLs) and not to their endogenous native ligands.

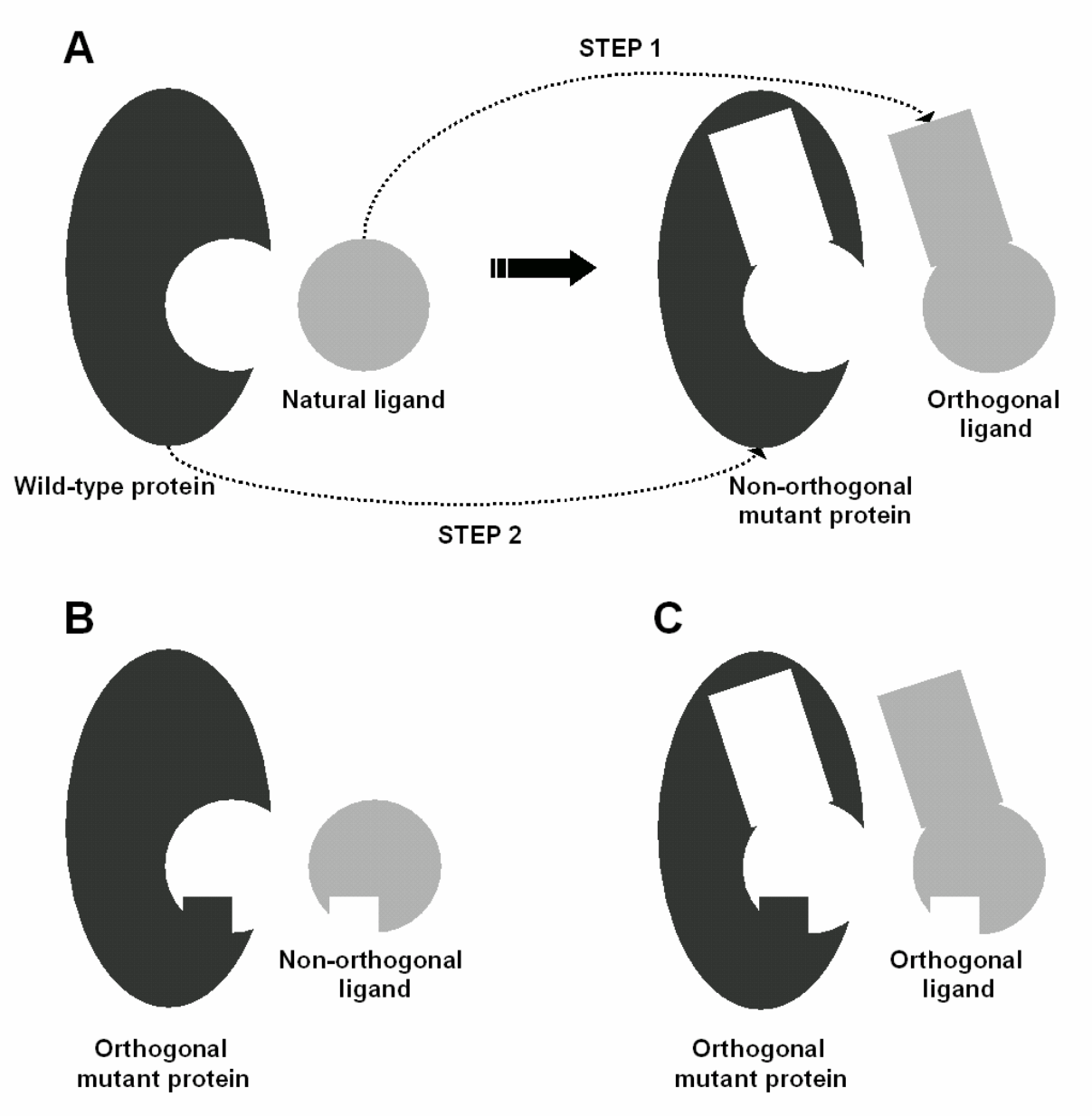

Figure 3.4 Definition of orthogonal ligands and proteins. **A** Step 1; a (small) molecule that binds to the protein of interest, i.e. the "key", is synthetically modified to eliminate its ability to bind to its wild- type target. Step 2; the (protein) target of interest, i.e. the "lock", is engineered to accept the orthogonal compound. **B** and **C** When the engineered lock no longer accepts the natural ligand, the target protein itself becomes orthogonal.

With the "neoceptor-neoligand" approach,[23] we envisaged to take the RASSL concept a step further by preparing synthetic ligands that are orthogonal, i.e. unresponsive, towards (ideally all) endogenous GPCRs. Using the adenosine receptor family as a model system the selective stimulation of an engineered (H272E) adenosine A_3AR mutant by synthetic (3'-modified) adenosine analogues was investigated. With ongoing efforts to further improve the potency and selectivity

of these A_3AR ligands, this RASSL approach can become a powerful method for functional validation of GPCRs.

Similar chemical genetic strategies have been reported for the design and synthesis of ligands for engineered nuclear hormone receptors, a family of transcriptional regulators that have both DNA binding and ligand-dependent transactivation properties.[31] We are convinced that the development of orthogonal ligand-receptor pairs will become important tools for the selective stimulation of a single member in a large family of receptors (whether GPCRs or other receptors).

3.3 References

[1] Lander, E. S. *et al. Nature* **2001**, *409*, 860.

[2] Bleicher, K. H.; Böhm, H.-T.; Müller, K.; Alanine, A. I. *Nature Rev. Drug Disc.* **2003**, *2*, 369.

[3] (i) Moro, S; Deflorian, F.; Spalluto, G.; Pastorin, G.; Cacciari, B.; Kim, S.-K.; Jacobson, K. A. *Chem. Commun.* **2003**, 2949. (ii) Klabunde, T.; Hessler, G. *Chembiochem.* **2002**, *10*, 928.

[4] Bondensgaard, K.; Ankersen, M.; Thogersen, H.; Hansen, B. S.; Wulff, B. S.; Bywater, R. P. *J. Med. Chem.* **2004**, *47*, 888.

[5] Palczewski, K.; Kumasaka, T.; Hori, T.; Behnke, C. A.; Motoshima, H.; Fox, B. A.; Le Trong, I.; Teller, D. C.; Okada, T.; Stenkamp, R. E.; Yamamoto, M.; Miyano, M. *Science* **2000**, *289*, 739.

[6] Unger, V. M.; Hargrave, P. A.; Baldwin, J. M.; Schertler, G. F. *Nature* **1997**, *389*, 203.

[7] Henderson, R.; Baldwin, J. M.; Ceska, T. A.; Zemlin, F.; Beckmann, E.; Downing, K. H. *J. Mol. Biol.* **1990**, *213*, 899.

[8] (i) Sakmar, T. P. *Curr. Opin. Cell Biol.* **2002**, *14*, 189. (ii) Becker, O. M.; Shacham, S.; Marantz, Y.; Noiman, S. *Curr. Opin. Drug Disc. Dev.* **2003**, *6*, 353. (iii) Archer, E.; Maigret, B.; Escrieut, C.; Pradayrol, L.; Fourmy, D. *Trends Pharmacol. Sci.* **2003**, *24*, 36. (iv) Bissantz, C.; Bernard, P.; Hibert, M.; Rognan, D. *Proteins Struct. Funct. Gen.* **2003**, *50*, 5-25. (v) Filipek, S.; Teller, D. C.; Palczewski, K.; Stenkamp, R. *Annu. Rev. Biophys. Biomol. Struct.* **2003**, *32*, 375. (vi) Oliveira, L.; Hulsen, T.; Hulsik, D. L.; Paiva, A. C. M.; Vriend, G. *FEBS Lett.* **2004**, *564*, 269.

[9] Shacham, S.; Topf, M.; Avisar, N.; Glaser, F.; Marantz, Y.; Bar-Haim, S.; Noiman, S.; Naor, Z.; Becker, O. M. *Med. Res. Rev.* **2001**, *21*, 472.

[10] Okada, T.; Palczewski, K. *Curr. Opin. Struct. Biol.* **2001**, *11*, 420.

[11] Gershengorn, M. C.; Osman, R. *Endocrinology* **2001**, *142*, 2.

[12] Fredholm, B. B.; IJzerman, A. P.; , Jacobson, K. A.; Klotz, K.-N.; Linden, J. *Pharmacol. Rev.* **2001**, *53*, 527.

[13] Klinger, M.; Freissmuth, M.; Nanoff, C. *Cell. Signalling* **2002**, *14*, 99.

[14] (i) Müller, C. E. *Curr. Topics Med. Chem.* **2003**, *3*, 445. (ii) Fishman, P.; Bar-Yehuda, S. *Curr. Topics Med. Chem.* **2003**, *3*, 463.

[15] Barbhaiya, H.; McClain, R.; Ijzerman, A. P.; Rivkees, S. A. *Mol. Pharmacol.* **1996**, *50*, 1635.

[16] Tucker, A. L.; Robeva, A. S.; Taylor, H. E.; Holeton, D.; Bockner, M.; Lynch, K. R.; Linden, J. *J. Biol. Chem.* **1994**, *269*, 27900.

[17] Kim, J.; Wess, J.; van Rhee, A. M.; Schoneberg, T.; Jacobson, K. A. *J. Biol. Chem.* **1995**, *270*, 13987.

[18] Gao, Z.-G.; Jiang, Q.; Jacobson, K. A.; IJzerman, A. P. *Biochem. Pharmacol.* **2000**, *60*, 661.

[19] Beukers, M. W.; den Dulk, H.; van Tilburg, E. W.; Brouwer, J.; IJzerman, A. P. *Mol. Pharmacol.* **2000**, *58*, 1349.

[20] Baraldi, P. G.; Cacciari, B.; Moro, S.; Romagnoli, R.; Ji, X. D.; Jacobson, K. A.; Gessi, S.; Borea, P. A.; Spalluto, G. *J. Med. Chem.* **2001**, *44*, 2735.

[21] Baraldi, P. G.; Cacciari, B.; Moro, S.; Spalluto, G.; Pastorin, G.; Da Ros, T.; Klotz, K. N.; Varani, K.; Gessi, S.; Borea, P. A. *J. Med. Chem.* **2002**, *45*, 770.

[22] Maconi, A.; Pastorin, G.; Da Ros, T.; Spalluto, G.; Gao, Z.-G.; Jacobson, K. A.; Baraldi, P. G.; Cacciari, B.; Varani, K.; Moro, S.; Borea, P. A. *J. Med. Chem.* **2002**, *45*, 3579.

[23] (i) Jacobson, K.A.; Gao, Z.-G.; Chen, A.; Barak, D.; Kim, S.-A.; Lee, K.; Link, A.; Van Rompaey, P.; Van Calenbergh, S.; Liang, B.T. *J. Med. Chem.* **2001**, *44*, 4125. (ii) Jacobson, K. A.; Kim, H. S.; Ravi, G.; Kim, S.-K.; Lee, K.; Chen, A.; Chen, W.; Barak, D.; Liang, B. T.; Gao, Z.-G. *Drug Dev. Res.* **2003**, 58, 330.

[24] Gao, Z.-G.; Chen, A.; Barak, D.; Kim, S. K.; Muller, C. E.; Jacobson, K. A. *J. Biol. Chem.* **2002**, *277*, 19056.

[25] Gao, Z.-G.; Kim, S. K.; Biadatti, T.; Chen, W.; Lee, K.; Barak, D.; Kim, S. G.; Johnson, C. R.; Jacobson, K. A. *J. Med. Chem.* **2002**, *45*, 4471.

[26] (i) Alaimo, P. J.; Shogren-Knaak, M. A.; Shokat, K. M. *Curr. Opin. Chem. Biol.* **2001**, *5*, 360. (ii) Shokat, K. M.; Velleca, M. *Drug Discovery Today* **2002**, *7*, 872.

[27] Bishop, A.; Buzko, O.; Heyeck-Dumas, S.; Jung, I.; Kraybill, B.; Liu, Y.; Shah, K.; Ulrich, S.; Witucki, L.; Yang, F.; Zhang, C.; Shokat, K. M. *Annu. Rev. Biophys. Biomol. Struct.* **2000**, *29*, 577.

[28] Hwang, Y. W.; Miller, D. L. *J. Biol. Chem.* **1987**, *262*,13081.

[29] (i) Specht, K. M.; Shokat, K. M. *Curr. Opin. Cell Biol.* **2002**, *14*, 155. (ii) Mayer, T. U. *Trends Cell Biol.* **2003**, *13*, 270.

[30] (i) Coward, P.; Wada, H. G.; Falk, M.S.; Chan, S. D. H.; Meng, F.; Akil, H.; Conklin, B. R. *Proc. Natl. Acad. Sci. USA* **1998**, *95*, 352. (ii) Redfern, C. H.; Coward, P.; Degtyarev, M. Y.; Lee, E. K.; Kwa, A. T.; Hennighausen, L.; Bujard, H.; Fishman, G. I.; Conklin, B. R. *Nat. Biotechnol.* **1999**, *17*, 165.

[31] (i) Koh, J. T.; Putnam, M.; Tomic-Canic, M.; McDaniel, C. M. *J. Am. Chem. Soc.* **1999**, *121*, 1984. (ii) Ye, H. F.; O'Reilly, K. E.; Koh, J. T. *J. Am. Chem. Soc.* **2001**, *123*, 1521. (iii) Tedesco, R.; Thomas, J. A.; Katzenellenbogen, B. S.; Katzenellenbogen, J. A. *Chem. Biol.* **2001**, *8*, 277. (iv) Shi, Y.; Koh, J. T. *Chem. Biol.* **2001**, *8*, 501. (v) Swann, S. L.; Bergh, J. J.; Farach-Carson, M. C.; Koh, J. T. *Org. Lett.* **2002**, *4*, 3863. (vi) Swann, S. L.; Bergh, J. J.; Farach-Carson, M. C.; Ocasio, C. A.; Koh, J. T. *J. Am. Chem. Soc.* **2002**, *124*, . (vii) Shi, Y.; Koh, J. T. *J. Am. Chem. Soc.* **2002**, *124*, 6921.

[32] van Rhee, A. M.; Jacobson, K. A. *Drug. Dev. Res.* **1996**, *37*, 1.

CHAPTER 4

EXPLORING HUMAN ADENOSINE A_3AR COMPLEMENTARITY AND ACTIVITY FOR ADENOSINE ANALOGUES MODIFIED IN THE RIBOSE AND PURINE MOIETY

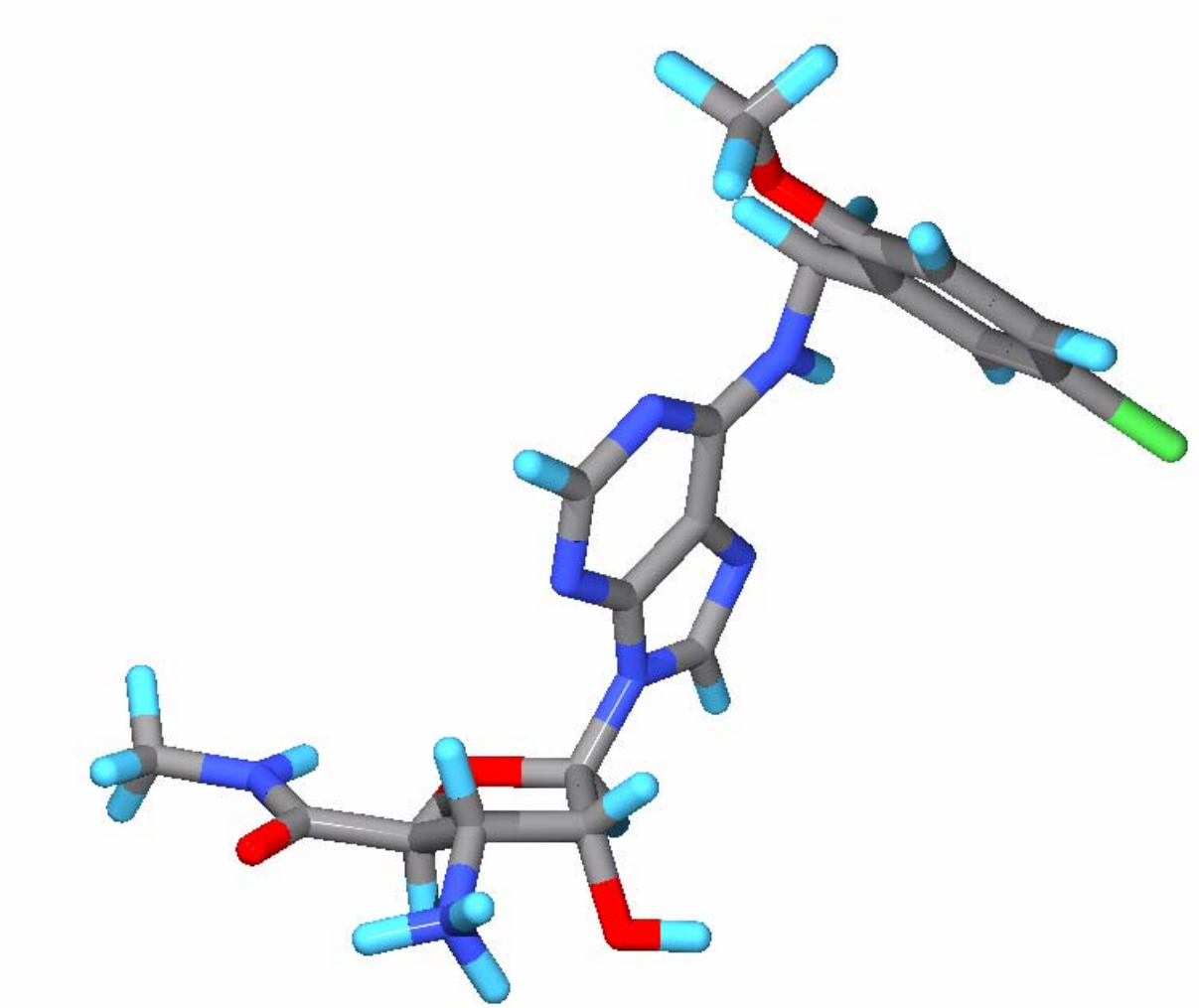

This chapter is published in part in:

Philippe Van Rompaey, Kenneth A. Jacobson, Ariel S. Gross, Zhan-Guo Gao, and Serge Van Calenbergh

Bioorg. Med. Chem. **2004**, *Accepted*.

4.1 Introduction

G protein-coupled receptors (GPCRs) with their typical seven-helix transmembrane (7TM) domains, constitute a large group of integral membrane proteins. Interacting with structurally diverse extracellular signals, GPCRs provide a molecular link for activation (or inhibition) of intracellular processes via given signal transduction pathways[1] and represent the most prominent family of validated drug targets.[2]

The regulatory actions of adenosine are mediated by four subtypes of GPCRs called adenosine receptors (ARs) that are ubiquitously expressed in the body and can be distinguished as A_1, A_{2A}, A_{2B} and A_3 receptors.[3] Activation of the A_3AR subtype, which is distributed in various organs (lung, liver, kidney, heart and brain)[4] has been shown to mediate adenylate cyclase inhibition[5] and phospholipase C[6] and D[7] stimulation. All four AR subtypes have been characterised on a pharmacological level as well as on a molecular level.[8] ARs from different species show a high amino acid sequence homology (82-93%) with the only exception being the A_3AR subtype, which only exhibits 74% primary sequence homology between rat and human or sheep.[9-10]

To be of therapeutic value, synthetic AR ligands need to be highly selective for a given receptor subtype and tissue targeted. Although several agonists have been synthesized that are selective for the known ARs subtypes,[3,11] so far the only AR agonist approved for clinical use is adenosine itself. Here we focus on the human (h)A_3AR subtype, the most recently identified member of the AR family.[12-14]

The A_3AR plays a crucial role in some of the physiological effects of adenosine.[15,16] In addition to cardio-[17-19] and cerebroprotective effects,[20,21] hA_3AR agonists may be therapeutically useful for the treatment of stroke,[22] inflammation[23] and in cancer therapy.[24] While full agonists maximally stimulate the receptor, partial agonists show reduced intrinsic activity, may exhibit fewer side effects[25,26] and may induce less receptor down-regulation and desensitisation than full agonists.[15] Partial A_3AR agonists can act as cardioprotective agents.[27] Selective antagonists for the A_3AR promise to be useful in the regulation of cell growth[28,29] and as anti-asthmatic,[30] cerebroprotective[20,31] and anti-inflammatory agents.[32]

Since its discovery in 1991,[12] the development of agonists of the A_3AR has been an active area of research. Many variations have been made on the adenosine scaffold in view of potent and selective A_3AR binding.[11,15,33] Generally, substitution at the 2'- and 8- positions has affinity- and efficacy-lowering effects.[11,15] Known A_3AR-selective alterations relevant to our work are N^6-modifications, such as 3-iodobenzyl (IB)[11,15,33,34] or 5-chloro-2-methoxybenzyl (CMB),[35] and smaller substituents like a Cl or CN at the 2-position[33-35] of the purine moiety. Both the 2- and N^6-purine modifications have been described with and without the 5'-methylcarbamoyl (MEC)[33] insertion in the nucleoside sugar moiety. Combinations of these groups are often additive in their potency enhancement and resulted in potent and moderately selective A_3AR agonists, such as Cl-IB-MECA and IB-MECA,[36] which are still used as reference tools for pharmacological study of the A_3AR.

Investigated to a lesser extent are 3'-modifications of the ribofuranosyl moiety.[37,38] We and others have shown that a 3'-amino substitution opens perspectives towards influencing the hA_3AR selectivity.[39,40] This stimulated us to investigate the effect on both affinity and efficacy of this 3'-amino modification when combined with the above mentioned variations at the 5'-, 2- and N^6-positions (Figure 4.1, derivatives **14**, **16** and **19**). By introducing an α-oriented methylene spacer (the so-called branching) between the 3'-carbon of the ribofuranosyl moiety and the amine function (Figure 4.1, derivatives **5**-**8**, **15** and **20**), we aimed to modulate the hydrogen bond donating effects of the 3'-amine, known to be crucial from our neoceptor work (Chapters 5 and 6).[39,41] We wanted to provide more insight into the effect of 3', 5', 2- and N^6-positional variations of the adenosine scaffold on hA_3AR affinity and to investigate the impact of such a combined substitution pattern on the hA_3AR efficacy.

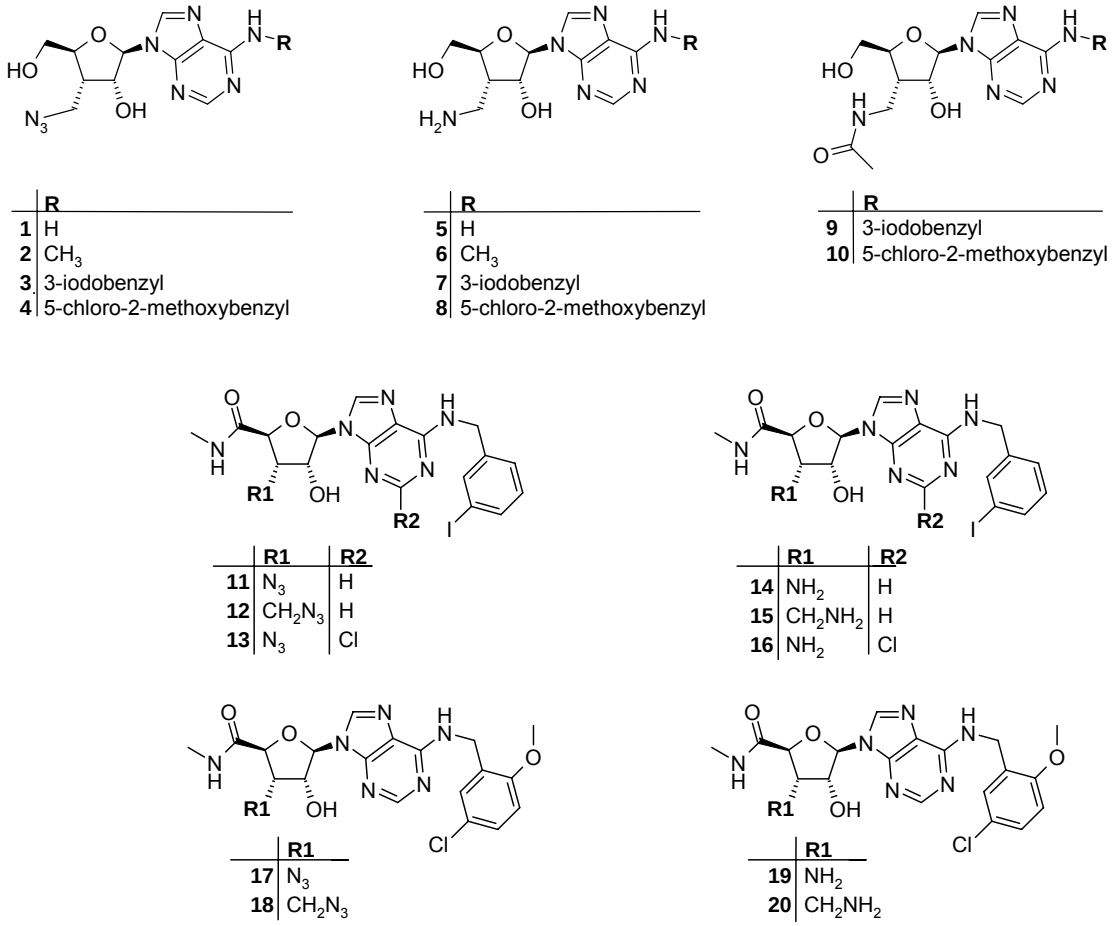

Figure 4.1 3', 5', 2- and N^6-modified adenosine analogues discussed in this Chapter.

4.2 Results and discussion

4.2.1 Chemistry

The synthesis of the 3', 5', 2- and N^6-substituted adenosine analogues **1**-**20** is described in Part I.

4.2.2 Biological activity

All analogues evaluated (i.e. **1**-**20**) are depicted in Figure 4.1. Modifications of the adenosine scaffold known to increase hA_3AR binding affinity and selectivity among adenosine agonists include: a 5'-uronamide moiety (as in **11**-**20**) and substitutions at

the 2- (as in **13** and **16**) and N^6-positions (as in **2**-**4** and **6**-**20**). We investigated the influence on hA_3AR affinity and intrinsic activity of combining these 5', 2- and N^6-modifications with the amino(methyl) substitution at the 3'-position that we[39,41] and others[40] recently reported.

Generally, substitution of the 2'- and 3'-hydroxyl groups of the ribofuranose moiety of AR agonists has been avoided. It has been demonstrated that modification of the 2'-position, compared to the 3'-position, had a negative impact on both potency and intrinsic activity.[37,38,42] However, a 3'-amino modification was recently shown to be beneficial for hA_3AR selectivity depending on the overall substitution pattern of the adenosine nucleoside.[40] This prompted us to investigate the boundaries of this 3'-amino substitution by insertion of a methylene spacer between the ribofuranose ring and the amine functional group.

4.2.2.1 Affinity and Selectivity

Looking at the analogues that exhibited < 1 μM affinities (in Table 4.1), it was clear that the 5'-uronamide modification for both the direct and branched-chain amine (as in **11**-**20** vs. **1**-**10**) improved the overall affinity. With exception of **3** and **7**, all compounds evaluated showed very good selectivity for the hA_3AR subtype. In the simple 3'-amino series the most potent compound **19** (K_i = 27 nM) showed a 300-fold selectivity over the A_1AR, compared to a 22-fold selectivity for its N^6-iodobenzyl substituted analogue **14**. Introduction of a chloro atom at the 2-position resulted in the selective and moderately potent (K_i = 132 nM) partial agonist **16**. All branched-chain analogues on the other hand had a good hA_3AR selectivity profile, but displayed weak binding characteristics, e.g. analogue **20** with a K_i of 557 nM having the highest affinity in this series. Introduction of the methylene spacer also affected intrinsic activity (see section 4.2.2.2.). In both the 3'-amino and 3'-aminomethyl series the affinity of the azido precursors was lower. This affinity difference was striking especially for the N^6-iodobenzyl substituted analogues: **11** (K_i = 2260 nM) vs. **14** (K_i = 137 nM) and **13** (K_i = 4270 nM) vs. **16** (K_i = 132 nM).

Table 4.1. Binding affinity (A_1AR, A_{2A}AR, or A_3AR) or functional activation (A_{2B}AR and A_3AR) of the adenosine derivatives at human adenosine receptors, n = 3 , unless noted.

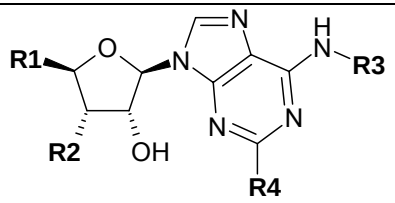

Compound	R1	R2	R3	R4	hA_1AR[a]	$hA_{2A}AR$[b]	$hA_{2B}AR$[c]	hA_3AR[d]	cAMP hA_3AR[g]
h	CH_2OH	NH_2	H	H	14%	6%	---	442,000±121,000	53±5
1	CH_2OH	CH_2N_3	H	H	25%	38%	---	53±1%	1.1±0.9
5	CH_2OH	CH_2NH_2	H	H	39%	33%	---	43±1%	23±8
2	CH_2OH	CH_2N_3	CH_3	H	69%	51%	---	20,600[e]	2.7±1.6
6	CH_2OH	CH_2NH_2	CH_3	H	42%	22%	---	48±3%	48±6
h	CH_2OH	NH_2	3-IB	H	93%	70%	---	870±180	---
3	CH_2OH	CH_2N_3	3-IB	H	27%	28%	---	61±1%	6.8±1.7
7	CH_2OH	CH_2NH_2	3-IB	H	72%	22%	---	8700[e]	9.2±2.1
9	CH_2OH	CH_2NHAc	3-IB	H	38%	0%	---	31,500[e]	20±5
8	CH_2OH	CH_2NH_2	CMB	H	61%	20%	0%	13,800±1400	18±3
10	CH_2OH	CH_2NHAc	CMB	H	---	---	---	4%[f]	1.4±0.2
11	MeUron	N_3	3-IB	H	64%	32%	0%	2260±480	0
14	MeUron	NH_2	3-IB	H	3080±380	67%	20%	137±41	37±5
12	MeUron	CH_2N_3	3-IB	H	24%	0%	0%	23±1%	23±4
15	MeUron	CH_2NH_2	3-IB	H	52%	6%	0%	1690±330	17±2
13	MeUron	N_3	3-IB	Cl	70%	29%	0%	4270±1400	0
16	MeUron	NH_2	3-IB	Cl	73%	50%	0%	132±60	30±6
17	MeUron	N_3	CMB	H	66%	34%	13%	376±83	0
19	MeUron	NH_2	CMB	H	8190±750	49%	7%	27±11	51±4
18	MeUron	CH_2N_3	CMB	H	54%	43%	19%	755±40	0
20	MeUron	CH_2NH_2	CMB	H	52%	2%	2%	557±164	30±6

[a] K_i (nM) or % inhibition of binding at 100 μM ([^{3}H]R-PIA, 2.0 nM) in CHO cells expressing hA_1AR. [b] % inhibition of binding at100 μM ([^{3}H]CGS21680,15 nM) in HEK-293 cells expressing $hA_{2A}AR$. [c] % activation (cAMP assay) at100 μM in CHO cells expressing $hA_{2B}AR$ (NECA is 100%). [d] K_i (nM) or % inhibition at 100 μM ([^{125}I]I-AB-MECA, 0.5 nM) in CHO cells expressing hA_3AR, unless noted. [e] n = 1. [f] at 10 μM. [g] Inhibition at 100 μM of forskolin-stimulated cAMP production at 10 μM, in CHO cells expressing the hA_3AR, as a percentage of the response of the full agonist Cl-IB-MECA (n=2). [h] affinities previously reported in ref. 39.

Focusing on the N^6-substituents, known to be important for hA_3AR selectivity,[36] we observed a difference between the 3'-amino and branched-chain 3'-aminomethyl series, depending on the modification at the 5'-position. In the 5'-hydroxy 3'-amino series, 3'-amino-N^6-iodobenzyladenosine (K_i = 870 nM) showed a significant 500-fold potency enhancement compared to 3'-aminoadenosine (K_i = 442 μM). In the 5'-hydroxy branched-chain series (as in **1**-**10**), however, contrary to what we recently reported for simple N^6-substituted adenosine analogues,[35] N^6-(5-chloro-2-methoxybenzyl) substitution (as in **8**, K_i = 13.8 μM) did not improve affinity over the N^6-iodobenzyl modification (as in **7**, K_i = 8.7 μM). The reduction of hA_3AR affinity upon acetamide formation (as in analogues **9** and **10**) indicated that introduction of a 3'-branching was the sterically maximal allowed modification.

In the 5'-uronamide series, both for the 3'-amino and branched-chain 3'-aminomethyl analogues, the influence of N^6-substitution on hA_3AR binding was consistent with our previous findings,[35] i.e. N^6-iodobenzyl (as in **14**, **15** and **16** with K_i = 137 nM, 1.7 μM and 132 nM respectively) was less affinity-enhancing than N^6-(5-chloro-2-methoxybenzyl) (as in **19** and **20** with K_i = 27 nM and 557 nM respectively).

4.2.2.2 Intrinsic activity

The results of the cyclic AMP-assay (in Table 4.1) indicated that all analogues were strong partial agonists at best. In the simple 5'-hydroxy 3'-amino series, 3'-aminoadenosine and 3'-amino-N^6-iodobenzyladenosine are known full agonists.[39] The 5'-uronamide analogues **14** and **19** were partial agonists, contrary to what was reported earlier.[40]

In the 3'-branched-chain series, comparison of the 5'-hydroxy derivatives **3**, **7** and **9** with the 5'-uronamides **12**, **15** and **20**, demonstrated a moderate influence of the 5'-methyluronamide modification on intrinsic activity. Thus, in general, introduction of a 3'-branching reduced the efficacy and, contrary to efficacy-reducing substitutions at the 2- and N^6-positions,[33,38] this effect could only partially be overcome by modification of the 5'-position.

A modification known to have contradictory effects on A_3AR binding and intrinsic activity is the introduction of a chlorine at the 2-position.[33] Comparing **14** with the 2-chloro substituted **16**, this modification did not alter the affinity nor the efficacy in this series.

An overall conclusion is that, contrary to the 3'-aminomethyl modification, the simple 3'-amino is better tolerated in terms of affinity and efficacy, resulting at best in (strong) partial agonists with moderate binding properties (as in analogues **14**, **16** and **19**) and low hA_3AR affinity antagonists for the branched-chain derivatives, with exception of **20**. In both series, the azido precursors (as in compounds **1**-**3**, **11**-**13, 17** and **18**) were full antagonists.

The 3'-amino modification has hydrogen bond donor properties like the 3'-hydroxyl group,[33,39] whereas for the 3'-azido, like the 3'-F,[37] this hydrogen bond pattern is no longer possible, resulting in a drop of efficacy.[38] For the branched-chain series, this difference in efficacy between the 3'-azidomethyl and 3'-aminomethyl analogues was less clear, which is most likely due to the steric impact of this modification.

4.3 Conclusion

From a pharmacological point of view the modulation of hA_3AR activity by selective agonists, partial agonists and antagonists is very important. We investigated the influence on affinity, selectivity and intrinsic activity of combined modifications at the 3'- and 5'-positions of the ribofuranosyl moiety with purine modifications at the 2- and N^6-positions. Various synthetic analogues displayed good hA_3AR selectivity and moderate-to-high affinities. More interesting, however, was the ability to tune the efficacy depending on the substituent introduced at the 3'-position. A 3'-amino function (as in **14**, **16** and **19**) resulted in (strong) partial agonist activity, whereas the azide precursors (as in **11**, **13** and **17**) converted these analogues into antagonists. Introduction of a methylene spacer between these functionalities and the ribofuranose ring (as in **1**-**10**, **12**, **15**, **18** and **20**) had an overall efficacy- and affinity-lowering effect.

The (branched-chain) amino and azido modifications at the 3'-position presented here, open interesting perspectives towards tuning the efficacy and selectivity for the A_3AR, starting from the adenosine agonist scaffold. Several analogues also represent valuable tools for the further exploration of the neoceptor concept, i.e. investigation of molecular complementarity at mutant A_3 (Chapter 5)[39] and mutant A_{2A} (Chapter 6)[41] adenosine receptors.

4.4 Experimental Part

*Biological evaluation was performed by the group of Dr. Kenneth A. Jacobson, at the Laboratory for Bioorganic Chemistry (NIDDK), NIH, Maryland, USA. For the detailed procedures on cell culture and membrane preparation, the binding assay and cyclic AMP accumulation assay we refer to the experimental part in our Bioorg. Med. Chem. research paper (**2004**, in press).*

4.5 References

[1] Gether, U. *Endocr. Rev.* **2000**, *21*, 90.

[2] Ballesteros, J. M.; Palczewski, K. *Curr. Opin. Drug Discov. Dev.* **2001**, *4*, 561.

[3] Fredholm, B. B.; IJzerman, A. P.; , Jacobson, K. A.; Klotz, K.-N.; Linden, J. *Pharmacol. Rev.* **2001**, *53*, 527.

[4] Salvatore, C. A.; Jacobson, M. A.; Taylor, H. E.; Linden, J.; Johnson, R. G. *Proc. Natl. Acad. Sci. U.S.A.* **1993**, *90*, 10365.

[5] Jacobson, K. A.; Suzuki, F. *Drug. Dev. Res*. **1996**, *39*, 289.

[6] Abbracchio, M. P.; Brambilla, R.; Kim, H. O.; von Lubitz, D. K. J. E.; Jacobson, K. A.; Cattabeni, F. *Mol. Pharmacol*. **1995**, *48*, 1083.

[7] Ali, H.; Choi, O. H.; Fraundorfer, P. F.; Yamada, K.; Gonzaga, H. M. S.; Beaven, M. A. *J. Pharmacol. Exp. Ther*. **1996**, *276*, 837.

[8] Collis, M. G.; Hourani, S. M. O. Adenosine receptor subtypes. *Trends Pharmacol. Sci.* **1993**, *14*, 360.

[9] Linden, J.; Taylor, H. E.; Robeva, A. S.; Tucker, A. L.; Stehle, J. H.; Rivkees, S. A.; Fink, J. S.; Reppert, S. M. *Mol. Pharmacol*. **1993**, *44*, 524.

[10] Ji, X.-D.; von Lubitz, D.; Olah, M. E.; Stiles, G. L.; Jacobson, K. A. *Drug Dev. Res*. **1994**, *33*, 51.

[11] Müller, C. E. *Curr. Med. Chem.* **2000**, *7*, 1269.

[12] Meyerhof, W.; Muller-Brechlin, R.; Richter, D. *FEBS Lett.* **1991**, *284*, 155.

[13] Zhou, Q. Y.; Li, C.; Olah, M. E.; Johnson R. A.; Stiles, G. L.; Civelli, O. *Proc. Natl. Acad. Sci. USA* **1992**, *89*, 7432.

[14] Salvatore, C. A.; Jacobson, M. A.; Taylor, H. E.; Linden, J.; Johnson, R. *Proc. Natl. Acad. Sci. USA* **1993**, *90*, 10365.

[15] Müller, C. E. *Curr. Topics Med. Chem.* **2003**, *3*, 445.

[16] Fishman, P.; Bar-Yehuda, S. *Curr. Topics Med. Chem.* **2003**, *3*, 463.

[17] Stambaugh, K.; Jacobson, K. A.; Jiang, J. L.; Liang, B. T. *Am. J. Physiol.* **1997**, *273*, H501.

[18]Liang, B. T.; Jacobson, K. A. *Proc. Natl. Acad. Sci. USA* **1998**, *95*, 6995.

[19] Liang, B. T.; Jacobson, K. A. *Curr. Pharm. Des.* **1999**, *5*, 1029.

[20] von Lubitz, D. K.; Lin, R. C.; Popik, P.; Carter, M. F.; Jacobson, K. A. *Eur. J. Pharmacol.* **1994**, *263*, 59.

[21] von Lubitz, D. K.; Lin, R. C.; Boyd, M.; Bischofberger, N.; Jacobson, K. A. *Eur. J. Pharmacol.* **1999**, *367*, 157.

[22] Jacobson, K. A. *Trends in Pharmacol. Sci.* **1998**, *19*, 184.

[23] Singer, B. F.; Fotheringham, J. A.; Mayne, M. B.; Geiger, J. D. *FASEB J.* **2001**, *15* A566.

[24] Ohana, G.; Bar-Yehuda, S.; Barer, F.; Fishman, P. *J. Cell. Physiol.* **2001**, *186*, 19.

[25] Volpini, R.; Camaioni, E.; Costanzi, S.; Vittori, S.; Klotz, K.-N.; Cristalli, G.; *Nucleosides Nucleotides* **1999**, *18*, 2511.

[26] Clarke, W. P.; Bond, R. A. *Trends Pharmacol. Sci.* **1999**, *19*, 270.

[27] Jacobson, K. A.; Kim, H. S.; Ravi, G.; Kim, S. K.; Lee, K.; Chen, A.; Chen, W.; Kim, S. G.; Barak, D.; Liang, B. T.; Gao, Z.-G. *Drug Dev. Res.* **2003**, *58*, 330.

[28] Jacobson, K. A.; Moro, S.; Kim, Y. C.; Li, A. H. *Drug Dev. Res.* **1998**, *45*, 113.

[29] Brambilla, R.; Cattabeni, F.; Ceruti, S.; Barbieri, D.; Franceshi, C.; Kim, Y.; Jacobson, K. A.; Klotz, K. N.; Lohse, M. J.; Abbracchio, M. P. *Naunyn-Schmiedeberg's Arch. Pharmacol.* **2000**, *361*, 225.

[30] Beaven, M. A.; Ramkumar, V.; Ali, H. *Trends Pharmacol. Sci.* **1994**, *15*, 13.

[31] von Lubitz, D. K. J. E.; Carter, M. F.; Deutsch, S. I.; Lin, R. C. S.; Mastropaolo, J.; Meshulam, Y.; Jacobson, K. A. *Eur. J. Pharmacol.* **1995**, *275*, 23.

[32] Ramkumar, V.; Stiles, G. L.; Beaven, M. A.; Ali, H. *J. Biol. Chem.* **1993**, *268*, 16887.

[33] Gao, Z.-G.; Kim, S.-K.; Biadatti, T.; Chen, W.; Lee, K.; Barak, D.; Kim, S. G.; Johnson, C. R.; Jacobson, K. A. *J. Med. Chem.* **2002**, *45*, 4471.

[34] Gao, Z.-G.; Blaustein, J. B.; Gross, A. S.; Melman, N.; Jacobson, K. A. *Biochem. Pharmacol.* **2003**, *65*, 1675.

[35] Ohno, M.; Gao, Z.-G.; Van Rompaey, P.; Tchilibon, S.; Kim, S.-K.; Harris, B. A.; Gross, A. S.; Duong, H. T.; Van Calenbergh, S.; Jacobson, K. A. *Bioorg. Med. Chem.* **2004**, *12*, 2995.

[36] Kim, H. O.; Ji, X.-D.; Siddiqi, S. M.; Olah, M. E.; Stiles, G. L.; Jacobson, K. A. *J. Med. Chem.* **1994**, *37*, 3614.

[37] Lim, M. H.; Kim, H. O.; Moon, H. R.; Lee, S. J.; Chun, M. W.; Gao, Z.-G.; Melman, N.; Jacobson, K. A.; Kim, H. K.; Jeong, L. S. *Bioorg. Med. Chem. Lett.* **2003**, *13*, 817.

[38] Gao, Z.-G.; Jeong, L. S.; Moon, H. R.; Kim, H. O.; Choi, W. J.; Shin, D. H.; Elhalem, E.; Comin, M. J.; Melman, N.; Madedova, L.; Gross, A. S.; Rodriguez, J. B.; Jacobson, K. A. *Biochem. Pharmacol.* **2004**, *67*, 893.

[39] Jacobson, K. A.; Gao, Z.-G., Chen, A.; Barak, D.; Kim, S.-A.; Lee, K.; Link, A.; Van Rompaey, P.; Van Calenbergh, S.; Liang, B. T. *J. Med. Chem.* **2001**, *44*, 4125.

[40] DeNinno, M. P.; Masumane, H.; Chenard, L. K.; DiRico, K. J.; Eller, C.; Etienne, J. B.; Tickner, J. E.; Kennedy, S. P.; Knight, D. R.; Kong, J.; Oleynek, J. J.; Tracey, W. R.; Hill, R. J. *J. Med. Chem.* **2003**, *46*, 353.

[41] Kim, S.-K.; Gao, Z.-G.; Van Rompaey, P.; Gross, A. S.; Chen, A.; Van Calenbergh, S.; Jacobson, K. *J. Med. Chem.* **2003**, *46*, 4847.

[42] Kim, H. O.; Park, J. G.; Moon, H. R.; Gunaga, P.; Lim, M. H.; Chun, M. W.; Jacobson, K. A.; Kim, H.-D.; Jeong, L. S. *Nucleosides Nucleotides* **2003**, *22*, 927.

CHAPTER 5

NEOCEPTOR CONCEPT BASED ON MOLECULAR COMPLEMENTARITY IN GPCRs: A MUTANT A_3AR WITH SELECTIVELY ENHANCED AFFINITY FOR AMINE-MODIFIED NUCLEOSIDES

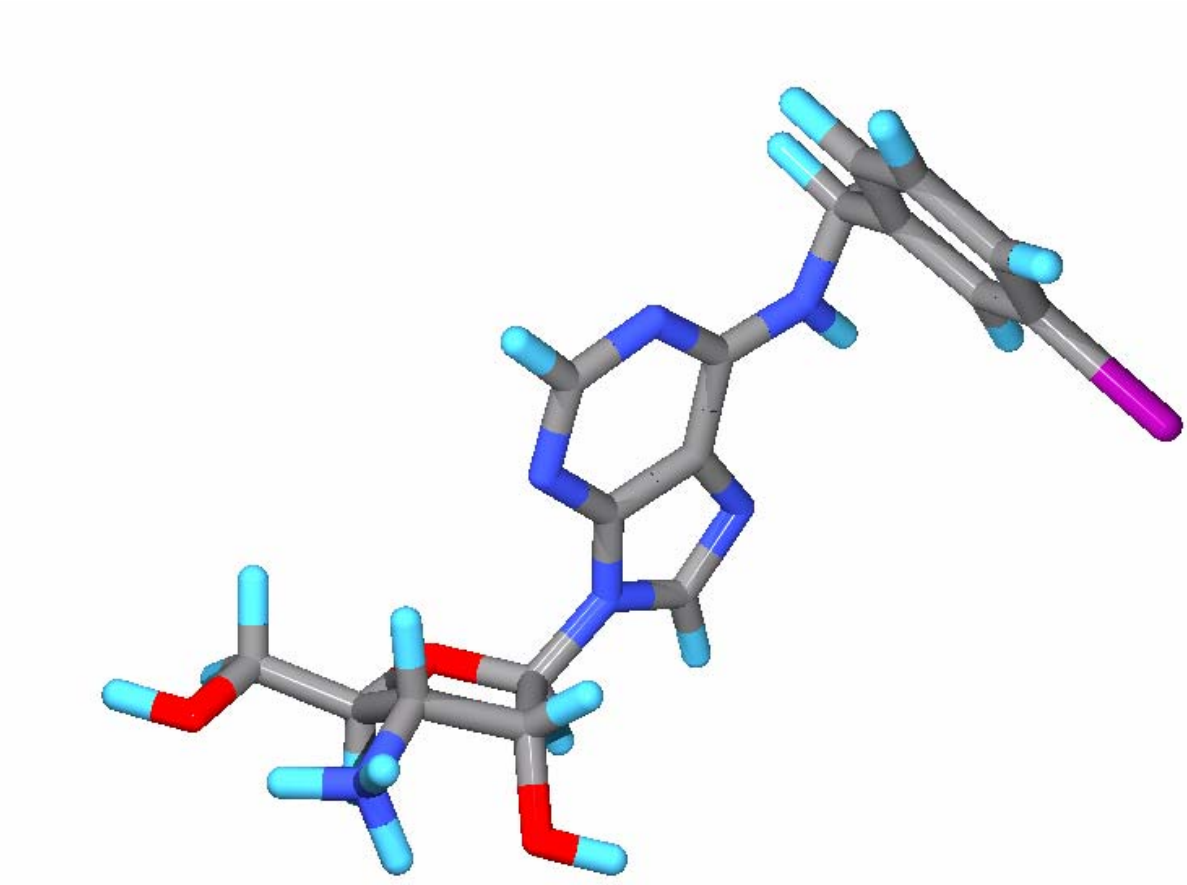

This chapter is published in part in:

Kenneth A. Jacobson, Zhan-Guo Gao, Aishe Chen, Dov Barak, Soon-Ai Kim, Kyeong Lee, Andreas Link, Philippe Van Rompaey, Serge Van Calenbergh, Bruce T. Liang

J. Med. Chem. **2001**, *44*, 4125.

5.1 Introduction

Therapeutic intervention using agonists is subject to side effects related in part to the widespread occurrence of the corresponding receptor throughout the body.[1,2] Currently, the specificity of a given drug for a target organ is usually achieved through manipulation of its pharmacokinetic properties. Past attempts to overcome this problem included generation of prodrugs that were to be preferentially activated at the target organ, either through enhanced metabolic processes or through a unique enzymatic system characteristic to the organ.[3] Our goal was to introduce and investigate a novel concept for therapeutic intervention at a specific anatomical and/or physiological locus, through a combination of receptor engineering, agonist design, and gene therapy. Elements of this potentially general approach include (a) engineering of a receptor protein to recognize synthetic ligands, for which it was selectively modified according to the molecular complementarity of the respective binding elements, while retaining its capacity for signal transduction (neoceptor); (b) synthesis of novel agonists that are not effective at the native receptor but do activate the engineered receptor (neoligand); and (c) a delivery vector to provide for selective expression of the neoceptor in the target area.

One of the numerous cases where agonist therapy has been problematic due to the widespread occurrence of receptors is the adenosine receptor (AR) family. For example, the hypotensive and bradycardiac side effects of adenosine agonists have been in part responsible for the difficulty of developing adenosine-based therapeutics for cardio- and cerebropotection.[1,3-6] The only adenosine agonist approved so far for clinical use has been adenosine itself, based on its short duration of action in the treatment of supraventricular tachycardia and in radionuclide imaging.[7] Thus, engineering of novel receptor-ligand interactions in the adenosine receptor family, through specific tailoring of both the receptors and the ligands, would provide a suitable and relevant system for investigation of the neoceptor-neoligand concept.

Adenosine is released in large amounts during ischemia and has been shown to be protective in the heart,[8] brain,[5,9] and other organs. Adenosine, when elevated prior to ischemia in cardiac tissue,[10,11] “preconditioned” the heart and protected it against injury during a subsequent period of prolonged ischemia. Synthetic agonists selective

for either A_1AR or A_3AR simulated this preconditioning effect.[12] The beneficial effects were seen following acute activation of A_1AR or chronic activation of A_3ARs. In addition to cardioprotection, adenosine A_3AR ligands have been proposed for the treatment of stroke,[13] inflammation,[14] and glaucoma.[15] In a model of global brain ischemia in gerbils, both A_1AR and A_3AR selective agonists had protective effects,[5] as judged by the histochemical and behavioral outcome following recovery. Thus, there has been much interest in the development of new therapeutic agents acting at adenosine A_3AR.

Ligand recognition in adenosine receptors, principally A_1AR and A_{2A}AR, has been extensively investigated using mutagenesis and molecular modeling.[16-20] The putative nucleoside binding site, which is highly homologous among subtypes of the adenosine receptors, is proposed to involve transmembrane helices (TMs) 3, 5, 6, and 7. Two conserved His residues (6.52 and 7.43, by the notation of van Rhee and Jacobson,[21] see p. 61) in TMs 6 and 7 of A_1AR and A_{2A}AR are considered to be among the most important amino acids involved in binding to adenosine. An assembly of aromatic amino acid side chains in the human A_{2A}AR, principally in TMs 5 and 6, is proposed to recognize the adenine moiety. The ribose moiety is likely coordinated to hydrophilic residues in TMs 3 and 7.[19,22,23] In fact, several hydroxyl-containing residues, Thr88 (3.36) and Ser277 (7.42) of the human A_{2A}AR, have been shown to be associated exclusively with agonist, but not antagonist, recognition.[19,22]

In the present study, we have utilized this hypothetical bound orientation of adenosine to identify a site on TM7 thought to be in proximity to the ribose moiety and amenable to introduction of a charged group intended for electrostatic interaction with the ligand. The site chosen was the conserved His (H272), which we have mutated to Glu. According to molecular modeling, this mutation would be expected to decrease the affinity of simple adenosine analogues,[19,23,24] except when strategically modified by the introduction of an amino group on the ribose moiety. Since alteration of the ribose moiety substitution pattern was also known to greatly diminish the affinity at adenosine receptors,[25] such substitution would ensure that the neoligand would not activate endogenous receptors at an effective concentration for the neoceptor. Our results suggested both the viability of the neoceptor-neoligand

concept and the need for further optimization of the A_3AR neoceptor-neoligand interactions.

5.2 Results

5.2.1 Design of a neoceptor: Creation of a mutant A_3AR that is activated selectively by novel agonist derivatives

On the basis of previous studies of ligand recognition in adenosine receptors,[16,19,23,24] a His residue in TM7 of the A_3AR was selected as the site for mutagenesis, i.e. the introduction of a negative charge to be complementary to an amine derivatized ligand. We examined the recognition of both known adenosine ligands (Figure 5.1) and synthetic agonist analogues (Figure 5.2) designed as neoligands, for selective recognition by the H272E mutant receptor (see below).

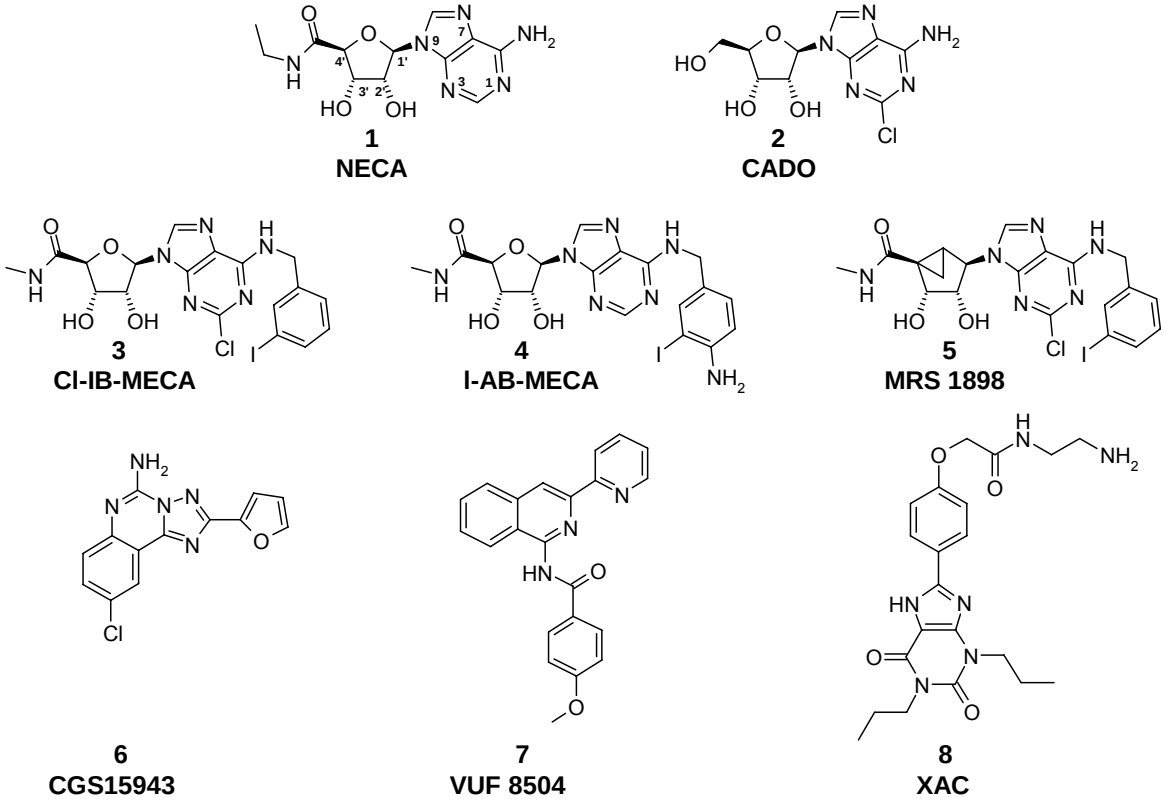

Figure 5.1 Known A_3AR agonists (**1**-**5**) and antagonists (**6**-**8**). Wild-type and mutant receptor affinities appear in Table 5.1.

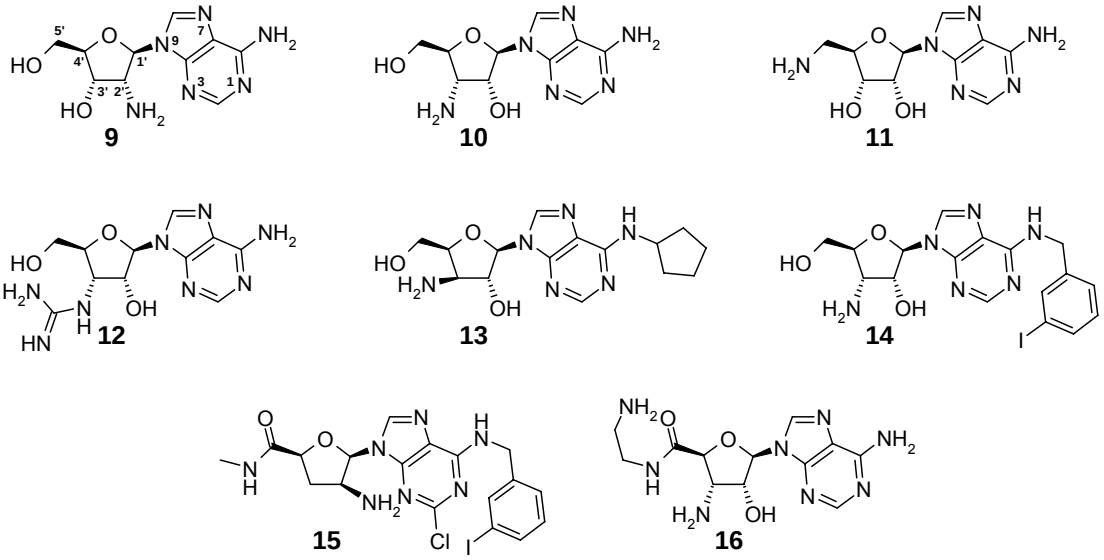

Figure 5.2 Derivatives of adenosine (**9**-**16**) tested as novel A_3AR agonists. Wild-type and mutant receptor affinities appear in Table 5.2.

5.2.2 Mutant vs wild-type A_3AR for known adenosine receptor ligands

The receptor binding affinities of various adenosine agonist and antagonist derivatives were measured in standard binding assays using wild-type and H272E mutant human A_3ARs. The high affinity of the radioligand [^{125}I]I-AB-MECA **4**[26] was retained in the mutant receptor, thus enabling the determination of the affinities of a wide range of competing ligands. K_i values for these ligands are shown in Table 5.1, and representative binding curves are shown in Figure 5.3. The closest mimic of adenosine itself was 2-chloroadenosine **2**,[27] which was 18-fold less potent in binding at the H272E mutant receptor than at the wild-type receptor.

Table 5.1 Binding affinity of known adenosine agonists and antagonists at wild-type and mutant (H272E) human A_3AR[a,b]

		K_i (nM)			K_i (nM)	
agonists		**WT**	**H272E**	**antagonists**	**WT**	**H272E**
1		169±32	3200±770	**6**	253±87	3260±994
2		650±130	11600±4200	**7**	61.7±23.4	1690±343
3		4.3±1.6	20.1±3.6	**8**	110±45	20100±4500
4	[^{125}I]AB-MECA	1.2±0.2	2.1±0.3			
5		1.6±0.3	9.9±2.6			

[a]Structures provided in Figure 5.1. [b]Results are from three independent experiments performed in duplicate, using [^{125}I]AB-MECA at a concentration of 1 nM.

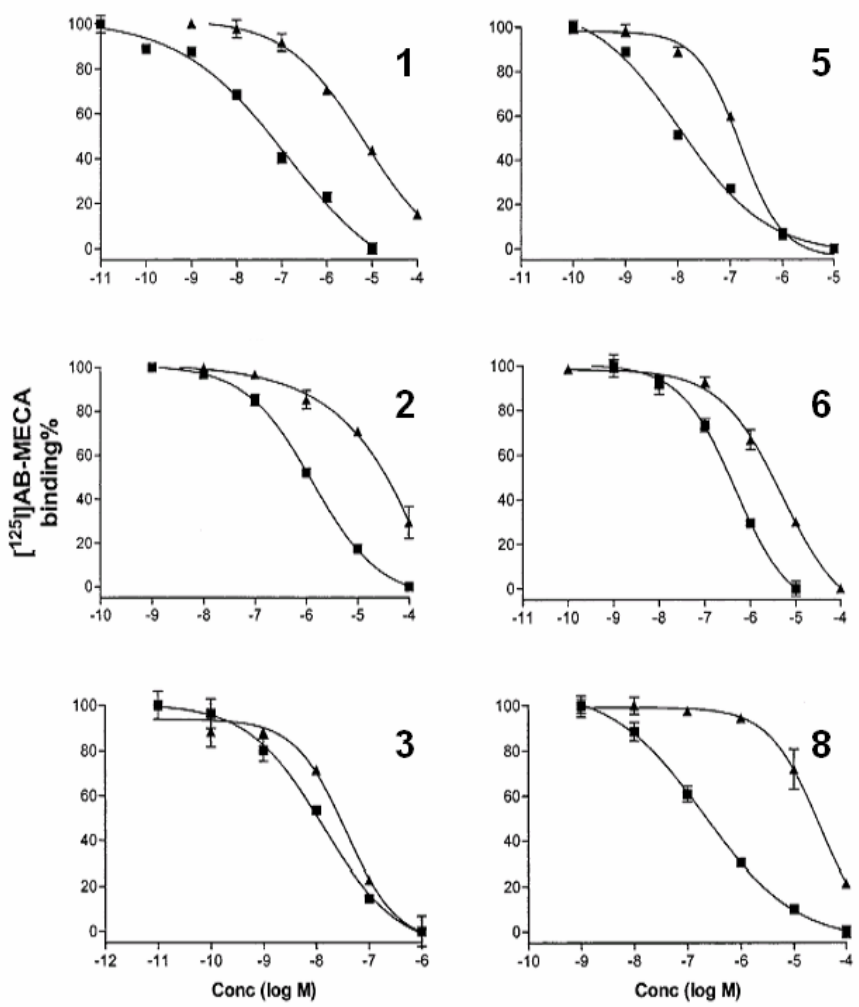

Figure 5.3 Binding of known A_3AR agonists and antagonists to wild type and mutant receptors ((■), wild type; (▲), H272E mutant receptor).

In most other cases, the affinity of competing ligands **1**-**8** was significantly reduced in the mutant receptor. For example, compound **1** was 19-fold less potent at the mutant receptor than the wild-type receptor. The potent antagonist **8**,[19] which contains a distal amino group, was 180-fold less potent at the mutant than the wild-type receptor. Other ligands, such as potent A_3AR agonists **3** and the rigid analogue **5**,[13,28] were shifted to lower affinity in binding to the mutant receptor by smaller factors, i.e. 5- and 6-fold, respectively.

5.2.3 Synthesis of neoligands

The amino derivatives of adenosine **9**-**10**, the N^6-substituted **13**, and a 5′-uronamide **16** were available from previous synthetic efforts.[29-31,35] Derivative **11** was

commercially available from Sigma Chemical Co. Preparation of 3'-guanidinoadenosine (**12**) is discussed in *J. Med. Chem.* **2001**, *44*, 4125. Synthesis of the N^6-iodobenzyladenosine analogue **14** is described in Part I.

5.2.4 Binding to mutant vs wild-type A_3AR

The receptor binding affinities of amine-functionalized adenosine derivatives were measured in standard binding assays using wild-type and H272E mutant human A_3AR expressed in COS-7 cells.[6,26,32,33] K_i values for these ligands are shown in Table 5.2, and representative binding curves are shown in Figure 5.4.

Table 5.2 Binding affinity of amine-derivatized adenosine analogues at wild-type and mutant (H272E) human A_3AR and rat adenosine receptors[a,b]

	K_i (μM)			K_i (μM)	
compound	**WT**	**H272E**	**compound**	**WT**	**H272E**
9	**c**	301±142	**13**	0.54±0.13	0.19±0.08
10	442±121	75±32	**14**	0.87±0.18	0.32±0.10
11	**c**	425±217	**15**	4.6±1.3	2.3±0.57
12	130±340	33.3±7.1	**16**	19.6±3.10	9.6±3.5

[a]Structures provided in Figure 5.2. [b]Results are from three independent experiments performed in duplicate, using [^{125}I]AB-MECA at a concentration of 1 nM at human A_3AR expressed in COS-7 cells [c]IC_{50} values of compounds **9** and **11** at the wild type receptor were estimated to be approximately 1 mM. The inhibition of [^{125}I]AB-MECA binding by **9** and **11** at the highest concentration examined (1 mM) was 51 and 54%, respectively.

The introduction of an amino group on the ribose moiety of adenosine resulted in either equipotency or enhanced binding affinity at the H272E mutant relative to wild-type A_3AR, depending on the position of the amino group. 3′-Amino-3′-deoxyadenosine **10** proved to be 7-fold more potent at the H272E mutant than the wild-type receptor. Two other isomers, 2′-amino-2′-deoxyadenosine **9** and 5′-amino-5′-deoxyadenosine **11**, an inhibitor of adenosine kinase,[34] did not display significantly enhanced affinity. The affinity of a 3′-guanidino analogue **12** was enhanced by 4-fold in the mutant versus wild-type receptors. A 2-aminoethyl analogue of **1**, i.e. **16**[35] was only 2-fold more potent at the mutant receptor. A 3′-amino-N^6-iodobenzyl analogue, **14**, showed a 3-fold enhancement at the mutant vs wild-type receptors, with a K_i value of 320 nM.

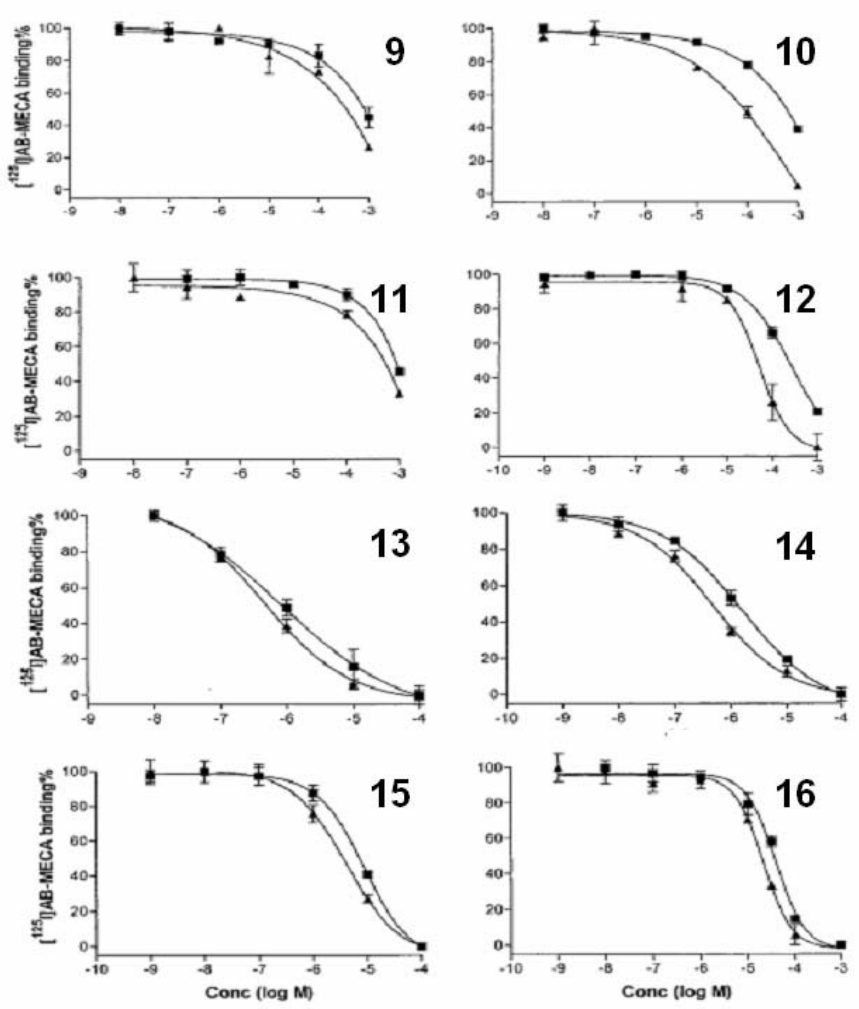

Figure 5.4 Binding of novel adenosine derivatives at wild-type and H272E mutant adenosine A_3AR ((■), wild type; (▲), H272E mutant receptor).

The ability of both mutant and wild-type receptors to activate second messengers was demonstrated. Both compounds **2** and **13** at 10 μM inhibited cyclic AMP production[36] stimulated by forskolin in COS-7 cells expressing either the wild-type or H272E mutant receptor (Figure 5.5). Furthermore, both the wild-type and H272E mutant receptors in the presence of 10 μM of compound **3** were shown to fully activate phospholipase C (data not shown), as determined by the method reported.[37]

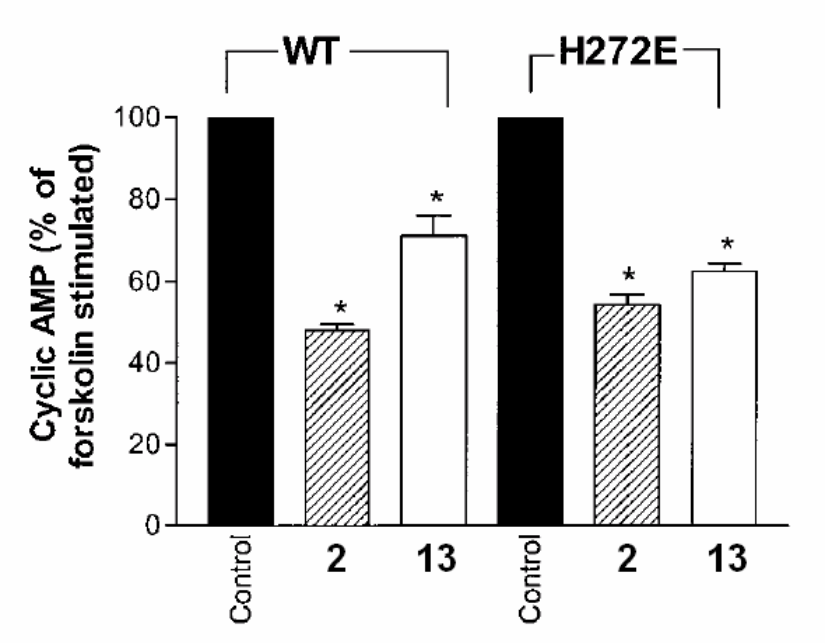

Figure 5.5 Cyclic AMP production by COS-7 cells expressing wild-type and H272E mutant human A_3AR after addition of compound **2** (10 μM) or compound **13** (10 μM). Values are means (SEM of three independent experiments performed in duplicate. For values marked with an asterisk, $P < 0.05$ compared with control.

5.2.5 Molecular modeling

A model of the human A_3AR was built in homology to the recently published X-ray structure of bovine rhodopsin.[38] The model included the seven TMs and the second extracellular loop (EL2). In this model, residue His272 was within interaction distance from Glu19 (1.39) in TM1 (see Nπ-Oε distance, 2.40 Å; Figure 5.6**A**). An analogous interaction had already been proposed for the A_{2A}AR,[23,24] in order to explain the observed involvement of both residues in agonist binding. In the present model, the carboxylate group of Glu19 appeared to interact also with Tyr265 (7.36) and Ser73 (2.65), resulting in a relatively rigid juxtaposition of the imidazole moiety of His272 relative to other elements of the ligand binding environment (Figure 5.6**B**).

Examination of the optimized model of the **2**-A_3AR complex showed that the N^6-amine nitrogen was located within H-bonding distances of the amide oxygen of Asn243 (6.50) and Oγ of Ser247 (6.52). The 2′-hydroxy substituent of the ribose ring was adjacent to both the Oε of Gln167 and Nζ of Lys152. The corresponding 3′-hydroxy substituent was within H-bonding distance from His272, and the 5'-oxygen interacted with Ser271 (7.42) and Asn274 (7.45) in TM7. Thus, **2** seemed to

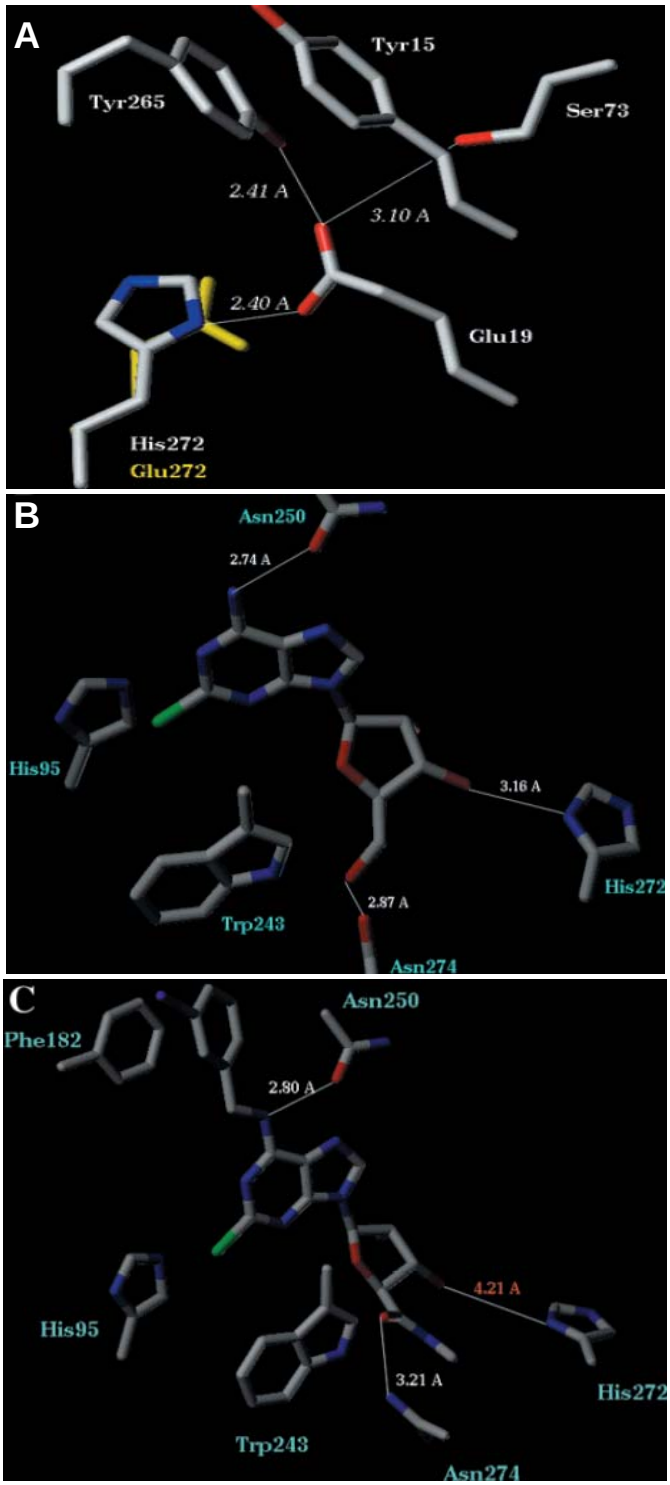

Figure 5.6 (**A**) Details of the putative H-bonding interactions among residues in proximity to the binding site of the human A_3AR either in the native receptor (His in blue and white) or for the H272E mutant (Glu in yellow). H-bonding distances to the carboxylate group of Glu19 are shown. (**B**) Docked conformation of non selective adenosine agonist **2** showing its position with respect to critical residues in the putative binding site of the wild-type human A_3AR. (**C**) Docked conformation of A_3AR selective adenosine agonist **3** showing its position with respect to critical residues in the putative binding site of the wild-type human A_3AR.

be accommodated by interactions with residues of TMs 6 and 7 and of EL2, with both 2′- and 3′-ribose hydroxy substituents proximal to basic residues.

In the optimized model of the **3**-A_3AR complex (Figure 5.6**C**) the N^6-benzyl substituent appeared to be wedged between TM5 and TM6, interacting with residues Phe182 (5.43), Ile186 (5.47), and Phe187 (5.48). Consequently, the whole ligand was displaced away from TM7, compared to the corresponding complex of **2**. The N^6 was still within interaction distance from Ser247 but was over 5 Å away from the amide oxygen of Trp243. Furthermore, the 3′-hydroxy substituent did not seem to interact with His272 (the 3′-O-Nτ distance was 4.21 Å). Reorientation of the latter was prevented by interaction with Glu19 (see above).

Modeling was used to test the hypothesis that an electrostatic interaction between the positively charged ligand and the now negatively charged ribose-binding region of the receptor led to the affinity enhancement of **10** at the H272E mutant receptor. Replacement of His272 by glutamate resulted in a structure with two adjacent carboxylates, one of which was most likely protonated. Since the mobility of Glu19 was restricted by interactions with Tyr265 and Ser73, the carboxylate group of Glu272 was held in an orientation that prevented a direct H-bond interaction with the 3′-hydroxy ribose substituent (Figure 5.6**A**). This was consistent with the 20-fold lower affinity of the H272E mutant toward agonists, such as **1** or **2**, while the corresponding effect on the agonists related to **3** was much smaller. The notion that, due to the H272E mutation, a polar interaction was lost was also consistent with the 15-20-fold affinity decrease of the mutant receptor toward the three antagonists examined (Table 5.1). In all of those cases, modeling suggested that Glu272 could not replace His in accommodating the A_3AR ligands through H-bonding interactions.

5.3 Discussion

We have investigated an approach to target agonist therapy to a specific organ or tissue based on selective activation of mutant receptors by synthetic ligands. Toward this goal we have both mutated the A_3AR and chemically modified the corresponding

agonists, aiming to preserve the structural complementarity required for agonist function.

On one hand, adenosine analogues carrying modifications of the ribose 2′- and 3′-substituents were known to be mostly inactive as agonists.[25] Thus, we concentrated on aminoadenosines in order to avoid activation of the wild-type A_3AR. On the other hand, simple aminoadenosines were nearly isosteric with the corresponding adenosines, implying that the former could act as agonists, provided a proper juxtaposition of its binding elements with those of an appropriate receptor could be achieved. For instance, introduction by mutagenesis of an acidic residue within the ligand binding site could have resulted in an electrostatic interaction with the amine substituent of the ligand.

Position 272 on TM7 of the human A_3AR (7.43) was selected for such mutagenesis, since it appeared to play an important role across the GPCR family. In rhodopsin, this is the location of the Lys residue that forms a Schiff base with retinal. In all four of the adenosine receptors this site is occupied by His, which has been proposed to be critical for recognition of the ribose or ribose-like moiety common to all adenosine agonists thus far reported. At the A_3AR, His at this site was proposed as the basis for enhanced affinity of xanthine-7-ribosides relative to the parent xanthines.[27] In the A_1AR, mutation of this His to Ala resulted in decreased affinity of both agonists and antagonists. In the A_{2A}AR, this site has been mutated to Ala with the loss of high-affinity binding of both agonists and antagonists,[19] while mutation to Tyr preserved the ability to bind ligands.[24] Thus, substitution that preserved H-bonding capability was allowed at this critical site. Substitution of His272 with Glu was the first example of a non aromatic residue at this position in adenosine receptors that still allowed ligand recognition. It was especially surprising in light of the proposal that in the human A_{2A}AR this His appeared to be coupled spatially to a Glu in TM1 through the formation of a H-bond.[24]

The affinities of the aminoadenosine analogues **9**-**16**, for the H272E mutant A_3AR were higher than for the corresponding wild type, demonstrating that in principle A_3AR could be engineered for selective interaction with synthetic agonists. In particular this was evident from the 7-fold affinity enhancement of **10** toward the

mutated receptor. Thus, the notion that the H272E mutant A_3AR could be selectively activated in the presence of wild-type A_3AR appeared feasible.

The role of residue His272 in accommodating A_3AR agonists and antagonists, as well as the consequences of its replacement by glutamate were investigated by molecular modeling[19,23] of the ligand-receptor complexes. The 3′-amino group was intended for a direct electrostatic interaction with the negatively charged ribose-binding region of the mutant receptor, yet molecular modeling did not support this notion. In brief, the higher affinity of 3′-amino-3′-deoxyadenosine at the engineered A_3AR appeared to result from the lack of a repulsion (positively charged ligand and a positively charged His272 side chain in the WT receptor), rather than the attractive force of opposite charges. It is also possible that a water molecule fills the space between the 3′-amino group and Glu272, thus allowing water mediated H-bonding.

Previous models of an interaction between His278 of A_{2A}AR (position equivalent to 272 in the A_3AR)[23] and adenosine suggested the involvement of both of the ribose secondary hydroxy substituents on binding. Yet substitution of glutamate at position 272 had a larger effect on **10** than on **9**, indicating that His/Glu272 interacted predominantly with the 3′-ribose substituent. Conversely, for aminoadenosines where N^6 was substituted by a cycloalkyl (**13**) or iodobenzyl (**14**, **15**), the effect of Glu272 was small, irrespective of the position of the amino ribose substituent (Table 5.2).

From molecular models of the human A_3AR complexed with **10** (Figure 5.7) it appears that the nearly 1000-fold lower affinity, relative to **2,** results from a loss of a H-bond interaction of the 3′-hydroxy substituent and the electrostatic repulsion of the 3′-amine substituent and His272. Replacement at position 272 by glutamate did not restore binding with the 3′-substituent. As already mentioned Glu272 was not available for direct contact with the ligand due to an interaction with Glu19. The gain of affinity for the aminoadenosines seemed therefore to depend on relief of electrostatic repulsion, being more pronounced for **10** than for **13** and **14,** where the ligands would be displaced toward TM5 (including the 3′-amine substituent).

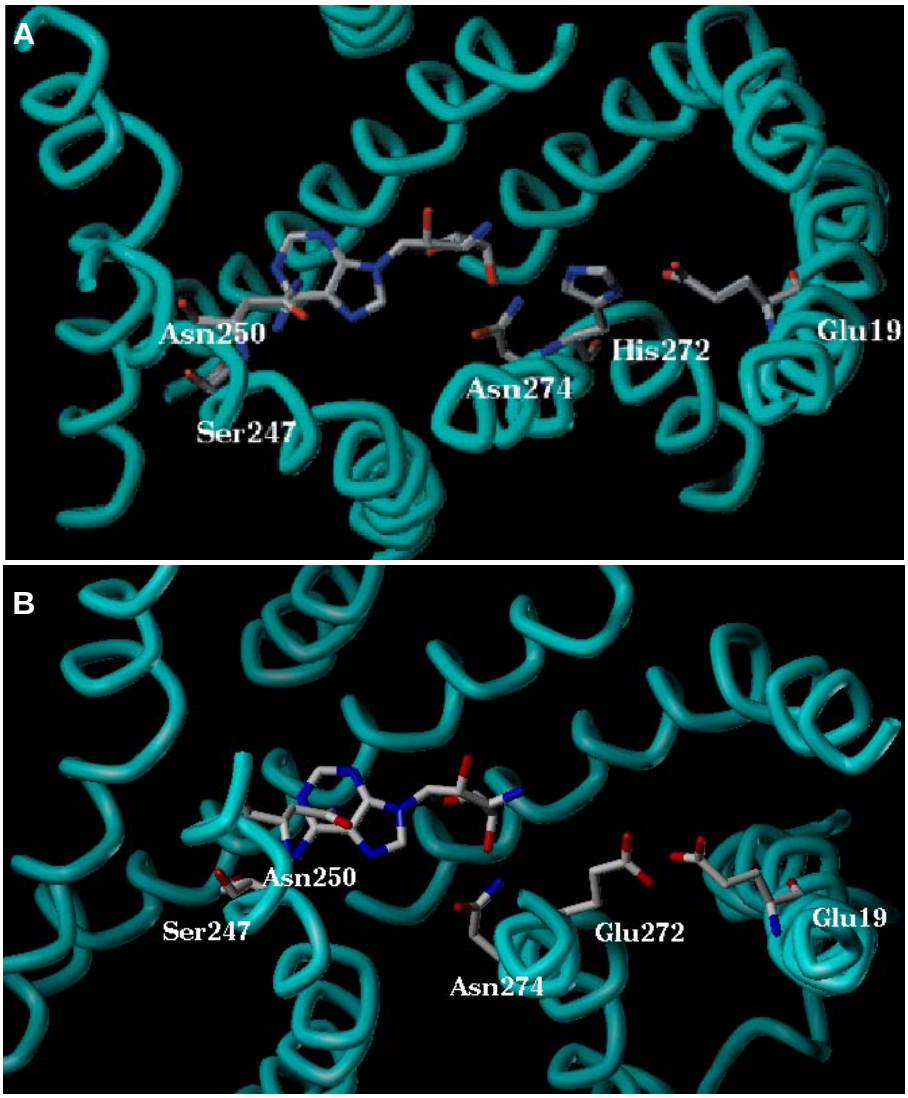

Figure 5.7 Docked conformation of the neoligand **10** in relation to the helical bundle and EL2 of the wild-type human A_3AR (**A**) and H272E mutant human A_3AR (**B**). View from the the extracellular region (showing TM side chains mentioned in the text).

The notion that Glu272 did not interact directly with the ligands was consistent with the finding that the A_3AR affinity toward *N*-benzyl-substituted analogues (i.e. **3**, **4** and **5**) was less sensitive to the nature of the residue at position 272. On the other hand, the corresponding affinity toward **2** was 20-fold lower (Table 5.1). Furthermore, the affinity of the H272E mutant A_3AR toward **2** was only 7-fold higher than that toward the 3′-amino derivative **10**, suggesting that the binding environments for the two ligands were similar. In fact, the lower affinity toward **10** was likely due to repulsive interactions with Lys152, which, according to our model, was vicinal to the 2′-hydroxy substituent. This proximity may also be responsible for the low affinity of the human A_3ARs toward the aminoadenosine **9**.

The lack of Glu272 participation in ligand accommodation, in particular in interaction with 3′-aminoadenosines, due to its interaction with Glu19 suggests that replacement of Glu19 by a residue that would not restrict the mobility of Glu272 may result in a receptor with considerably higher affinity toward aminoadenosines such as **10** and **14**. Replacement of Ser73 by a non polar residue such as Ala, on the other hand, may allow enhanced mobility of the Glu272-Glu19 assembly toward TM7 (see above), bringing the Glu272 carboxylate within interaction distance of the ligands. Thus, the doubly mutated H272E/E19X and H272E/S73X mutant A_3ARs may be more suitable as neoceptors for the aminoadenosine neoligands. Alternatively, on neoligand level, the introduction of a methylene spacer between the ribose sugar moiety and the amine function (by-passing the restricted mobility of Glu272), should enhance the affinity of aminoadenosines such as **10** and **14**. In fact this is what inspired us to synthesize the branched-chain derivatives mentioned in Chapter 4. Unfortunately, due to stable expression problems of the A_3 neoceptor, these analogues have not been evaluated yet for this purpose.

The notion that GPCRs can be engineered to accommodate unnatural ligands has been investigated in other cases. Schwartz and co-workers[39,40] engineered GPCRs to have the ability to bind zinc ions through complexation with multiple His residues. More recently Conklin and co-workers[41] engineered the κ opioid receptor to respond exclusively to small molecule ligands and not to the receptor's natural ligand. In this study, impressive selectivity toward bremazocine was achieved, demonstrating the extent to which receptor properties could be modified without compromising functionality. Strader and co-workers[42] also studied the microscopic complementarity of functionality in receptor binding. However, no attempt was made to modify both the receptors and the ligands in the manner proposed in the present study.

The feasibility of a tailor-made agonist (neoligand) to interact selectively with a mutant receptor (neoceptor) opens interesting perspectives for a (futuristic) therapeutic approach, in which such a neoceptor would be introduced specifically into a target organ through gene transfer.[43,44] Gene transfer to the heart has been demonstrated,[45-47] and gene therapy toward the goal of cardioprotection has already been proposed.[4] The transfection of the A_1AR or A_3AR into a cardiac myocyte culture enhances the protective effect of either endogenous adenosine or an exogenously

added, synthetic agonist of the appropriate receptor. By this approach, a neoceptor could be genetically delivered to a target organ, followed by the administration of a selective, tailor-made ligand, as needed.

5.4 Experimental section

*Biological evaluation and molecular modeling was performed by the group of Dr. Kenneth A. Jacobson, at the Laboratory for Bioorganic Chemistry (NIDDK), NIH, Maryland, USA. For the detailed procedures on the preparation of mutant receptors, radioligand binding studies, cyclic AMP assay and molecular modeling we refer to the experimental part in our J. Med. Chem. paper (**2001**, 44, 4125).*

5.4.1 Chemistry

Commercially available compounds **1**-**3**, **6**, **8** were from Sigma Chemical Co. Compound **5**[28] was available from previous synthetic efforts. Compound **7**[51] was the gift of Prof. Ad IJzerman of the LACDR, Leiden, The Netherlands.

5.5 References

[1] Kowaluk, E. A.; Jarvis, M. F. *Expert Opin. Invest. Drugs* **2000**, *9*, 551.

[2] Saxena, P. R.; De Vries, P.; Wang, W.; Heiligers, J. P.; Maassen vandenBrink, A.; Bax, W. A.; Yocca, F. D. *Naunyn-Schmiedebergs Arch. Pharmakol.* **1997**, *355*, 295.

[3] Maillard, M.; Nikodijevic, O.; LaNoue, K. F.; Berkich, D. A.; Ji, X.-D.; Bartus, R.; Jacobson, K. A. *J. Pharm. Pharmacol.* **1994**, *83*, 46.

[4] Liang, B. T.; Jacobson, K. A. *Proc. Natl. Acad. Sci. U.S.A.* **1998**, *95*, 6995.

[5] von Lubitz, D. K. J. E.; Lin, R. C.-S.; Popik, P.; Carter, M. F.; Jacobson, K. A. *Eur. J. Pharmacol.* **1994**, *263*, 59.

[6] Jarvis, M. F.; Schutz, R.; Hutchison, A. J.; Do, E.; Sills, M. A.; Williams, M. *J. Pharmacol. Exp. Therap.* **1989**, *251*, 888.

[7] Lerman, B. B.; Wesley, R. C.; Belardinelli, L. *Circulation* **1989**, *80*, 1536.

[8] Ely, S. W.; Berne, R. M. *Circulation* **1992**, *85*, 893.

[9] Abbracchio, M. P.; Cattabeni, F. *Ann. N. Y. Acad. Sci.* **1999**, *890*, 79.

[10] Murry, C. E.; Jennings, R. B.; Reimer, K. A. *Circulation* **1986**, *74*, 1124.

[11] Downey, J. M. *Trends Cardiovasc. Med.* **1992**, *2*, 170.

[12] Strickler, J.; Jacobson, K. A.; Liang, B. T. *J. Clin. Invest.* **1996**, *98*, 1773.

[13] Jacobson, K. A. *Trends Pharmacol. Sci.* **1998**, *19*, 184.

[14] Singer, B. F.; Fotheringham, J. A.; Mayne, M. B. *FASEB J.* **2001**, *15*, A566.

[15] Mitchell, C. H.; Peterson-Yantorno, K.; Carre, D. A.; McGlinn, A. M.; Coca-Prados, M.; Stone, R. A.; Civan, M. M. *Am. J. Physiol.* **1999**, *276*, C659.

[16] Olah, M. E.; Ren, H.; Ostrowski, J.; Jacobson, K. A.; Stiles, G. L. *J. Biol. Chem.* **1992**, *267*, 10764.

[17] Townsend-Nicholson, A.; Schofield, P. R. *J. Biol. Chem.* **1994**, *269*, 2373.

[18] Tucker, A. L.; Robeva, A. S.; Taylor, H. E.; Holeton, D.; Bockner, M.; Lynch, K. R.; Linden, J. *J. Biol. Chem.* **1994**, *269*, 27900.

[19] Kim, J.; Wess, J.; van Rhee, A. M.; Schöneberg, T.; Jacobson, K. A. *J. Biol. Chem.* **1995**, *270*, 13987.

[20] Rivkees, S. A.; Barbhaiya, H.; IJzerman, A. P. *J. Biol. Chem.* **1999**, *274*, 3617.

[21] van Rhee, A. M.; Jacobson, K. A. *Drug Dev. Res.* **1996**, *37*, 1.

[22] Jiang, Q.; van Rhee, A. M.; Kim, J.; Yehle, S.; Wess, J.; Jacobson, K. A. *Mol. Pharmacol.* **1996**, *50*, 512.

[23] IJzerman, A. P.; von Frijtag Drabbe Künzel, J. K.; Kim, J.; Jiang, Q.; Jacobson, K. A. *Eur. J. Pharmacol.* **1996**, *310*, 269.

[24] Gao, Z.-G, Jiang, Q.; Jacobson, K. A.; IJzerman, A. P., *Biochem. Pharmacol.* **2000**, *60*, 661.

[25] Jacobson, K. A.; Siddiqi, S. M.; Olah, M. E.; Ji, X.-d.; Melman, N.; Bellamkonda, K.; Meshulam, Y.; Stiles, G. L.; Kim, H. O. *J. Med. Chem.* **1995**, *38*, 1720.

[26] Olah, M. E.; Gallo-Rodriguez, C.; Jacobson, K. A.; Stiles, G. L. *Mol. Pharmacol.* **1994**, *45*, 978.

[27] Jacobson, K. A.; Kim, H. O.; Siddiqi, S. M.; Olah, M. E.; Stiles, G. L.; von Lubitz, D. K. J. E. *Drugs Future* **1995**, *20*, 689.

[28] Lee, K.; Ravi, R. G.; Ji, X.-d.; Marquez, V. E.; Jacobson, K. A. *Biorg. Med. Chem. Lett.* **2001**, *11*, 1333.

[29] Azhayev, A. V.; Ozols, A. M.; Bushnev, A. S.; Dyatkina, N. B.; Kochetkova, S. V.; Victorova, L. S.; Kukhanova, M. K.; Krayevski, A. A.; Gottikh, P. B. *Nucleic Acids Res.* **1979**, *6*, 625.

[30] Robins, M. J.; Hawrelak, S. D.; Hernandez, A. E.; Wnuk, S. F. *Nucleosides Nucleotides* **1992**, *11*, 821.

[31] Van Calenbergh, S.; von Frijtag Drabbe Künzel, J. K.; Blaton, N. M.; Peeters, O. M.; Rozenski, J.; Van Aerschot, A.; De Bruyn, A.; De Keukeleire, D.; IJzerman, A. P.; Herdewijn, P. *J. Med. Chem.* **1997**, *40*, 3765.

[32] Schwabe, U.; Trost T. *Naunyn-Schmiedebergs Arch. Pharmakol.* **1980**, *313*, 179.

[33] Gao, Z.; Li, B. S.; Day, Y. J.; Linden, *J. Mol. Pharmacol.* **2001**, *59*, 76.

[34] Wiesner, J. B.; Ugarkar, B. G.; Castellino, A. J.; Barankiewicz, J.; Dumas, D. P.; Gruber, H. E.; Foster, A. C.; Erion, M. D. *J. Pharmacol. Exp. Ther.* **1999**, *289*, 1669.

[35] Gallo-Rodriguez, C.; Ji, X.-D.; Melman, N.; Siegman, B. D.; Sanders, L. H.; Orlina, J.; Fischer, B.; Pu, Q.-L.; Olah. M. E.; van Galen, P. J. M.; Stiles, G. L.; Jacobson, K. A. *J. Med. Chem.* **1994**, *37*, 636.

[36] van Tilburg, E. W.; von Frijtag Drabbe Künzel, J.; de Groote, M.; Vollinga, R. C.; Lorenzen, A., IJzerman, A. P. *J. Med. Chem.* **1999**, *42*, 1393.

[37] Chen, A.; Gao, Z. G.; Barak, D.; Liang, B. T.; Jacobson, K. A. *Biochem. Biophys. Res. Comm.* **2001**, *284*, 596.

[38] Palczewski, K.; Kumasaka, T.; Hori, T.; Behnke, C. A.; Motoshima, H.; Fox, B. A.; Trong, I. L.; Teller, D. C.; Okada, T.; Stenkamp, R. E.; Yamamoto, M.; Miyano, M. *Science* **2000**, *289*, 739.

[39] Elling, C. E.; Nielsen, S. M.; Schwartz, T. W. *Nature* **1995**, *374*, 74.

[40] Holst, B.; Elling, C. E.; Schwartz, T. W. *Mol. Pharmacol.* **2000**, *58*, 263.

[41] Coward, P.; Wada, H. G.; Falk, M. S.; Chan, S. D.; Meng, F.; Akil, H.; Conklin, B. R. *Proc. Natl. Acad. Sci. U.S.A.* **1998**, *95*, 352.

[42] Fong, T. M.; Yu, H.; Cascieri, M. A.; Underwood, D.; Swain, C. J.; Strader, C. D. *J. Biol. Chem.* **1994**, *269*, 14957.

[43] Mack, C. A.; Patel, S. R.; Schwarz, E. A.; Zanzonico, P.; Hahn, R. T.; Ilercil, A.; Devereux, R. B.; Goldsmith, S. J.; Christian, T. F.; Sanborn, T. A.; Kovesdi, I.; Hackett, N.; Isom, O. W.; Crystal, R. G.; Rosengart, T. K. J. *Thorac. Cardiovasc. Surg.* **1998**, *115*, 168.

[44] Harvey, B. G.; Hackett, N. R.; El-Sawy, T.; Rosengart, T. K.; Hirschowitz, E. A.; Lieberman, M. D.; Lesser, M. L.; Crystal, R. G. *J Virol.* **1999**, *73*, 6729.

[45] Logeart, D.; Hatem, S. N.; Rucker-Martin, C.; Chossat, N.; Nevo, N.; Haddada, H.; Heimburger, M.; Perricaudet, M.; Mercadier, J.-J. *Human Gene Ther.* **2000**, *11*, 1015.

[46] Svensson, E. C.; Marshall, D. J.; Woodard, K.; Lin, H.; Jiang, F.; Chu, L.; Leiden, J. M. *Circulation* **1999**, *99*, 201.

[47] Shah, A. S.; Lilly, R. E.; Kypson, A. P.; Tai, O.; Hata, J. A.; Pippen, A.; Silvestry, S. C.; Lefkowitz, R. J.; Glower, D. D.; Koch, W. J. *Circulation* **2000**, *101*, 408.

[48] van Muijlwijk-Koezen, J. E.; Timmerman, H.; van der Goot, H.; Mengge, W. M. P. B.; Frijtag von Drabbe-Künzel, J.; de Groote, M.; IJzerman, A. P. *J. Med. Chem.* **2000**, *43*, 2227.

CHAPTER 6

MODELING THE ADENOSINE RECEPTORS:

COMPARISON OF THE BINDING DOMAINS OF A_{2A}AR AGONISTS AND ANTAGONISTS

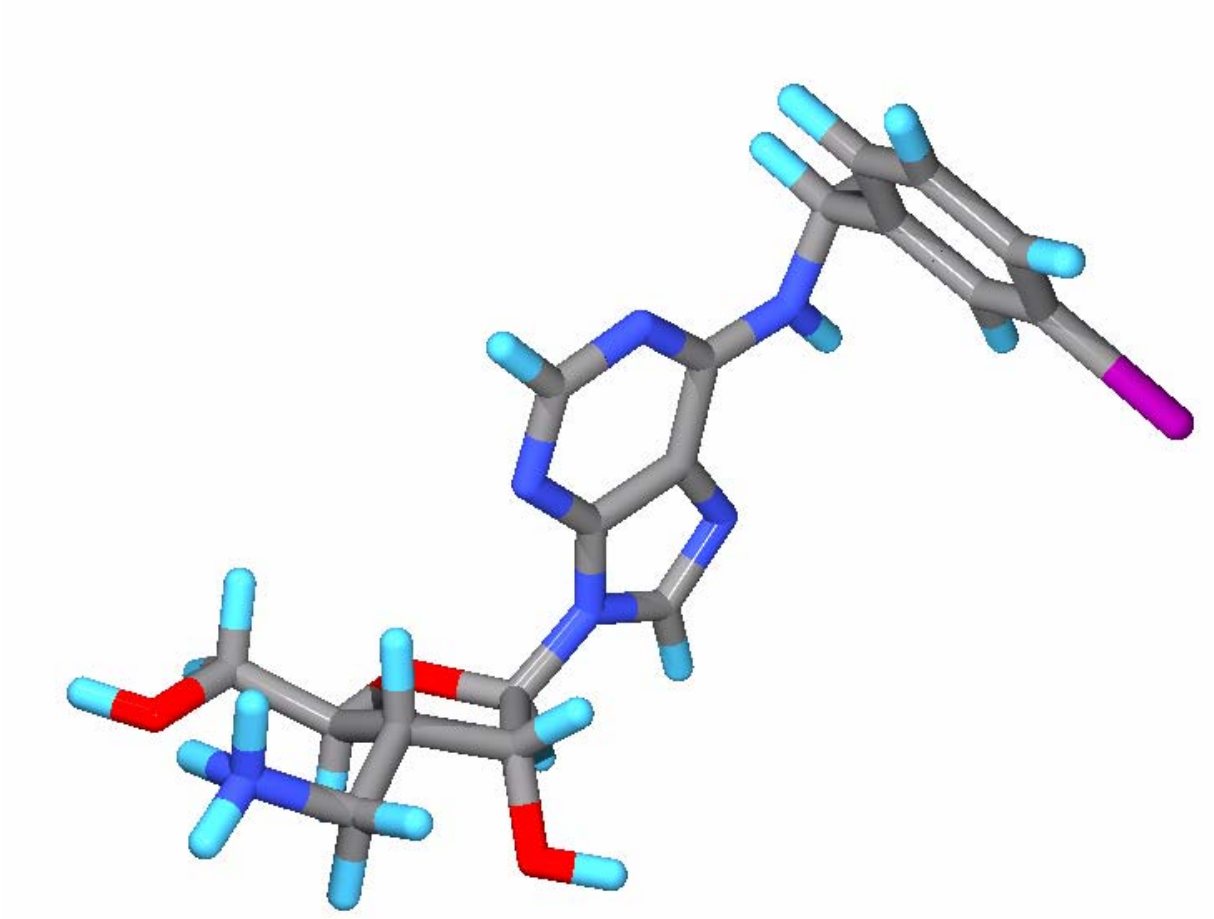

This chapter is published in part in:

Soo-Kyung Kim, Zhan-Guo Gao, Philippe Van Rompaey, Ariel S. Gross, Aishe Chen, Serge Van Calenbergh, Kenneth A. Jacobson.

J. Med. Chem. **2003**, *46*, 4847.

6.1 Introduction

As mentioned in Chapter 3-5 adenosine receptors (ARs), classified as A_1, A_{2A}, A_{2B}, and A_3 subtypes, represent a physiologically and pharmacologically important family of G protein-coupled receptors (GPCRs).[1]

A_{2A}AR agonists are also potentially useful for the treatment of cardiovascular diseases, such as hypertension, ischemic cardiomyopathy, inflammation, and atherosclerosis,[2] and A_{2A}AR antagonists have been proposed as novel therapeutics for Parkinson's disease and may also be active as cognition enhancers, neuroprotective and anti-allergic agents, analgesics, and positive inotropics.[3-5] Although the physiological effects mediated through the A_{2A}AR have been extensively investigated, only a few molecular modeling studies, which used a low-resolution rhodopsin template,[6,7] have explored the binding properties of agonists and antagonists at the A_{2A}AR. The development of more potent and/or selective A_{2A}AR agonists and antagonists is still being pursued intensively.

Extensive mutagenesis was carried out for both the A_1AR and A_{2A}AR and to a lesser extent for the A_{2B}AR and A_3AR.[1,8] The retinal binding site of rhodopsin,[9] a G protein-coupled photoreceptor, and the putative ligand binding sites on ARs, as deduced by using mutational analysis, overlap extensively. Most of the essential residues required for recognition of AR agonists and/or antagonists, which bind within the transmembrane helical domains (TMs) 3, 5, 6, and 7,[1] coincide largely with the corresponding amino acids of the binding site of *cis*-retinal in rhodopsin, although there are additional interaction sites within TMs 6 and 7 of the ARs.

In this chapter, a three-dimensional model of the A_{2A}AR was studied, based on the high-resolution structure of rhodopsin as a template.[7] We describe a comparison of the binding characteristics of A_{2A}AR agonist and antagonist ligands (Figure 6.1). We also made comparisons to our previously A_3AR model (Chapter 5),[10,11] which was derived with similar methods. Finally, the model was tested experimentally by making complementary changes in the structures of agonist ligands (e.g. introduction of amino groups into known ligands, resulting in adenosine derivatives **5**-**8**; Figure 6.2) and the A_{2A}AR, to form neoceptor-neoligand pairs.[12]

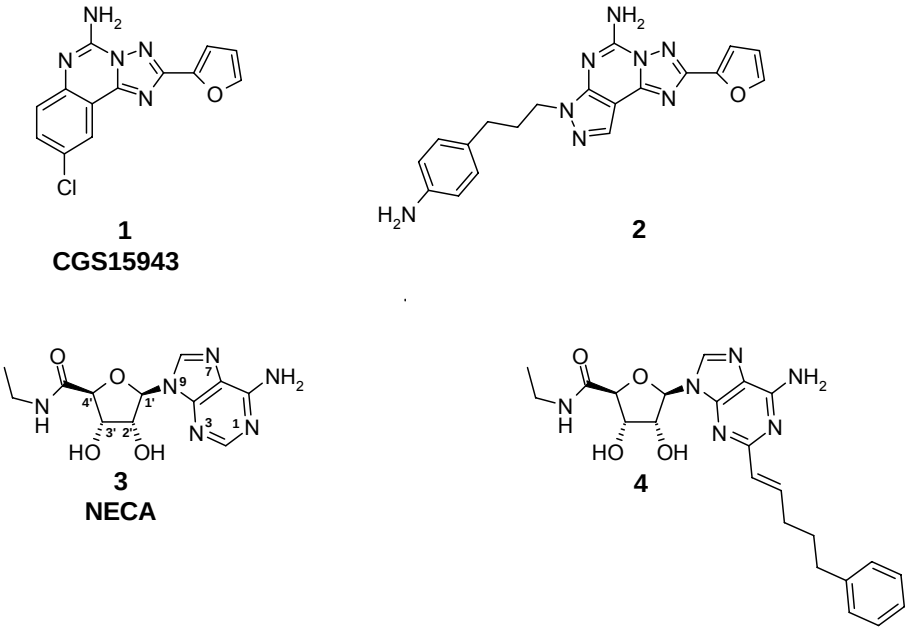

Figure 6.1 Structures of the known A_{2A}AR agonists and antagonists used in initial receptor docking**. 1**, CGS15943, non selective antagonists; **2**, A_{2A}AR-selective antagonists; **3**, non selective agonist; **4**, A_{2A}AR-selective agonist (rA_{2A}AR: 3.5 nM, rA_1AR: 1017 nM, A_1AR/A_{2A}AR: 291).[18]

6.2 Results and discussion

6.2.1 Synthesis of neoligands

The amino derivatives **5** was commercially available from Sigma Chemical Co. and **8** was available from previous synthetic efforts.[13] Synthesis of adenosine nucleoside analogues **6** and **7**, modified at the 3'- and N^6-position, is described in Part I.

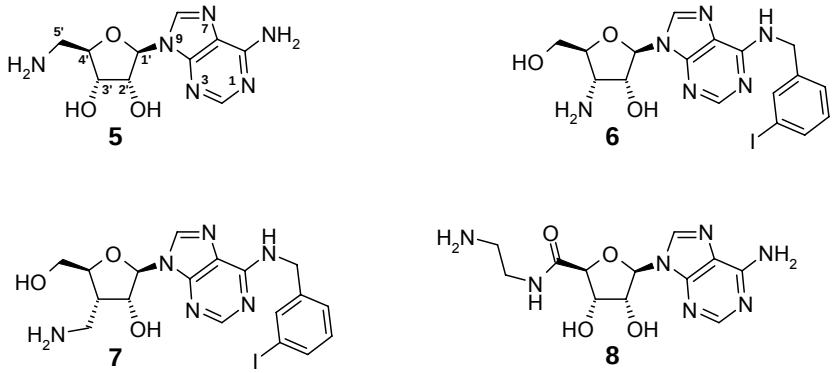

Figure 6.2 Structures of the A_{2A}AR agonists containing amino groups for electrostatic interaction with negatively charged side chains of mutant A_{2A}ARs. Compounds **5**, **6**, and **8** were used in the previous neoceptor study of the A_3AR.[17]

6.2.2 Construction of the A_{2A}AR molecular model

Construction of the A_{2A}AR molecular model and molecular modeling was performed by the group of Dr. Kenneth A. Jacobson, at the Laboratory for Bioorganic Chemistry (NIDDK), NIH, Maryland, USA. For the detailed procedures regarding these topics we refer to *J. Med. Chem.* **2003**, *46*, 4847.

6.2.3 Binding of a known agonist and antagonist to mutant human A_{2A}ARs

A variety of negatively charged side chains were substituted in the A_{2A}AR at hydrophilic positions in TMs 3 and 7 predicted to be in proximity to the bound ribose moiety. Radioligand binding studies showed that T88D and T88E mutant receptors were able to bind the non selective AR antagonist **1** but not the non selective AR agonist **3** (Figure 6.3 and Table 6.1). Similarly, the T88A mutation was already shown to substantially decrease agonist but not antagonist affinity.[14] For the Q89D mutant receptor, the binding affinity of agonist **3** was increased approximately 14-fold. Its Ala mutation also increased agonist and antagonist binding affinity and its H/R mutation affected only antagonist affinity.[14] However, S277E, H278D, and H278E mutations did not affect the binding of either the agonist **3** or the antagonist **1**. These findings contrasted with the selective decrease of agonist affinity in the S277A mutant receptor and the inability of the H278A mutant receptor to bind either agonist or antagonist radioligand.[6] A total of six mutations-T88D, T88E, Q89D, S277E, H278D, and H278E-did not alter the binding affinity of the antagonist **1**.

6.2.4 Ligand docking

A crystallographic determination of the human A_{2A}AR structure would be a better method by which to analyze the conformational implications of our mutagenesis experiments; however, presently no structure is available. While such studies are underway,[15] no structure of close homology to the receptor is available. Thus, we resorted to the widely used, however imprecise, method of rhodopsin-based

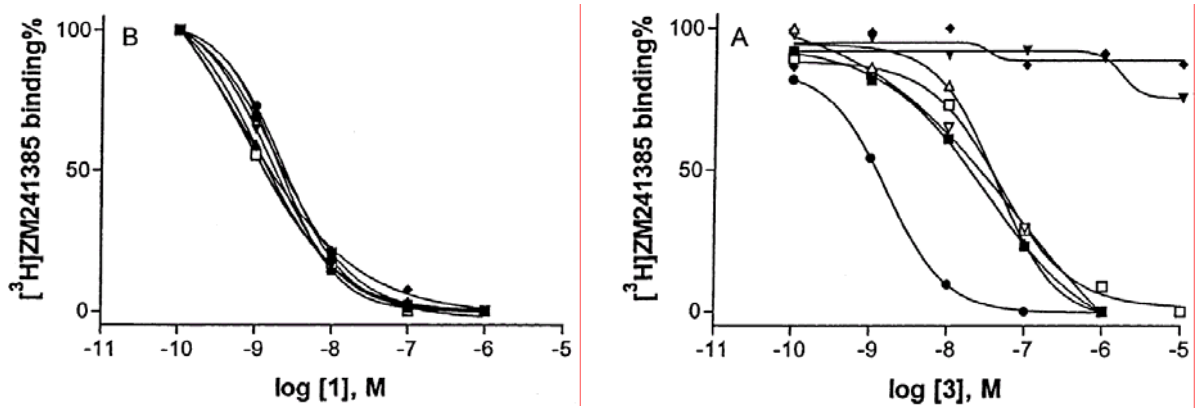

Figure 6.3 Effect of the antagonist CGS15943 **1** and agonist NECA **3** on the binding of the radiolabeled antagonist [^{3}H]ZM241385 to the human A_{2A}AR. Membranes (10-20 μg of protein) from COS-7 cells transfected with wild type (■) or mutant receptors of T88D (▼), T88E (♦), Q89D (●), S277E (□), H278D (▲), or H278E (▼) were incubated with 1.0 nM [^{3}H]ZM241385 in duplicate, together with increasing concentrations of the competing compounds, in a final volume of 0.4 mL of Tris HCl buffer (50 mM, pH 7.4) at 25 °C for 120 min. Results were from a representative experiment.

homology modeling of Family 1 GPCRs. Rhodopsin-based homology modeling is not an automatic method for obtaining a realistic structure for a given GPCR, but rather requires time-consuming custom treatment according to known pharmacological data.[16] Here, both agonists and antagonists were docked in the human A_{2A}AR model. In general, docking of agonists to GPCR models is subject to even greater uncertainty than antagonist since the template consists of the inactive state of rhodopsin.

Table 6.1 Binding affinity of the antagonist **1** and the non selective agonist **3** at WT and mutant human A_{2A}ARs[a]

	K_i (nM) or % displacement	
mutant receptor	**1**	**3**
WT	0.84±0.22	21.4±8.7
T88D	0.91±0.09	20% at 10 μM
T88E	0.67±0.17	0% at 10 μM
Q89D	0.35±0.12	1.5±0.4
S277E	1.0±0.3	29.2±6.3
H278D	0.41±0.14	19.1±3.4
H278E	0.52±0.06	24.6±8.3

[a]Membranes from COS-7 cells transfected with WT or mutant A_{2A}AR cDNA were incubated with 1.0 nM [^{3}H]ZM241385 in duplicate, together with increasing concentrations of the competing compounds, in a final volume of 0.4 mL of Tris HCl buffer (50 mM, pH 7.4) at 25 °C for 120 min. The K_i values are expressed as mean ± standard error from three independent experiments.

Often multiple modes of docking of a given agonist or antagonist ligand are observed.[17] Selection of preference of one docking mode in such cases is based on diverse pharmacological data, rather than on computational results alone. In the present study, the introduction of complementary functional groups on the ligand and receptor is meant to overcome the problem of ambiguity of docking modes in GPCR modeling.

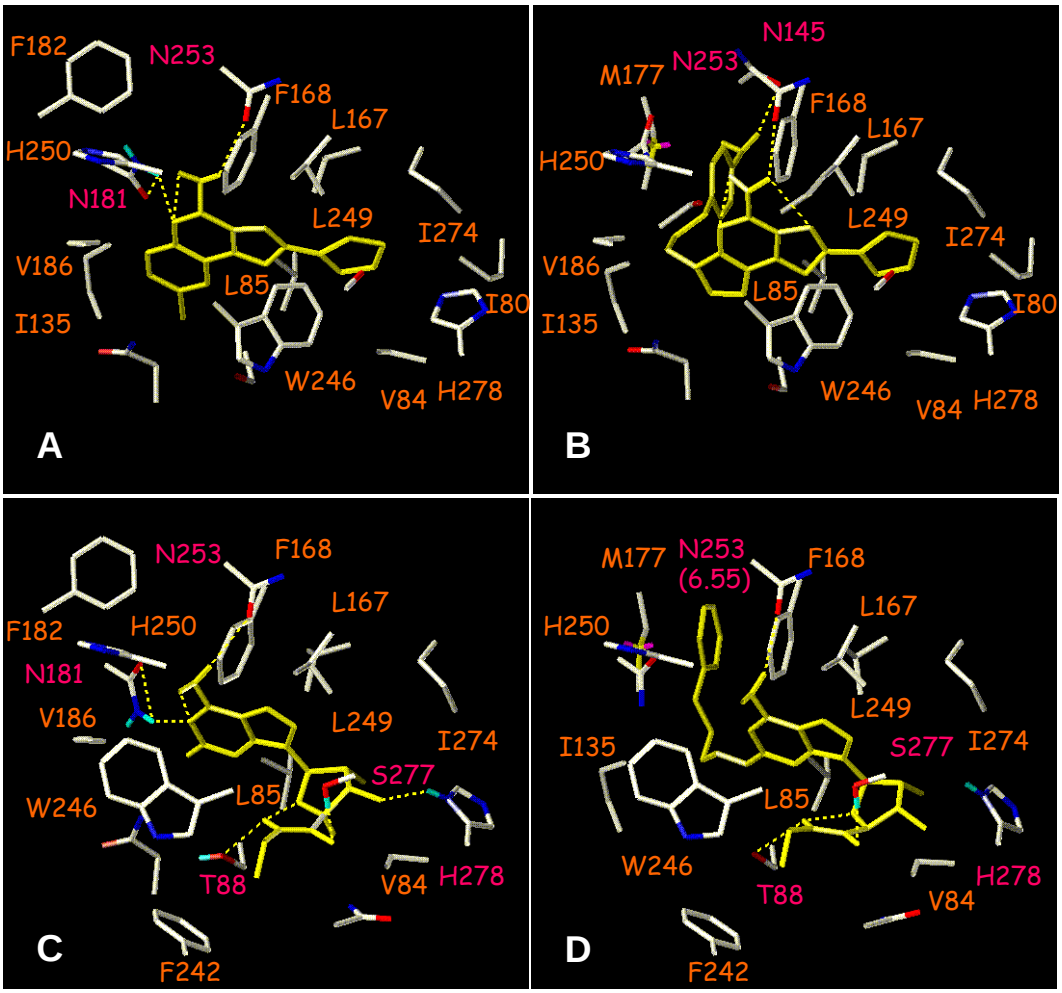

Figure 6.4 The complex of the A_{2A}AR with agonists and antagonists: (**A**) **1**, a non selective antagonist; (**B**) **2**, an A_{2A}AR-selective antagonist; (**C**) **3**, a non selective agonist; (**D**) **4**, an A_{2A}AR-selective agonist. All ligands are represented in yellow. The amino acids of the A_{2A}AR that are depicted in red and orange participated in the hydrophilic and hydrophobic interactions, respectively.

The most general structural distinction between agonists and antagonists is that only an agonist requires a ribose ring, or more specifically, the 3′- and 5′-ribose substituents that interact directly with the A_{2A}AR. To explain the different binding properties of antagonists and agonists at the A_{2A}AR, representative ligands were

were docked within the human A_{2A}AR model. The result showed overlapped binding modes for antagonists and agonists (Figures 6.4 and 6.5).

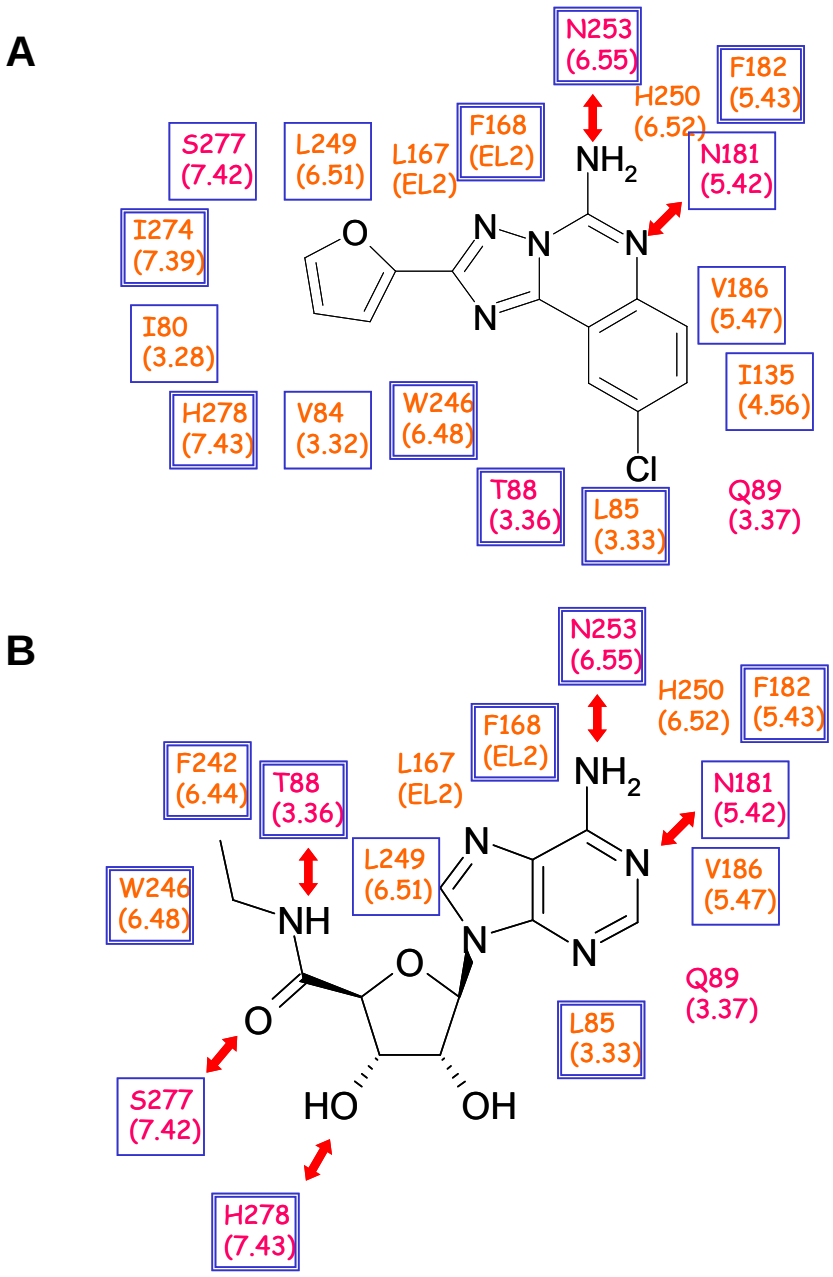

Figure 6.5 Detailed interactions with **1** (**A**) and **3** (**B**) in the putative A_{2A}AR binding site. The residues in the double-squared box are highly conserved among G protein-coupled receptors, and those in the single-squared box are conserved amino acids among ARs.

6.2.5 Agonist binding

Our present model is consistent with several experimental results concerning recognition of ribose-containing ligands (i.e. adenosine agonists): (1) The hydrophilic interactions at S277 (7.42) and H278 (7.43) were required for high-affinity binding of agonists but not antagonists.[14] The toleration of ligand binding in the S277E and H278D/E mutant receptors suggested that the acidic residues in the mutant receptors retained the ability to form an H-bond with the ligand, i.e. at the 3′-OH group. With respect to the 5′-carbonyl group of **3**, the model suggested that a weak H-bond, or alternately a water mediated H-bond, was possible. (2) Radioligand binding studies (Figure 6.3 and Table 6.1) showed that T88D and T88E mutant receptors were able to bind the antagonist **1** but not the agonist **3**. Similarly, the T88A mutation was already shown to substantially decrease agonist but not antagonist affinity.[14] Thus the reason that mutation of T88 was specific for diminishing the affinity of the ribosides appeared to be the proximity of this residue to agonists but not antagonists based on the docking result. (3) Replacement of H278 with other aromatic residues was not tolerated in ligand binding.[6]

To better understand the increase of A_{2A}AR selectivity on substitution of the 2-position of the adenine ring, we performed the docking of the (*E*)-2-phenylpentenyl derivative of NECA **4**.[18] Additional hydrophobic interactions between the phenylpentenyl moiety at the 2-position of the adenine ring and the hydrophobic pocket formed from TM4 and TM5 increased the A_{2A}AR affinity, similar to the result shown for the A_{2A}AR-selective antagonist binding. The interaction sites of the additional phenyl rings were very close to each other. The superimposition of the bound conformations of the A_{2A}AR-selective agonist **4** and antagonist **2** in their putative binding sites demonstrated the partial overlap of the binding sites of the adenine and triazolopyrimidine rings and their C-2 and N^7 substituents (Figure 6.6).

The A_{2A}AR complex with its agonist showed a preference for the intermediate conformation about the glycosydic bond. There might be subtle differences in binding requirements, conformational preferences, and local environments among subtypes of ARs, although most of the amino acid sequences in the putative binding sites (TM regions) are conserved among the four types of ARs. The electrostatic potential

maps of the A_{2A}AR and A_3AR showed some differences in the shape and electrostatic nature of their binding sites near the second extracellular loop (Figure 6.7).

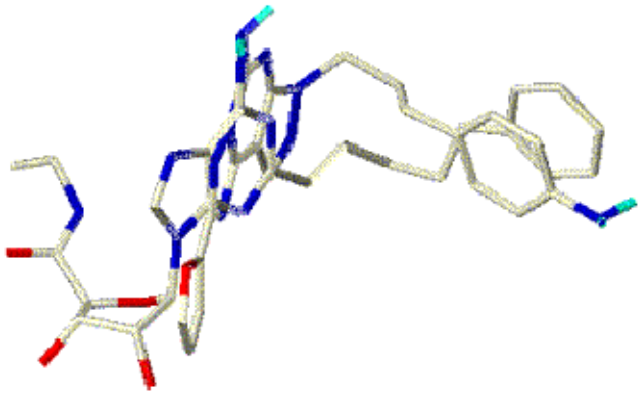

Figure 6.6 Superimposition of the bound conformations of the A_{2A}AR-selective antagonist **2** and agonist **4** in the putative binding sites. The colors represent atom type.

6.2.6 Conformational hypothesis for activation of the A_{2A}AR

Agonist binding was significantly different than antagonist binding in the region of the ribose ring, as expected from the requirement for a ribose ring in the agonist but not in the antagonist. Thus, the putative ribose-binding region is probably involved in receptor activation. For the A_3AR,[10] Jacobson and co-workers tried to gain insight into the distinct structural requirements for binding and activation by using ligand effects on cyclic AMP production in intact CHO (Chinese hamster ovary) cells and docking a few adenosine analogues. An interesting result concerned the conserved W243 (6.48) side chain in the A_3AR, which was involved in recognition of the classical (non nucleoside) A_3AR antagonists but not adenosine-derived ligands and which displayed a characteristic movement (counter clockwise rotation, as viewed from the exofacial side) exclusively upon docking of agonists.[10] We concluded similarly for the A_{2A}AR that a significant distinction between agonists and antagonists was whether ligand binding could effect the movement of W246 (6.48) side chain (Figure 6.4). Additional binding of the ribose 5′-substituents shown in the agonist complex induced the movement of the side-chain of W246 (6.48). That conformational change might disrupt a network of H-bonding of W246 (6.48), as well

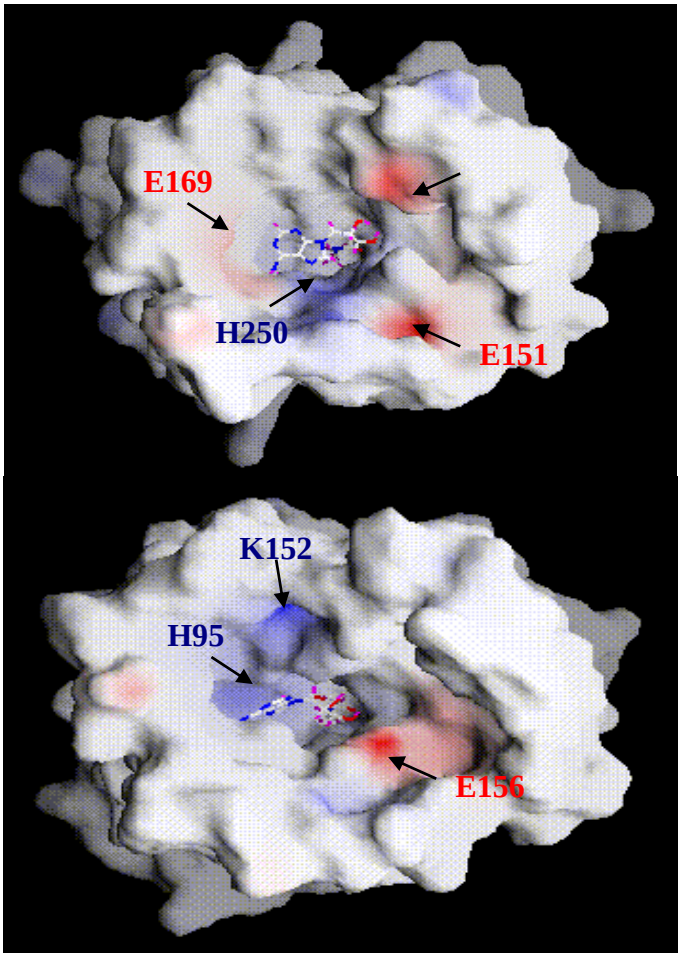

Figure 6.7 Electrostatic potential map made with the Grasp program. Putative binding sites of the A_{2A}AR (**top**) and A_3AR (**bottom**), with the second extracellular loop removed from the extracellular view. NECA **3** is represented as a stick model. Blue and red color potential indicates the electronic positive and negative, respectively.

as hydrophobic interactions of W246 (6.48) with residues from TMs 3, 6, and 7, thus facilitating a conformational change upon receptor activation. If the A_{2A}AR behaves like the A_3AR,[10] then flexibility of the ribose moiety and specific recognition elements at the 3′- and 5′-positions, to permit the movement of TM6, would be important for agonism at the A_{2A}AR. The modeling result indicated that the overall flexibility and binding elements of the ribose ring were important for distinguishing the receptor interactions of agonists and antagonists. It also correlated with recent studies[19] based on electron paramagnetic resonance and fluorescence spectroscopy, which suggested an outward movement of the cytoplasmic end of TMs 3 and 6, as well as an anticlockwise rotation of TM6 around its helical axis as viewed from the extracellular side.

6.2.7 Amino derivatives of adenosine as neoligands for neoceptors derived from the A_{2A}AR

The current model, like the A_3AR model,[10] suggested the ribose moiety was in proximity to hydrophilic residues of TM3. This hypothesis was tested experimentally by making complementary changes in the structures of the agonist ligand (i.e. introducing a positively charged ammonium group) and the receptor (i.e. introducing a negatively charged carboxylate group) to provide a new electrostatic interaction as the basis of neoceptor-neoligand pairs. Four amino derivatives (Figure 6.2) were tested in binding to a variety of Asp and Glu mutant receptors (Table 6.2). The 5′-aminoethyluronamide **8** (equivalent to appending an amino group at the end of the 5′-substituent of **3**) displayed a large selective enhancement in binding to the T88D mutant receptor (Figure 6.8). Also, compound **7** displayed a significant enhancement of affinity at the same mutant receptor. However, other possible electrostatic interactions of the ribose 3′-amino groups of compounds **6** and **7** with negatively charged mutant receptors, such as H278E, as suggested in the model, were not supported in the binding assay.

Table 6.2 Binding affinity of amino derivatives of adenosine (see Figure 6.2) at wt and mutant human A_{2A}ARs[a]

	K_i (μM)			
mutant receptor	**5**	**6**	**7**	**8**
WT	543±51	67±13	79±16	46.1±4.2
T88D	407±142	18±7	6.5±1.9	4.4±1.6
T88E	492±161	57±8	64±28	57±19
Q89D	52±9	6.4±0.9	58±18	3.6±1.0
S277E	604±125	88±36	67±11	41±8
H278D	-	87±36	59±19	121±32
H278E	-	64±5	56±6	72±14

[a]Membranes from COS-7 cells transfected with WT or mutant A_{2A}AR cDNA were incubated with 1.0 nM [^{3}H]ZM241385 in duplicate, together with increasing concentrations of the competing compounds, in a final volume of 0.4 mL of Tris HCl buffer (50 mM, pH 7.4) at 25 °C for 120 min. The K_i values are expressed as mean ± standard error from three independent experiments.

For the docking studies of neoceptor and neoligand,[12] three mutant receptors (i.e. T88D, S277D, and H278E) were optimised through a molecular dynamics (MD) procedure after the mutation of each side chain. T88, S277, and H278 residues in the inactive state of A_{2A}AR preferred the gauche (*g*) rotamer conformation, which also

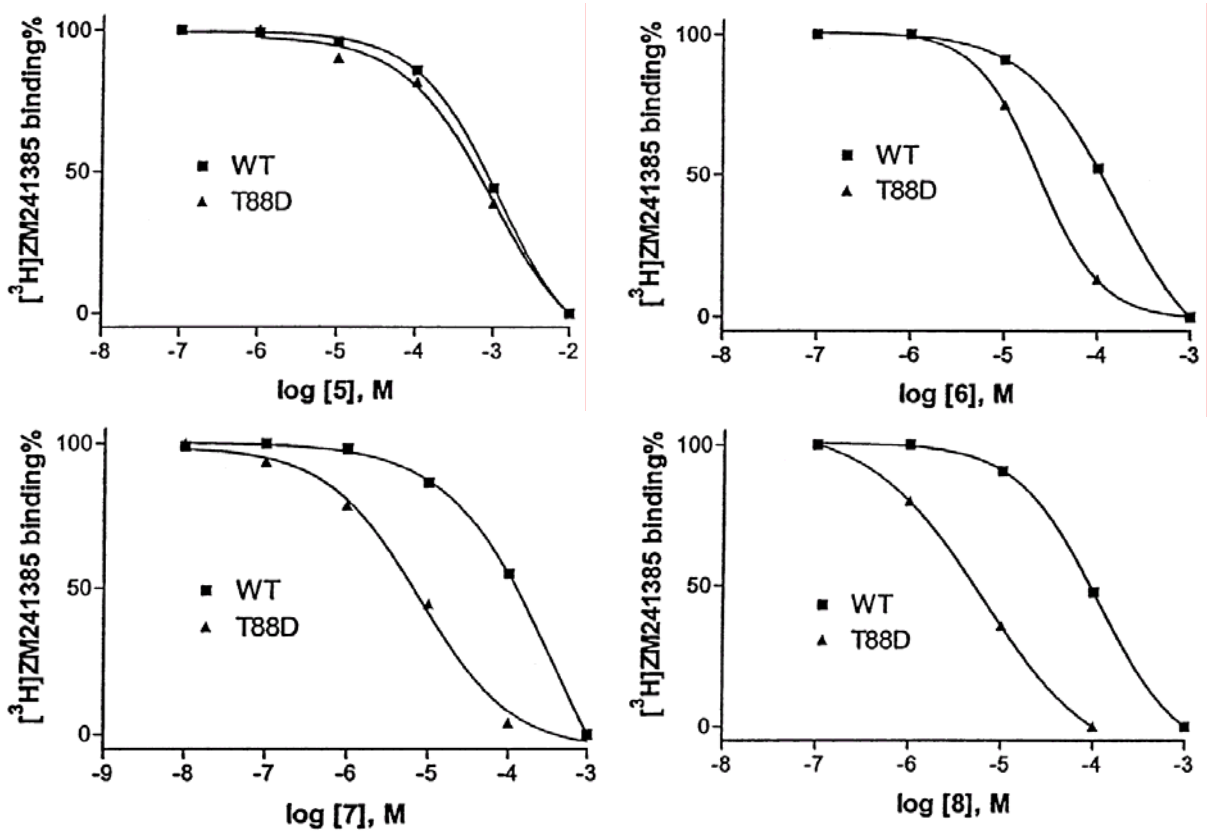

Figure 6.8 Effect of the amino derivatives of adenosine **5**, **6**, **7** and **8** on the binding of the radiolabeled antagonist [^{3}H]ZM241385 to the human A_{2A}AR. Membranes (10-20 μg of protein) from COS-7 cells transfected with wild type or T88D mutant receptor. Membranes were incubated with 1.0 nM [^{3}H]ZM241385 in duplicate, together with increasing concentrations of the competing compounds, in a final volume of 0.4 mL of Tris HCl buffer (50 mM, pH 7.4) at 25 °C for 120 min. Results were from a representative experiment. The K_i values were from three independent experiments and are listed in Table 6.2.

occurred in the bound state of the A_{2A}AR/**3** complex. However, in the T88D mutant receptor, the side chain of aspartate residue was in the trans (*t*) form, because of new H-bonding of the carboxylate group with N181 (5.42). Thus, there was a local conformational change with respect to the wild type in the position and direction of the aspartate side chain. This conformational change was consistent with the binding profile of the neoceptor. Initially, on the basis of the model of the unoccupied native A_{2A}AR, the 5′-amino derivative **5** was expected to display an enhanced affinity for the neoceptor T88D. However, **5** did not display an increase of binding affinity, whereas compound **8** with the extended ammonium group was enhanced in affinity.

The docking result of compound **8** (Figure 6.9**A**) suggested the possibility of the salt bridge and H-bonding between acidic residues of D88 and the terminal ammonium

ion, but the loss of H-bonding at the 3′- and 5′-position, as suggested in **3** binding to the wild-type A_{2A}AR.

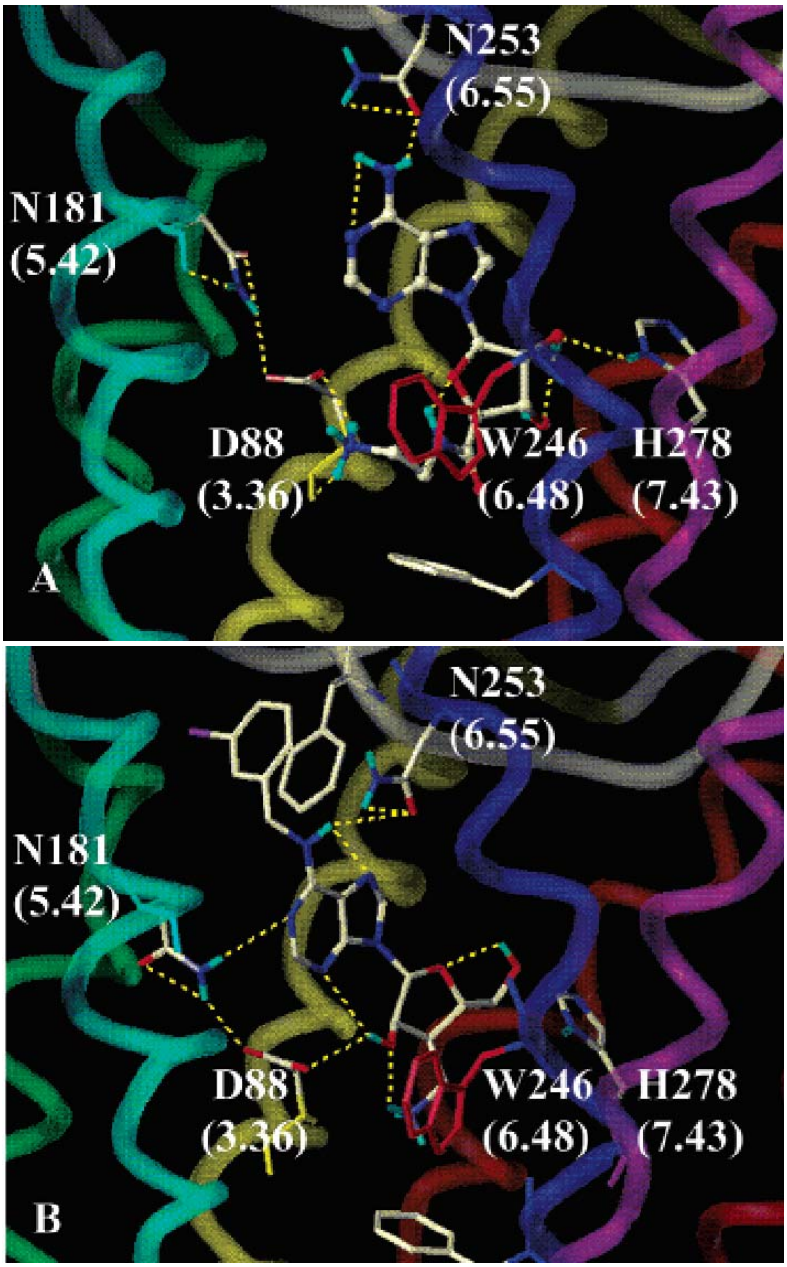

Figure 6.9 Complex of the T88D neoceptor with neoligand. (**A**) Compound **8** with 5′-aminoethyluronamide group. (**B**) Compound **7** with a 3′-aminomethyl group (represented in the protonated form). The neoligands are represented as ball-and-stick models. The intermolecular H-bonding between neoceptor and neoligand is displayed as yellow color. The W246 (6.48) of the T88D A_{2A}AR in red shows the movement of the indole side chain upon ligand binding.

Compound **7** was additionally substituted at the N^6-position and also displayed binding enhancement at the T88D mutant receptor. In the docking of **7**, a different binding mode that was energetically unfavorable in the A_{2A}AR/**3** complex was

suggested, because with side-chain geometry that was identical to that of the A_{2A}AR/**3** complex, it was impossible for the 3′-ammonium group of **7** to interact with the side chain of D88. In its complex, the conjugation of H-bonding between D88 and 3′-ammonium ion through the 2′-OH group was suggested. An additional interaction of the N^6-benzyl group of **7** with the second extracellular loop, especially through hydrophobic interaction with F168, was evident in the model (Figure 6.9**B**); however, there was no interaction of the 5′-OH with this neoceptor. The conformational search of compounds **6** and **7** indicated that the lowest-energy conformer of compound **7** had more stable intramolecular H-bonding of the 2′-OH group and the 3′-ammonium ion than was displayed by compound **6**. It was consistent with the experimental result: i.e. compound **7** showed a greater increase of binding affinity to its neoceptor than compound **6** did. Thus, we identified new neoceptor (T88D)-neoligand pairs consistent with the theoretical model, even though the binding affinities to the T88D neoceptor were still low compared to the endogenous ligand binding to the wild-type A_{2A}AR.

6.3 Conclusion

The molecular modeling results provided insight into the binding requirements for agonists and antagonists at the A_{2A}AR. Structural differences between the A_{2A}AR and the A_3AR include the microenvironment surrounding docked agonist. Structural similarities between the A_{2A}AR and the A_3AR include the hydrophobic region surrounding W246 (6.48), and the proposed rotation of TM6 to induce receptor activation. The introduction of a hydrophilic moiety such as ribose into an otherwise hydrophobic region destabilizes the inactive ground state of the receptor and thus would facilitate activation. Furthermore, this study is intended to facilitate further design of adenosine analogues targeted for improved A_{2A}AR affinity and selectivity, i.e. neoceptor-neoligand pairs.[12] The identification of the T88D receptor as a new neoceptor that may be activated selectively by synthetic ligands, such as **7** and **8**. Moreover, the putative electrostatic interaction, which enhances affinity by anchoring the ligand in the agonist binding site, also serves to validate the model.

6.4 Experimental section

*Biological evaluation and molecular modeling was performed by the group of Dr. Kenneth A. Jacobson, at the Laboratory for Bioorganic Chemistry (NIDDK), NIH, Maryland, USA. For the detailed procedures on site-directed mutagenesis, the transient expression of wild-type and mutant receptors in COS-7 cells, membrane preparation, radioligand binding assay, radioligand binding studies and molecular modeling we refer to the experimental part in our J. Med. Chem. paper (**2003**, 46, 4847).*

6.5 References

[1] Fredholm, B. B.; IJzerman, A. P.; Jacobson, K. A.; Klotz, K.-N.; Linden, J. *Pharmacol. Rev.* **2001**, *53*, 527-552.

[2] Stone, T. W.; Collis, M. G.; Williams, M.; Miller, L. P.; Karasawa, A.; Hillaire-Buys, D. Adenosine: Some Therapeutic Applications and Prospects. In *Pharmacological Sciences: Perspectives for Research and Therapy in the Late 1990s*; Cuello, A. C., Collier, B., Eds.; Birkhauser Verlag: Basel, Switzerland, 1995; pp 303- 309.

[3] Richardson, P. J.; Kase, H.; Jenner, P. G. *Trends Pharmacol. Sci.* **1997**, *18*, 338-344.

[4] Ledent, C.; Vaugeois, J. M.; Schiffmann, S. N.; Pedrazzini, T.; El Yacoubi, M.; Vanderhaeghen, J. J.; Costentin, J.; Heath, J. K.; Vassart, G.; Parmentier, M. *Nature (London)* **1997**, *388*, 674-678.

[5] Baraldi, P. G.; Cacciari, B.; Spalluto, G.; Borioni, A.; Viziano, M.; Dionisotti, S.; Ongini, E. *Curr. Med. Chem.* **1995**, *2*, 707-722.

[6] Kim, J.; Wess, J.; van Rhee, A. M.; Schöneberg, T.; Jacobson, K. A. *J. Biol. Chem*. **1995**, *270*, 13987-13997.

[7] IJzerman, A. P.; van der Wenden, E. M.; van Galen, P. J. M.; Jacobson, K. A. *Eur. J. Pharmacol.: Mol. Pharmacol*. **1994**, *268*, 95-104.

[8] Gao, Z.-G.; Chen, A.; Barak, D.; Kim, S.-K.; Müller, C. E.; Jacobson, K. A. *J. Biol. Chem*. **2002**, *277*, 19056-19063.

[9] Palczewski, K.; Kumasaka, T.; Hori, T.; Behnke, C. A.; Motoshima, H.; Fox, B. A.; Le Trong, I.; Teller, D. C.; Okada, T.; Stenkamp, T. E.; Yamamoto, M.; Miyano, M. *Science* **2000**, *289*, 739-745.

[10] Gao, Z.-G.; Kim, S.-K.; Biadatti, T.; Chen, Q.; Lee, K.; Barak, D.; Kim, S. G.; Johnson, C. R.; Jacobson K. A. *J. Med. Chem.* **2002**, *45*, 4471-4484.

[11] Our most recent model of the human A_3AR (by Dr. Soo-Kyung Kim) is now available on the pdb ftp site. Entry in PDB format (compressed): pdblo74.ent. Z.; Entry in mmCIF format (compressed): lo74.cif. Z. See http://www.rcsb.org/pdb/latest_news.html#models_removal2.

[12] Jacobson, K. A.; Gao, Z. G.; Chen, A.; Barak, D.; Kim, S. A.; Lee, K.; Link, A.; Van Rompaey, P.; Van Calenbergh, S.; Liang, B. T. *J. Med. Chem*. **2001**, *44*, 4125-4136.

[13] Gallo-Rodriguez, C.; Ji, X.-D.; Melman, N.; Siegman, B. D.; Sanders, L. H.; Orlina, J.; Fischer, B.; Pu, Q.-L.; Olah. M. E.; van Galen, P. J. M.; Stiles, G. L.; Jacobson, K. A. *J. Med. Chem.* **1994**, *37*, 636.

[14] Jiang, Q.; van Rhee, M.; Kim. J.; Yehle, S.; Wess, J.; Jacobson, K. A. *Mol. Pharmacol*. **1996**, *50*, 512-521.

[15] Weiss, H. M.; Grisshammer, R. *Eur. J. Biochem*. **2002**, *269*, 82-92.

[16] Archer, E.; Maigret, B.; Escrieut, C.; Pradayrol, L.; Fourmy, D. *Trends Pharm. Sci.* **2003**, *24*, 36- 40.

[17] Chambers, J. J.; Nichols, D. E. *J. Comput. Aided Mol. Des*. **2002**, *16*, 511-520.

[18] Vittori, S.; Camaioni, E.; Francesco, E. D.; Volpini, R.; Monopoli, A.; Dionisotti, S.; Ongini, E.; Cristalli, G. *J. Med. Chem*. **1996**, *39*, 4211-4217.

[19] Farrens, D. L.; Altenbach, C.; Yang, K.; Hubell, W. L.; Khorana, H. G. *Science* **1996**, *274*, 768-770.

PART III
BIOLOGICAL EVALUATION OF THE MODIFIED THYMIDINE ANALOGUES

Biological results in this part were published in:

Eur. J. Org. Chem. **2003**, *15*, 2911.

CHAPTER 7

GENERAL BACKGROUND

7.1 Pseudororation and conformational flexibility of nucleosides

Due to its inherent flexibility the sugar ring of nucleosides, in solution, rapidly equilibrates between two extreme forms of ring pucker (Figure 7.1):

- the north (N) or C3'-*endo*-C2'-*exo* conformation, and
- the opposite south (S) or C2'-*endo*-C3'-*exo* conformation.

Complete conformational definition of a nucleoside usually involves the determination of three structural parameters:[1]

- (1) the glycosyl torsion angle χ (Figure 7.1**A**-**D**), which determines the *syn* or *anti* position of the base relative to the sugar moiety (*syn* when the C2 carbonyl of pyrimidines or N3 of purines lies over the sugar ring, *anti* when these atoms are oriented in the opposite direction);
- (2) the torsion angle γ (Figure 7.1**C**), which defines the orientation of the 5'-hydroxyl with respect to C3' (represented are the three main rotamers;
- (3) the puckering of the furanose ring and its deviation from planarity, which are described by the phase angle of pseudorotation[2] *P* (0-360°, Figure 7.1**B**) and the maximum out-of-plane pucker ν_{max}.

The value of *P* depends on the five endocyclic sugar torsion angles ν_0-ν_4 (see below). By convention, a phase angle *P* = 0° corresponds to a N conformation, with a symmetrical twist form $^3T_2$, whereas the S antipode, $^2T_3$, possesses phase angle *P* = 180°. The conformation of the furanose ring around the pseudorotational cycle alternates every 18° between envelope (*E*) and twist (*T*) conformations. The superscripts and subscripts represent, respectively, atoms displaced above and

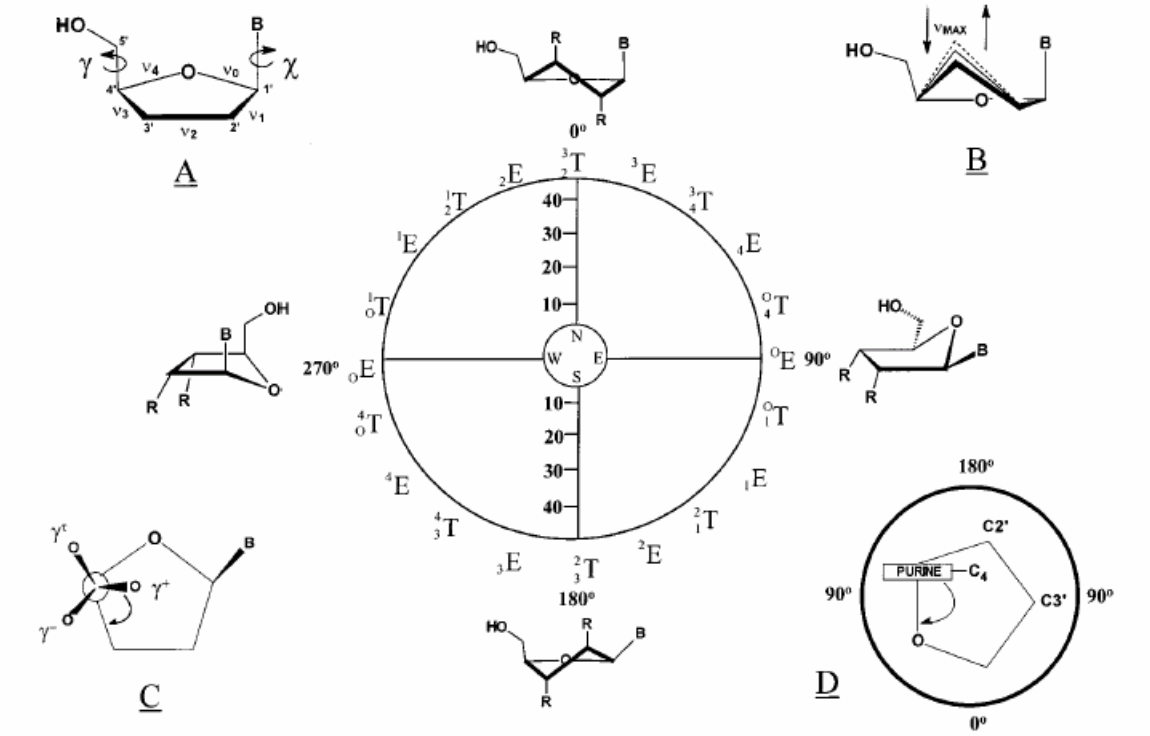

Figure 7.1 Pseudorotational cycle (center) illustrating the nucleoside ring pucker parameter *P* and description of other nucleoside structural parameters. Different twist (T) or envelope (E) form are obtained for every 18° torsion in the furanose ring angles from *P* = 0° to 360°. **A** General view and labeling of ring torsion angles ν_0-ν_4. **B** Description of maximum out-of-plane pucker parameter ν_{max}. **C** Definition of angle γ. **D** Definition of angle χ for a purine nucleoside.

below the C4'-O4'-C1' plane (relative to other atoms). Atoms displaced on the same side as C5' are called *endo*, those on the opposite side are called *exo*. Although *P* and the torsion angles γ and χ are interdependent, the preferred ring pucker is known to be the strongest conformational parameters and is determined by the interplay of the anomeric and *gauche* effect.[1,3]

A broad definition of the anomeric effect is: *"In a fragment C-**X**-C-**Y**, where ligand **X** carries one or two lone pairs of electrons and **Y** represents an electronegative ligand, the gauche conformers along the central X-C bond are preferred over the trans form."*[4] In nucleosides and related sugars this means that an electronegative ligand **L** at C1' is driven to adopt the pseudoaxial position (*gauche* C4'-O4'-C1'-**L**). Preference for a pseudoaxial position at C1' means a drive toward the N form in the β-D-series (S form in the α-D-series). In practice, matters are complicated by the stereo-electronic competition at the anomeric center (C1'),[5] and the fact that the anomeric strength of a given aglycon varies with the chemical nature of nearby substituents.[6] The *gauche*

effect describes the tendency of a vicinal fragment **X**-C-C-**Y** to adopt a *gauche* conformation along the central C-C bond in cases where **X** and **Y** represent electronegative ligands or electron pairs (although dipole-dipole repulsions and steric factors can work in favor of the antiperiplanar form).

A standard method for assessing the solution conformation of a furanose ring involves the NMR measurement of three-bond ^{1}H-^{1}H coupling constants ($^{3}J_{HH}$, of the ring hydrogens) and subsequent analysis of these data with the program PSEUROT.[7] This program assumes a model of equilibration between the north and south pseudorotational conformers. With knowledge of the five endocyclic torsion angles of a given conformer (ν_0-ν_4, see Figure 7.1**A**), *P* can be calculated through the use of equation 1.[1] The puckering amplitude ν_{max} is related to *P* and ν_0 through equation 2.[1]

$$\tan P = (\nu_2 + \nu_4) - (\nu_1 + \nu_3) / (3.077 * \nu_0) \qquad \text{(equation 1)}$$

$$\nu_{max} = \nu_0 / \cos P \qquad \text{(equation 2)}$$

PSEUROT calculates the *P* and ν_{max} values of the two conformers (and their mole fraction) that best fit the experimental $^{3}J_{HH}$ data. This is done by correlation of the experimental $^{3}J_{HH}$ (exocyclic H-C-C-H dihedral angles ϕ_i^{HH}) to the corresponding endocyclic torsion angles (ν_i), through a generalized Karplus equation,[8] from which *P* is calculated. The correlation of ϕ_i^{HH} with ν_i given by via equation 3.

$$\phi_i^{HH} = (A_i * \nu_i) + B_i \quad i = 0, 1, 2, 3, 4 \qquad \text{(equation 3)}$$

In the initial parametrization of PSEUROT, A_i and B_i constants were determined for β-ribofuranosyl and 2-deoxy-β-ribofuranosyl rings through the analysis of a database[9] containing the crystal structures of 178 nucleosides and nucleotides. Using these values, estimates of A_i and B_i for other ring systems (e.g. β-arabinofuranosyl systems) were made,[10] and these values are included in the 6.2 version[11] of PSEUROT. More recently, computational methods have been used to determine these constants for other ring systems.[14]

In the solid state, usually only one of the two solution conformations is present due to the influence of crystal packing forces.[1,9] Recent studies suggest that the majority of enzymes[15] and receptors[16] have strict conformational requirements for nucleoside substrate binding, i.e. only one conformational form is favoured in the active site. So, conformational data of nucleosides, both from (solid) X-ray structure or (solution) NMR analysis, has to be interpreted with care (in structure-activity-relationship studies), since the binding conformation is likely to be altered by the enzyme. In Chapter 8, we conducted a conformational analysis on thymidine analogues as TMPKmt inhibitors. The prepared derivatives (designed to show improved TMPKmt affinity) were only moderately active. Hence, we investigated more closely their conformational preferences in solution and correlated these findings with their probable enzyme bound conformation.[17]

7.2 References and notes

[1] (i) Altona, C.; Sundaralingam, M. *J. Am. Chem. Soc*. **1972**, *94*, 8205. (ii) Altona, C.; Sundaralingam, M. *J. Am. Chem. Soc*. **1973**, *95*, 2333. (iii) Saenger, W. *Principles of Nucleic Acid Structure*; Springer-Verlag: New York, **1984.**

[2] (i) Kilpatrick, J. E.; Pitzer, K. S.; Spitzer, R. *J. Am. Chem. Soc.* **1947**, *69*, 2483. (ii) Pitzer, K. S.; Donath, W. F. *J. Am. Chem. Soc.* **1959**, *81*, 3213.

[3] Plavec, J.; Tong, W.; Chattopadhyaya, J. *J. Am. Chem. Soc.* **1993**, *115*, 9734.

[4] (i) *The Anomeric Effect and its Associated Stereoelectronic Effects*; Thatcher, G. R. J., Ed.; ACS Symposium Series; American Chemical Society: Washington, DC, **1993**. (ii) Kirby, A. J. *The Anomeric Effect and Related Stereoelectronic Effects at Oxygen*; Springer-Verlag: Berlin, **1983**.

[5] Krol, M. C.; Huige, C. J. M.; Altona, C. *J. Comput. Chem*. **1990**, *11*, 765.

[6] (i) Thibaudeau, C.; Földesi, A.; Chattopadhyaya, J. *Tetrahedron* **1998**, *54*, 1867. (ii) Thibaudeau, C.; Plavec, J.; Chattopadhyaya, J. *J. Org. Chem*. **1996**, *61*, 266.

[7] (i) van Wijk, J.; Haasnoot, C. A. G.; de Leeuw, F. A. A. M.; Huckriede, B. D.; Westra Hoekzema, A.; Altona, C. *PSEUROT 6.2* **1993**; Leiden Institute of Chemistry, Leiden University. (ii) de Leeuw, F. A. A. M.; Altona, C. *J. Comput. Chem.* **1983**, *4*, 428. (c) Altona, C. *Recl. Trav. Chem. Pays-Bas* **1982**, *101*, 413.

[8] (i) Haasnoot, C. A. G.; de Leeuw, F. A. A. M.; Altona, C. *Tetrahedron* **1980**, *36*, 2783. (ii) Haasnoot, C. A. G.; de Leeuw, F. A. A. M.; de Leeuw, H. P. M.; Altona, C. *Org. Magn.*

Reson. **1981**, *15*, 43. (iii) Altona, C.; Francke, R.; de Haan, R.; Ippel, J. H.; Daalmans, G. J.; Westra Hoekzema, A. J. A.; van Wijk, J*. Magn. Reson. Chem.* **1994**, *32*, 670. (iv) van Wijk, J.; Huckriede, B. D.; Ippel, J. H.; Altona, C. *Methods Enzymol.* **1992**, *211*, 286.

[9] De Leeuw, H. P. M.; Haasnoot, C. A. G.; Altona, C. *Isr. J. Chem*. **1980**, *20*, 108.

[10] De Leeuw, F. A. A. M.; Altona, C. *J. Chem. Soc.*, *Perkin Trans. 2.* **1982**, 375.

[11] When only three vicinal $^3J_{HH}$ coupling constants along the ring bonds exist, two of the five conformational parameters must be kept fixed during the minimization. This fixing is usually not much of a problem when the equilibrium is strongly one-sided (major form >85%) but may lead to wide ranges of possible conformational parameters otherwise. These ranges can be narrowed by increasing the ratio of the number of data points vs the number of parameters. To achieve this, two different strategies can be employed: (i) measurement of the NMR spectra over a wide range of temperatures; (ii) the inclusion of other coupling information in the calculation. Chattopadhyaya and co-workers have recently developed a new Karplus-type relation between vicinal proton-fluorine coupling constants and the corresponding H-C-C-F torsion angles including correction terms for substituent.[13] The latest PSEUROT release (version 6.3) incorporates the published Karplus parameters for $^3J_{HF}$ and allows simultaneous analysis of $^3J_{HH}$ and $^3J_{HF}$ experimental coupling constants, which greatly facilitates the conformational analysis of fluorinated furanose rings because of the increase in the number of experimental data points over the puckering parameters *P* and ν_{max}.[14] The conformational analysis of the thymidine analogues in Chapter 8 was performed with the PSEUROT 6.2, but NMR experiments were carried out at five temperature intervals (278K-333K).

[12] Thibaudeau, C.; Plavec, J.; Chattopadhyaya, J. *J. Org. Chem*. **1998**, *63*, 4967.

[13] (i) van Wijk, J.; Haasnoot, C. A. G.; de Leeuw, F. A. A. M.; Huckriede, B. D.; Westra Hoekzema, A. J. A.; Altona, C. *PSEUROT 6.3* **1999**; Leiden Institute of Chemistry, Leiden University. (ii) Mikhailopulo, I. A.; Pricota, T. I.; Sivets, G. G.; Altona, C. A. *J. Org. Chem.* **2003**, *68*, 5897.

[14] (i) Thibaudeau, C.; Kumar, A.; Bekiroglu, S.; Matsuda, A.; Marquez, V. E. Chattopadhyaya, J. *J. Org. Chem.* **1998**, *63*, 5447. (ii) Plavec, J.; Tong, W.; Chattopadhyaya, J. *J. Am. Chem. Soc.* **1993**, *115*, 9734. (iii) Crnugelj, M.; Dukhan, D.; Barascut, J.-L.; Imbach, J.-L.; Plavec, J. *J. Chem. Soc.*, *Perkin Trans. 2* **2000**, 255. (iv) Callam, C. S.; Lowary, T. L. *J. Org. Chem.* **2001**, *66*, 8961. (v) Houseknecht, J. B.; Altona, C.; Hadad, C. M.; Lowary, T. *J. Org. Chem.* **2002**, *67*, 4647.

[15] (i) Marquez, V. E.; Siddiqui, M. A.; Ezzitouni, A.; Russ, P.; Wang, J.; Wagner, R. W.; Matteucci, M. D. *J. Med. Chem.* **1996**, *39*, 3739. (ii) Ezzitouni, A.; Marquez, V. E. *J. Chem. Soc., Perkin Trans. 1* **1997**, 1073. (iii) Marquez, V. E.; Ezzitouni, A.; Russ, P.; Siddiqui, M. A.; Ford, H.; Feldman, R. J.; Mitsuya, H.; George, C.; Barchi, J. J. *J. Am. Chem. Soc.* **1998**, *120*,

2780. (iv) Ford, H.; Dai, F.; Mu, L.; Siddiqui, M. A.; Nicklaus, M. C.; Anderson, L.; Marquez, V.; Barchi, J. J. *Biochemistry* **2000**, *39*, 2581. (v) Choi, Y.; George, C.; Strazewski, P.; Marquez, V. E. *Org. Lett.* **2002**, *4*, 589. (vi) Choi, Y.; George, C.; Comin, M. J.; Barchi, J. J.; Kim, H. S.; Jacobson, K. A.; Balzarini, J.; Mitsuya, H.; Boyer, P. L.; Hughes, S. H.; Marquez, V. *J. Med. Chem.* **2003**, *46*, 3292. (vii) Russ, P.; Schelling, P.; Scapozza, L.; Folkers, G.; De Clercq, E.; Marquez, V. E. *J. Med. Chem.* **2003**, *46*, 5045.

[16] (i) Jacobson, K. A.; Ji, X.-D.; Li, A.-H.; Melman, N.; Siddiqui, M. A.; Shin, K.-J.; Marquez, V. E.; Ravi, R. G. *J. Med. Chem.* **2000**, *43*, 2196. (ii) Kim, H. S.; Ravi, R. G.; Marquez, V. E.; Maddileti, S.; Wihlborg, A.-K. Erlinge, D.; Malmsjo, M.; Boyer, J. L.; Harden, T. K.; Jacobson, K. A. *J. Med. Chem.* **2002**, *45*, 208. (iii) Kim, H. S.; Ohno, M.; Xu, B.; Kim, H. O.; Choi, Y.; Ji, X. D.; Maddileti, S.; Marquez, V. E.; Harden, T. K.; Jacobson, K. A. *J. Med. Chem.* **2003**, *46*, 4974.

[17] Van Rompaey, P.; Nauwelaerts, K.; Vanheusden, V.; Rozenski, J.; Munier-Lehmann, H.; Herdewijn, P.; Van Calenbergh, S. *Eur. J. Org. Chem.* **2003**, *15*, 2911.

CHAPTER 8

MYCOBACTERIUM TUBERCULOSIS THYMIDINE MONOPHOSPHATE KINASE INHIBITORS: BIOLOGICAL EVALUATION AND CONFORMATIONAL ANALYSIS OF 2'- AND 3'-MODIFIED THYMIDINE ANALOGUES

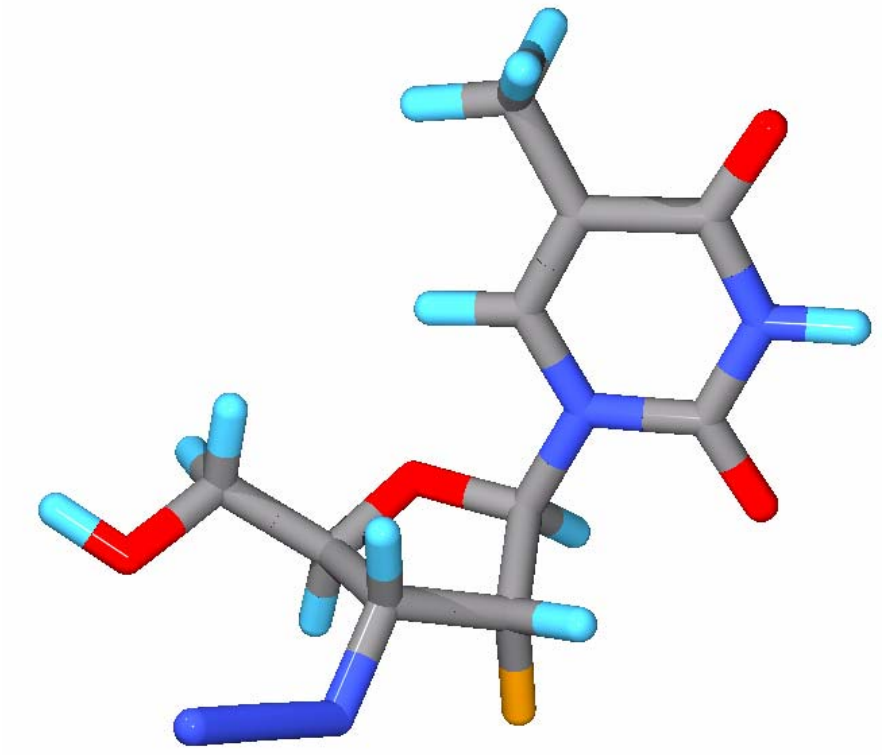

This chapter is published in part in:

Philippe Van Rompaey, Koen Nauwelaerts, Veerle Vanheusden, Jef Rozenski, Hélène Munier-Lehmann, Piet Herdewijn and Serge Van Calenbergh

Eur. J. Org. Chem. **2003**, *15*, 2911-2918.

8.1 Introduction

Each year *Mycobacterium tuberculosis*, the intracellular parasite that causes tuberculosis (TB), kills approximately 2 million people.[1] The World Health Organization (WHO) declared TB a global health emergency and estimates that between 2002 and 2020 approximately 1000 million people will be newly infected and 36 million will die from TB.[2,3] Major contributors to the resurgence of this pulmonary disease and its worsening impact are the breakdown in health services, the pandemic of AIDS and the emergence of multidrug-resistant (MDR)-TB.[3] The immune system can "wall off" the bacilli, allowing TB to stay dormant for years and to emerge when the immune system is weakened. This explains why TB is a leading cause of death among HIV-positive persons.[3,4] The current treatment strategy of TB is based on an intensive 6 to 8-month regimen of multiple antibiotics such as rifampicine, isoniazid, pyrazinamide and ethambutol or streptomycin.[5] However, *Mycobacterium tuberculosis* strains resistant to some or all of these major anti-TB drugs have emerged and are associated with high death rates of 50-80%.[6] The "MDR" prefix refers to the simultaneous resistance to at least isoniazid and rifampicin, the two most potent anti-TB drugs, caused primarily by inconsistent, partial or improper treatment regimens.

These facts impose the need to identify new targets and to develop new anti-TB drugs in order to optimise and/or shorten the current TB treatment and to combat resistance. In that light, *Mycobacterium tuberculosis* thymidine monophosphate kinase (TMPKmt), an essential enzyme of nucleotide metabolism that catalyses the reversible phosphorylation of thymidine monophosphate (dTMP) to thymidine diphospate (dTDP), has recently been introduced as a novel potential target for chemotherapeutic intervention.[7,8] Although the global fold of the TMPKmt enzyme is similar to that of other TMPK isozymes, it has a low degree of amino acid sequence identity with the *E. coli* (26 %), yeast (25 %) and human (22 %) isozymes, making it an attractive target for blocking mycobacterial DNA synthesis.[8]

The X-ray structure of the dTMP-TMPKmt complex (Figure 8.1) indicated that the main binding interactions between dTMP and the enzyme involve both its pyrimidine base (i.e. stacking interaction with Phe70 and *O*4 and *N*3 participating in hydrogen

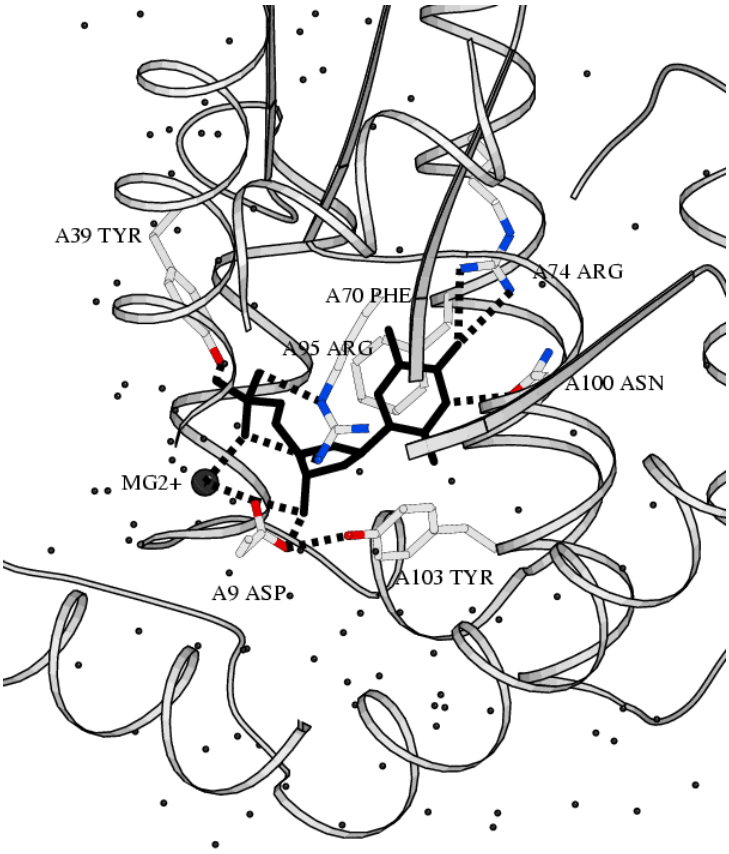

Figure 8.1 Schematic representation of the most important amino acid residues of TMPKmt interacting with **dTMP** (in **black**). The main bonding forces between dTMP and the enzyme are: (i) a stacking interaction between the pyrimidine ring and Phe70, (ii) a hydrogen bond between *O*4 of thymine and the Arg74 side-chain, which results in a preference for thymine over cytosine, (iii) a hydrogen bond between Asn100 and *N*3 of the thymine ring, (iv) a hydrogen bond between the 3'-hydroxyl of dTMP and the terminal carboxyl of Asp9, that in its turn interacts with the magnesium ion that is responsible for positioning the phosphate oxygen of dTMP, and (v) hydrogen bonds and an ionic interaction between the 5'-*O*-phosphoryl and Tyr39, Arg95 and Mg^{2+}, respectively. The presence of Tyr103 close to the 2'-position is believed to render the enzyme catalytically selective for 2'-deoxy nucleotides versus ribo nucleotides.

bonding with Arg74 and Asn100) and its ribofuranose ring moiety (i.e. hydrogen bond between the 3'-hydroxyl of dTMP and the terminal carboxyl of Asp9).[8] The presence of a tyrosine residue (Tyr103) close to the 2'-position allows the enzyme to discriminate between 2'-deoxynucleotides and ribonucleotides, only transforming the former.[8] Also this X-ray analysis revealed the substrate to adopt the "Southern" conformation.[8]

The fact that thymidine (dT) and 3'-azido-3'-deoxythymidine (AZT) proved to be competitive inhibitors of TMPKmt with low μM affinity,[9] led towards the synthesis and biological evaluation of several dT nucleoside and nucleotide analogues.[9-11] In this

paper we continue our search for nucleosidic TMPKmt inhibitors by combining favourable modifications at C-3' (N_3, NH_2) with the beneficial effects observed upon introduction of an α-chloro or α-fluoro substituent at C-2' (Figure 8.2).[10,11] Using NMR spectroscopy and pseudorotational analysis, we examined the solution state conformation of the sugar ring of the synthesized analogues to gain better insight into the molecular determinants of TMPKmt inhibition.

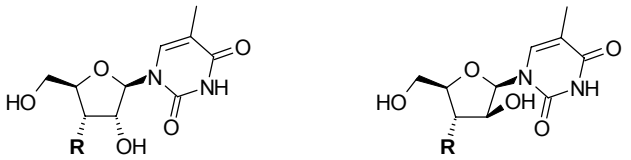

1 R = NH_2
2 R = N_3

3 R = NH_2
4 R = N_3

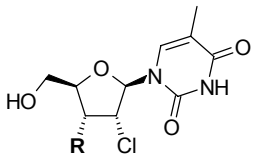

5 R = NH_2
6 R = N_3

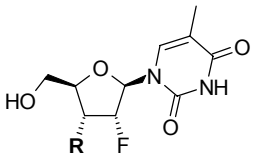

7 R = NH_2
8 R = N_3

Figure 8.2 2'- and 3'-modified thymidine analogues discussed in this Chapter.

8.2 Results and Discussion

8.2.1 Chemical Synthesis

The synthesis of the 2'- and 3'-modified thymidine analogue (**1**-**8**) is described in Part I.

8.2.2 TMPKmt affinity (Inhibition studies)

Results of the binding studies are presented in Table 8.1. The 3'-azido and 3'-amino substituents are intended for direct interaction with Asp 9. With the 2'-modifications we explored if an α-chloro or α-fluoro substituent in the vicinity of Tyr103 would be sterically tolerated.

Table 8.1 Kinetic parameters of *Mycobacterium tuberculosis* thymidylate kinase with the 2'- and 3'-modified thymidine analogues

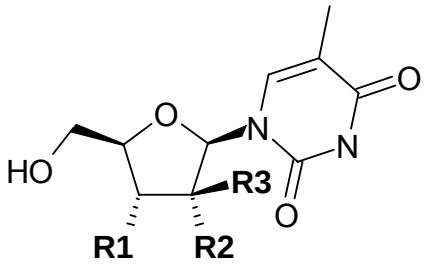

Analogue	R1	R2	R3	K_i (μM)
dT[9]	OH	H	H	27
AZT[9]	N_3	H	H	28
1	N_3	OH	H	740
2	NH_2	OH	H	750
3	N_3	H	OH	215
4	NH_2	H	OH	1260
5	N_3	Cl	H	170
6	NH_2	Cl	H	145
7	N_3	F	H	118
8	NH_2	F	H	190

As expected, the introduction of the 2'-hydroxyl function in **1** and **2** had adverse effects on the affinity, due to an unfavourable interaction with the nearby tyrosine residue (Tyr103). Indeed, the affinity markedly improves when the 2'-hydroxyl adopts the opposite *arabino* configuration in **3** (K_i = 215 μM), or when the 2'-*ribo*-hydroxyl (in **1** and **2**) is replaced by a chloro or fluoro atom in **5** (and **6**) and **7** (and **8**), respectively. The incorporation of a fluoro atom into the sugar moiety of nucleosides has great impact on the biological and chemical characteristics of these molecules.[12] The strong electronegative fluorine alters the electronic properties of the molecule and specifically tunes the conformation of the furanose ring.[12] Also, the 2'-α-fluoro atom in **7** (and **8**) isosterically replaces a hydrogen atom and is known to greatly enhance the stability of the glycosidic bond.[13] Still, the affinity for **5** (and **6**) and **7** (and **8**) is moderate, i.e. > 100 μM. This was not expected, since earlier work of our group suggested "to combine a 2'-chlorine and 3'-azido group".[10] Furthermore, the 3'-amino analogues **6** and **8**, showed no enhanced TMPKmt affinity compared to their 3'-azido forms **5** and **7**, indicating that the positively charged 3'-amine is not optimally oriented to form an ionic interaction with Asp9. These results prompted us to investigate the preferred puckering of the furanose ring of the 2'- and 3'-modified **5** (and **6**) and **7** (and **8**) pairs.

8.2.3 NMR spectroscopy

NMR spectroscopy in D_2O permits extension of the results to the in vivo/ in vitro situation and was used for the pseudorotational analysis[14] of nucleosides **5** (and **6**) and **7** (and **8**). The complete conformational analysis of a nucleoside (or nucleotide) usually comprises the determination of three principal structural parameters: (1) the glycosidic torsion angle χ, which determines the *syn* or *anti* position of the base relative to the sugar moiety; (2) the torsion angle γ, which determines the orientation of the 5'-hydroxyl with respect to the C3'; and (3) the puckering of the furanose ring and its deviation of planarity, described by the phase angle of pseudorotation *P* (0-360°) and the maximum out-of-plane pucker ν_{max} (30-46°).[14] Here, we only focussed on the latter, since (a) the ring puckering is known to be the main determinant in controlling the γ- and χ-angles;[15] (b) most probably a strong preference for a specific C4′-C5′ rotamer (γ-angle) is induced by the enzyme upon binding; and (c) as evidenced by the crystal structure data,[8] TMPKmt binds its substrates with the base in the *anti* position (χ-angle).

In solution, the relative strengths and interplay of important anomeric and *gauche* effects[15,16] drive the preference of the flexible furanose ring moiety of *N*-nucleosides between the north (N) and south (S) type puckered pseudorotamers. By convention, a phase angle $P = 0°$ corresponds to the absolute N conformation possessing a symmetrical twist form $^3T_2$ (C3'-*endo*-C2'-*exo*), whereas the S antipode twist, $^2T_3$ (C2'-*endo*-C3'-*exo*), is represented by $P = 180°$.[14] Along the pseudorotational cycle, the conformation of the furanose ring alternates between envelope (*E*) and twist (*T*) conformations every 18°. We measured vicinal proton-proton coupling constants ($J_{1',2'}$, $J_{2',3'}$ and $J_{3',4'}$) of **5** (and **6**) and **7** (and **8**) at 500 MHz in D_2O (ca. 40mM) in a 278-333 K range at pD 7.4 (Table 8.2.).

Subsequently, we used the computer program PSEUROT 6.2[17] to calculate, at each temperature interval, the best fit of five conformational parameters, i.e. *P* and ν_{max} for both N and S conformers and the mole fraction of S (X_S), based on the three experimental coupling constants (Table 8.2 and Table 8.3).

Table 8.2 $^3J_{H,H}$ coupling constants (Hz)[a] and population of S conformers[b] at five distinct temperatures in the range from 278 to 333 K

Temp (K)	$^3J_{1',2'}$[a]	$^3J_{2',3'}$	$^3J_{3',4'}$	X_S (%)[b]
5				
278	4.70	5.55	6.21	45
288	4.76	5.59	6.25	45
300	4.92	5.61	6.39	46
318	5.06	5.63	6.43	47
333	5.20	5.67	6.49	48
6				
278	2.12	4.93	8.17	16
288	2.30	4.94	8.11	17
300	2.50	4.94	7.91	20
318	2.66	4.95	7.80	21
333	2.69	4.95	7.73	22
7				
278	1.27	4.73	9.31	3
288	1.54	4.78	9.24	5
300	1.66	4.81	9.19	7
318	1.69	4.88	9.07	8
333	1.72	4.89	9.05	8
8				
278	$\leq$ 1.00	4.30	9.70	$\leq$ 1
288	$\leq$ 1.00	4.49	9.92	$\leq$ 1
300	$\leq$ 1.00	4.79	9.97	$\leq$ 1
318	$\leq$ 1.00	4.81	10.01	$\leq$ 1
333	$\leq$ 1.00	4.82	10.07	$\leq$ 1

[a] $^3J_{H,H}$ recorded at 500 MHz in D_2O at pD 7.4. [b] The PSEUROT program (version 6.2)[17] has been used to derive populations as well as geometries of N and S coformers (Table 8.3) at stated temperature.

The preferred solution state conformation of **5**, **6**, **7**, and **8** is determined by a variety of factors, but is primarily influenced by the class and positioning of the 2'- and 3'-substituents and the complex interplay of the resulting four *gauche* interactions, i.e. *O*4'-C4'-C3'-R3, *O*4'-C1'-C2'-R2, R2-C2'-C3'-R3 and *N*1-C1'-C2'-R2. The mole fraction of S at 30 °C (X_S) shows these analogues prefer the "northern" type ring puckering (Table 8.4). In combination with the 3'-azide modification, the 2'-chloro derivative **5** (P_N = -2.7°, $\nu_{max, N}$ = 37.5°) virtually adopts a $^3T_2$ (C3'-*endo*-C2'-*exo* twist) conformation, whereas the 2'-fluoro analogue **7** (P_N = 28.7°, $\nu_{max, N}$ = 34.6°) exhibits a conformation that lies between a ^3E (C3'-*endo* envelope) and $^3T_4$ (C3'-*endo*-C4'-*exo*

Table 8.3 Optimized pseudorotational parameters and errors of pseudorotational analysis[a] based on $^3J_{H,H}$ measured at five distinct temperatures in the range of 278 to 333 K

Analogue	P_N (deg)	$\nu_{max, N}$ (deg)	P_S (deg)	$\nu_{max, S}$ (deg)	Rms (Hz)[b]
5	-2.7	37.5	132.7	38.8	0.110
6	7.7	38.4	162.7	38.2	0.020
7	28.7	34.6	146.1[c]	36.0[c]	0.042
8	31.2	36.5	151.8[c]	30.0[c]	0.172

[a]The least-squares minimization program PSEUROT (version 6.2)[17] has been used for $^3J_{H,H}$ and equilibrium populations of N↔S equilibrium at various temperatures, see Table 8.2. [b]The rms deviation represents the deviation of calculated and experimental $^3J_{H,H}$: rms = $[1 / n\Sigma[J_i^{expt} - J_i^{theor} (P_N, \nu_{max, N}, P_S, \nu_{max, S})]^2]^{1/2}$ [c]The pseudorotational parameter was kept fixed during optimisation.

twist). For the 3'-amino modified compounds, the puckering of the 2'-chloro derivative **6** (P_N = 7.7°, $\nu_{max, N}$ = 38.4°), is in between a $^3T_2$ (C3'-*endo*-C2'-*exo* twist) and ^3E (C3'-*endo* envelope), whereas the 2'-fluoro derivative **8** (P_N = 31.2°, $\nu_{max, N}$ = 36.5°) is close to a $^3T_4$ (C3'-*endo*-C4'-*exo* twist). Our results show that when 3'-azido/amino and 2'-chloro/fluoro modifications are combined, the pseudo-axial position of the 2'-halogens and the resulting *O*4'-C1'-C2'-R2 *gauche* effect are directing the furanose ring towards the "northern" hemisphere of the pseudorotational circle. This *O*4'-C1'-C2'-R2 *gauche* interaction and its drive towards the N-type conformers is cooperative with the anomeric effect[16] and, as evidenced by the X_S-values of **5** (and **6**) (≤ 46 %) *vs.* **7** (and **8**) (≤ 6 %) (Table 8.4), relates to the electronegativity of the 2'-substituents. This is in line with previous findings.[12,18] Marquez *et al.*[12] proved the pseudorotational equilibrium to be governed by the α- or β-oriented fluorine atoms at the 2'- or 3'-position and their tendency to adopt a pseudo-axial orientation. Furthermore, the comparative solution conformation analysis of both 3'-α-fluoro-thymidine (FLT) and AZT clearly demonstrated that the small, electronegative 3'-fluorine atom was practically locked in the pseudo-axial position (due to the strong O4'-C4'-C3'-F *gauche* interaction), whereas the sterically larger 3'-azide showed no clear positional preference.[12] Here however, without proper energetic quantification of the various stereoelectronic effects in **5** (and **6**) and **7** (and **8**), we can only postulate that the *O*4'-C1'-C2'-Cl/F *gauche* effect dominates the opposite O4'-C4'-C3'-N_3/NH_2 *gauche* effect and decreases as size increases and/or electronegativity decreases (*cf.* **5** (and **6**) *vs.* **7** (and **8**). Only the S-type conformers of **5** and **6** are relevant (for **7** (and **8**) X_S ≤ 6 %). The 2'-chloro-3'-azido modified **5** (P_S = 132.7°, $\nu_{max, N}$ = 36.5°) has a

conformation in between a $_1E$ (C1'-*exo* envelope) and $^2T_1$ (C2'-*endo*-C1'-*exo* twist), whereas the 3'-amino derivative **6** (P_S = 162.7°, $\nu_{max, N}$ = 36.5°) has a perfect ^2E (C2'-*endo* envelope) S-type conformation.

Table 8.4 Values for $\Delta H°$ and $\Delta S°$ of the N↔S conformational equilibria as obtained through van't Hoff plots, $\Delta G°$ and population of the S conformer at 303 K

Analogue	ΔH[a] (kJ/mol)	ΔS[a] (J/mol K)	ΔG[b] (kJ/mol)	X_S[c] (%)
5	1.8	4.6	0.38	46
6	5.7	6.8	3.6	19
7	13.7	22.4	7.0	6
8	21.1	1.2	20.7	≤ 1

[a]$\Delta H°$ and $\Delta S°$ were calculated from the slope and intercept of the line obtained through the least-squares fitting procedure of ln (X_S/X_N) to the reciprocal of temperature: ln (X_S/X_N) = -($\Delta H°$ / R) (1 / T) + ($\Delta S°$ / R). R is the gas constant (8.31 J/mol K). [b]Calculated Gibbs free energy at 303 K ($\Delta G° = \Delta H° - T\Delta S°$). [c]The population of the S conformer at 303 K through the relation X_S/X_N = K = exp(-ΔG^{303} / RT).

X-ray crystallographic analysis of TMPKmt complexed dTMP shows that the furanose ring of the substrate is biased towards the "south".[8,10] The preference of **5** (and **6**) and **7** (and **8**) for the opposite "northern" conformation results in the pseudo-equatorial positioning of the 3'-azide/amine and can explain their moderate affinity for TMPKmt. The 3'-hydroxyl function of dTMP interacts directly with an aspartate residue (Asp9) in the TMPKmt binding site.[8] The positional shift of the 3'-azido/amino substituents, when puckered in N, might result in an ineffective contact with this Asp9 and hence lower the affinity. The introduction of a methylene spacer between the 3'-azido/amino group and the C3', the so-called "branched chain", might restore the hampered interaction with Asp9 and consequently improve the affinity.

8.2.4 N↔S energy calculations

Generally, in the solid state, mainly influenced by crystal packing forces,[19] only one of the two solution conformations (N or S) is present.[15] Similarly, when a nucleoside (or nucleotide) binds to its target only one form is expected to be present. Although the N↔S energy difference is ≈ 4 kcal/mol for classic nucleosides and nucleotides,[15] it can explain their differences in binding affinity.[20] We estimated the enthalpy ($\Delta H°$)

and the entropy ($\Delta S°$) of the N↔S two-state pseudorotational equilibrium for **5** (and **6**) and **7** (and **8**) from the slopes and intercepts of the van't Hoff plots [ln (*X*s/*X*n) vs. 1/*T*] (Table 8.4). The signs of the thermodynamic parameters ($\Delta H°$, $\Delta S°$ and $\Delta G°$) are arbitrary chosen so that positive values indicate the drive of N↔S equilibrium to N, as is the case for **5** (and **6**) and **7** (and **8**)**,** whereas negative values would describe the drive towards S.

Note that at 30 °C the $\Delta H°$ and $\Delta S°$ contributions to the $\Delta G°$ of the pseudorotational equilibrium in **5** (and **6**) and **7** (and **8**) are quite different and that it is the significant $\Delta H°$ contribution that drives the pseudorotational equilibrium to the "north". Although the $\Delta G°$-values for **5** and **6** are positive, their $\Delta H°$ contribution to $\Delta G°$ is rather low (1.8 kJ/mol and 5.7 kJ/mol respectively) and indicates the N↔S equilibrium can be easily driven towards S by the enzyme upon binding. More likely, their rather poor affinity, i.e. $K_i \approx 150$ μM (Table 8.1), results from the steric clash between the larger 2'-α-chloro atom with Tyr103. In case of **5** (and **6**) however, this effect is not so dramatic as for the 2'-α-hydroxyl in **1** and **2**, which probably relates to the greater hydrophobicity of the chloro atom. The $\Delta H°$ contributions of **7** and **8** (13.7 kJ/mol and 21.1 kJ/mol respectively), on the other hand, suggest that the N↔S equilibrium is strongly biased towards N, the antipodal conformation of the S puckering preferred by TMPKmt.[8] Such an energy gap might not easily be overcome by TMPKmt and, together with the ineffective pseudo-equatorial position of the 3'-azide/amine, plausibly accounts for the moderate K_i-values of **7** and **8**. This conformational rigidity of **7** is also a possible explanation for the lack of anti-HIV-1 activity.[21] The strong tendency of **7** to adopt a N-type puckering probably hampers the activation of this nucleoside to its triphosphate counterpart by cellular kinases, known to prefer S conformers as substrates.[22]

8.3 Conclusion

In search for new treatment strategies against tuberculosis, *Mycobacterium tuberculosis* thymidine monophosphate kinase (TMPKmt) was previously introduced as a potential target for the rational design of inhibitors. Stimulated by the fact that

thymidine and 3'-α-azido-thymidine proved to be potent inhibitors, we further elaborated our research towards the rational design of new leads based on the TMPKmt crystal structure. This work describes the synthesis and biological evaluation of a number of 2'-and 3'-modified thymidine analogues (**1-8**).

As expected the combination of 3'-azide/amine and 2'-α/β-hydroxyl substitutions, i.e. for **1** (and **2**) and **3** (and **4**), decreased the affinity significantly due to interaction with a tyrosine residue (Tyr103) known to be in the vicinity of the 2'-position. To our surprise the combination of 3'-azide/amine and 2'-chloro/fluoro substituents (**5** (and **6**) and **7** (and **8**)), known to be beneficial for the TMPKmt affinity when introduced separately, only resulted in moderate binding properties. This prompted us to investigate the conformational aspects of these thymidine analogues. In solution the sugar ring of nucleosides and nucleotides is known to exist in a rapid dynamic equilibrium, between the extreme "northern" (N) and the opposite "southern" (S) conformations. When a nucleoside or a nucleotide binds to its target enzyme, like in the crystal, only one of the two solution conformations is expected to be present in the active site. Through the NMR spectral parameters of **5** (and **6**) and **7** (and **8**), i.e. vicinal coupling constants (*J*), and their subsequent analysis with the PSEUROT program we indicated these analogues to be biased strongly towards the N conformation of the furanose ring. Via van't Hoff plots we also calculated the energy ($\Delta H°$, $\Delta S°$ and the resulting $\Delta G°$) for the N$\leftrightarrow$S equilibria of **5** (and **6**) and **7** (and **8**). Keeping the binding affinity of these derivatives in mind, our conformational analysis and energy calculations show to have important implications on: (*i*) the appropriate positioning of the 2'- and 3'- substituents; (*ii*) the ability of the enzyme to induce an S-type puckering on its ligand.

The discrepancy between the conformation of the substrate from the target X-ray structure and the solution state conformation of the analogues examined, indicates the danger of only using crystal structural data for the formulation of structure-activity relationships. These findings will allow us to further rationally design other 2'- and 3'-modified thymidine analogues, considering the influence of the planned modification (at the 2'- and 3'-position) on both potential binding interactions and conformational preference.

8.4 Experimental Section

8.4.1 TMPK assay

*Biological evaluation was performed by Dr. Hélène Munier-Lehmann, at the Laboratoire de Chemie Structurale des Macromolecules (Institut Pasteur), Paris, France. For the detailed procedure on the TMPKmt assay we refer to the experimental part in our Eur. J. Org. Chem. research paper (**2003**,15, 2911).*

8.4.2 Pseudorotational analysis

NMR samples were prepared with 3 mg of compounds **5** (and **6**) and **7** (and **8**), dissolved in 250 μl D_2O and pD was adjusted to 7.4 (same conditions used during the TMPKmt assay). High resolution 1D ^1H spectra were recorded on a Varian 500 MHz Unity spectrometer, operating at 499.505 MHz. Quadrature detection was achieved by States-Haberkorn hypercomplex mode.[23] Coupling constants were examined for all four analogues between 278 K and 333 K. The ring conformations of the synthetic nucleosides were analysed with the program PSEUROT 6.2[17] (DOS version) running on a Pentium II 350-MHz personal computer. This version includes an improved generalized Karplus equation for the iterative generation of coupling constants based on the experimental data as described by Donders *et al.*[24] The standard values for substituent electronegativities (supplied with the 6.2 version)[17] were used in the iterations. For the azide function the λ-value of 0.85 was used.[12] For the calculations an iterative strategy was adopted in which the pseudorotational parameters, obtained for each set of coupling constants, were calculated repeatedly after minor changes were systematically made in the starting parameters. If there was reason to believe that a specific derivative preferred a particular ring puckering, the minor conformer was held fixed during the iteration. The quality of the data was measured in the RMS deviation of the calculated and experimental coupling constants. In general, the RMS deviation (between the experimental and calculated coupling constants) was less than 0.2, indicating the parameterisation of the program was well suited to the input data (Table 8.3).

8.4.3 N↔S energy calculations

For each compound, the mole fraction of S (X_S) at each temperature interval (Table 8.2.), obtained from the PSEUROT[17] analysis, was used to make the van't Hoff plots (not shown here). The slopes and intercepts of these van't Hoff plots were subsequently used to calculate the $\Delta H°$ and $\Delta S°$ of the N↔S two-state pseudorotational equilibrium of compounds **5** (and **6**) and **7** (and **8**) (Table 8.4). The correlation coefficients (R^2) of the van't Hoff plots are: 0.96 (**5**), 0.93 (**6**), 0.81 (**7**) and 0.92 (**8**). $\Delta G°$ and X_S were calculated at 303 K using the determined $\Delta H°$ and $\Delta S°$ values (Table 8.4).

8.4 References

[1] Stokstad, E. *Science* **2000**, *287*, 2391.

[2] Raviglione, M. D.; Snider Jr., D. E.; Kochi, A. *JAMA* **1995**, *273*, 220.

[3] http://www.who.int/mediacentre/factsheets/who104/en/index.html
(WHO Global tuberculosis programme – Tuberculosis Fact Sheet, **2002**)

[4] Nguyen, T.; Stout, B. *OutLook* **1999**, *17*, 1.

[5] http://www.who.int/gtb/dots/index.htm (WHO Global tuberculosis programme – An expanded DOTS framework for effective tuberculosis control, **2002**)

[6] Dooley, S. W.; Jarvis, W. R.; Martone, W. J.; Snyder Jr, D. E. *Ann. Intern. Med.* **1992**, *117*, 257.

[7] Munier-Lehmann, H.; Chaffotte, A.; Pochet, S.; Labesse, G. *Protein Science* **2001**, *10*, 1195.

[8] de la Sierra, L.; Munier-Lehmann, H.; Gilles, A. M.; Bârzu, O.; Delarue, M. *J. Mol. Biol.* **2001**, *311*, 87.

[9] Pochet, S.; Dugué, L.; Douguet, D.; Labesse, G.; Munier-Lehmann, H. *ChemBioChem* **2002**, *3*, 108.

[10] (i) Vanheusden, V.; Munier-Lehmann, H.; Pochet, S.; Herdewijn, P.; Van Calenbergh, S. *Bioorg. Med. Chem. Lett.* **2002**, *12*, 2695. (ii) Van Rompaey, P.; Vanheusden, V.; Pochet, S.; Munier-Lehmann, H.; Froeyen, M.; Herdewijn, P.; Van Calenbergh, S. *Collection Symposium Series* **2002**, *5*, 393.

[11] Vanheusden, V.; Munier-Lehmann, H.; Froeyen, M.; Dugué, L.; Heyerick, A.; De Keukeleire, D.; Pochet, S.; Herdewijn, P.; Van Calenbergh, S. *J. Med. Chem.* **2003**, *46*, 3811.

[12] (i) Herdewijn, P.; Van Aerschot, A.; Kerremans, L. Nucleosides Nucleotides **1989**, *8*, 65. (ii) Plavec, J.; Koole, L. H.; Sandström, A.; Chattopadhaya, J. *Tetrahedron* **1991**, *47*, 7363. (iii) Barchi Jr., J. J.; Jeong, L. S.; Siddiqui, M. A.; Marquez, V. E. *J. Biochem. Biophys. Methods* **1997**, *34*, 11.

[13] Codington, J. F.; Doerr, I. L.; Fox, J. J. *J. Org. Chem.* **1964**, *29*, 558.

[14] (i) Altona, C.; Sundaralingam, M. *J. Am. Chem. Soc.* **1972**, *94*, 8205. (ii) Altona, C.; Sundaralingam, M. *J. Am. Chem. Soc.* **1973**, *95*, 2333.

[15] Saenger, W. *Principles of Nucleic Acid Structure*, Springer-Verlag, New York, **1984**.

[16] Plavec, J.; Tong, W.; Chattopadhyaya, J. *J. Am. Chem. Soc.* **1993**, *115*, 9734.

[17] (i) van Wijk, J.; Haasnoot, C. A. G.; de Leeuw, F. A. A. M.; Huckriede, B. D.; Westra Hoezema, A.; Altona, C. *PSEUROT 6.2* **1993**, Leiden Institute of Chemistry, Leiden University. (ii) Altona, C. *Recl. Trav. Chem. Pays-Bas* **1982**, *101*, 413. (iii) de Leeuw, F. A. A. M.; Altona, C. *J. Comput. Chem.* **1983**, *4*, 428.

[18] Thidaudeau, C.; Plavec, J.; Garg, N.; Papchikhin, A.; Chattopadhyaya, J. *J. Am. Chem. Soc.* **1994**, *116*, 4038.

[19] De Leeuw, H. P. M.; Haasnoot, C. A. G.; Altona, C. *Isr. J. Chem.* **1980**, *20*, 108.

[20] Marquez, V. E.; Siddiqui, M. A.; Ezzitouni, A.; Russ, P.; Wang, J.; Wagner, R. W.; Matteucci, M. D. *J. Med. Chem.* **1996**, *39*, 3739.

[21] (i) Herdewijn, P.; Van Aerschot, A. *Bull. Soc. Chim. Belg* **1989**, *12*, 937. (ii) Huang, J.-T.; Chen, L.-C.; Wang, L.; Kim, M.-H.; Warshaw, J. A.; Armstrong, D.; Zhu, Q.-H.; Chou, T.-C.; Watanabe, K. A.; Matulic-Adamic, J.; Su, T.-L.; Fox, J. J.; Polsky, B.; Baron, P. A.; Gold, J. W. M.; Hardy, W. D.; Zuckerman, E. *J. Med. Chem.* **1991**, *34*, 1640.

[22] Van Roey, P.; Taylor, W. E.; Wu, C.G.; Schinazi, R. f. *Ann. N. Y. Acad. Sci.* **1990**, *616*, 29.

[23] States, D. J.; Haberkorn, R. A.; Ruben, D. J. *J. Magn. Res.*, **1982**, *48*, 286.

[24] Donders, L. A.; De Leeuw, F. A. A. M.; Altona, C. *Magn. Res. Chem.* **1989**, *27*, 556.

SUMMARY

In this work we have described the synthesis (**Part I**, **Chapter 1**-**2**) of various adenosine and thymidine analogues (Figure 1) and evaluated their behaviour on adenosine receptors (ARs, **Part II**, **Chapter 3**-**6**), a subfamily of G-protein coupled receptors, and as inhibitors of thymidine monophosphate kinase (**Part III**, **Chapter 7**-**8**), a potential drug target for treatment of tuberculosis.

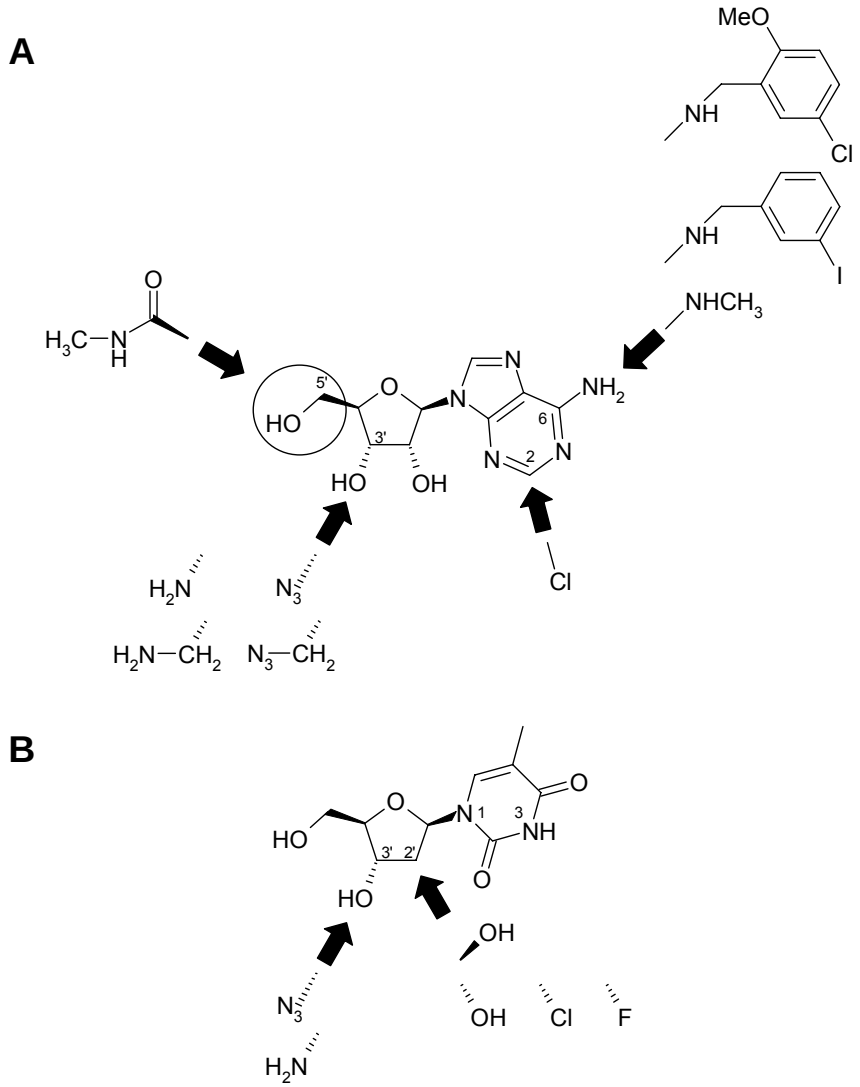

Figure 1 Overview of the modifications made on the adenosine (**A**) and thymidine (**B**) nucleoside scaffolds

In **Part II** we focussed on the human adenosine A_3 receptor (A_3AR) subtype, the most recently identified member of the ARs. Since its discovery, many variations have been made on the adenosine nucleoside scaffold in view of potent and

selective A_3AR binding. Known A_3AR selective alternations are (Figure 1**A**): N^6-modifications and smaller substituents at the 2-position of the purine moiety, both with and without the 5'-methylcarbamoyl insertion in the sugar moiety.

In this thesis, we have examined the effect of combining these variations with 3'-azido/amino(methyl) modifications, to provide more insight into the effect of combined substitution patterns on hA_3AR affinity and efficacy. Several analogues showed moderate to high A_3AR affinity and selectivity. Analogue **4.19** (K_i hA_3AR = 27 nM and A_1/A_3 selectivity > 350) emerged as the best in this series. An interesting feature was that the intrinsic activity could be tuned by varying the substituent introduced at the 3'-position:

- a 3'-amino function (as in **4.14**, **4.16** and **4.19**) resulted in (strong) partial agonist activity;
- the azide precursors (as in **4.11**, **4.13** and **4.17**) converted these analogues into antagonists;
- introduction of a methylene spacer "branching" (as in **4.1**-**10**, **4.12**, **4.15**, **4.18** and **4.20**) abolished all efficacy.

Moreover, we were interested in the role of these modified adenosine analogues as tools for the structure based exploration of ARs. By integrating organic synthesis and molecular engineering, we (in collaboration with the group of Dr. Kenneth A. Jacobson) investigated the molecular complementarity at both wild-type and mutant A_3 (**Chapter 5**) and A_{2A} (**Chapter 6**) adenosine receptors in the so-called "neoceptor-neoligand" concept. In absence of high-resolution structural knowledge of GPCRs, this concept was successfully used to both structurally and functionally validate the rhodopsin based homology models of the A_{2A} and A_3 adenosine receptors with adenosine derivatives such as **4.7** and **5.14**.

In **Chapter 5** we showed the affinities of the 3'-amino modified adenosine analogues (neoligands) to be higher for the H272E mutant A_3AR (neoceptor) than for the corresponding wild type receptor, demonstrating that the A_3AR (or a GPCR in general) could be engineered for selective interaction with synthetic agonists.

In **Chapter 6** we described the binding characteristics of A_{2A}AR agonist and antagonist ligands, using a rhodopsin based three-dimensional model of the A_{2A}AR TMs. In addition, we validated the model by making complementary changes in the structures of both agonist ligands and the A_{2A}AR, to form new neoceptor(T88D)-neoligand pairs.

In **Part III** (**Chapter 7**-**8**) we briefly studied the potential of thymidine analogues, modified in 2'- and 3'-position (Figure 1**B**), as inhibitors of Mycobacterium *tuberculosis* thymidine monophosphate kinase, an enzyme under investigation as new anti-tuberculosis target. Surprisingly, these analogues showed only moderate binding affinity (i.e. K_i between 118 and 1260 μM), prompting us to investigate their conformational features (i.e. preferred ring puckering). This analysis showed that especially derivatives **8.7** and **8.8** (with respectively K_i = 118 and 190 μM) are strongly biased towards the "northern" ring conformation, whereas X-ray crystallography suggests a preference of TMPKmt for ligands with the opposite "southern" ring pucker.

OVERVIEW OF EVALUATED COMPOUNDS

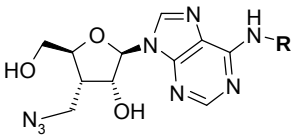

	R
4.1	H
4.2	CH_3
4.3	3-iodobenzyl

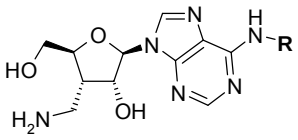

	R
4.5	H
4.6	CH_3
4.7	3-iodobenzyl (**6.7**)
4.8	5-chloro-2-methoxybenzyl

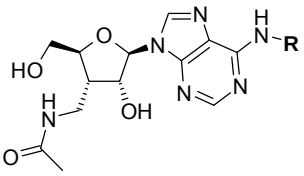

	R
4.9	3-iodobenzyl
4.10	5-chloro-2-methoxybenzyl

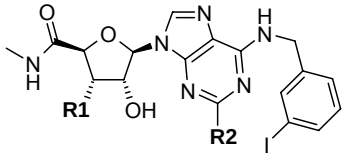

	R1	R2
4.11	N_3	H
4.12	CH_2N_3	H
4.13	N_3	Cl

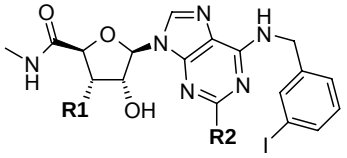

	R1	R2
4.14	NH_2	H
4.15	CH_2NH_2	H
4.16	NH_2	Cl

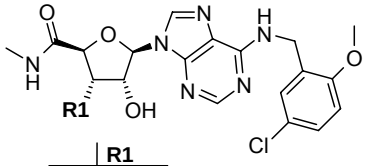

	R1
4.17	N_3
4.18	CH_2N_3

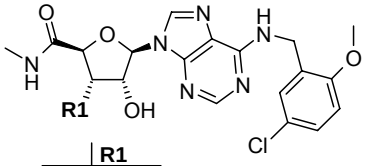

	R1
4.19	NH_2
4.20	CH_2NH_2

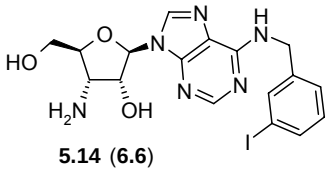

5.14 (**6.6**)

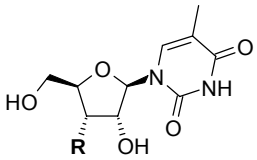

8.1 R = NH_2
8.2 R = N_3

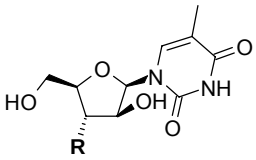

8.3 R = NH_2
8.4 R = N_3

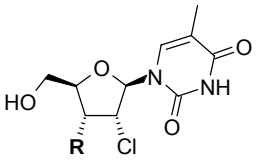

8.5 R = NH_2
8.6 R = N_3

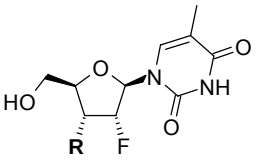

8.7 R = NH_2
8.8 R = N_3

LIST OF PUBLICATIONS

Jacobson, K.A.; Gao, Z.-G.; Chen, A.; Barak, D.; Kim, S.-A.; Lee, K.; Link, A.; Van Rompaey, P.; Van Calenbergh, S.; Liang, B.T. Neoceptor Concept Based on Molecular Complementarity in GPCRs: A Mutant Adenosine A_3 Receptor with Selectively Enhanced Affinity for Amine-Modified Nucleosides. *J. Med. Chem.* **2001**, 44, 4125-4136.

Vanhoenacker, G.; Van Rompaey, P.; De Keukeleire, D.; Sandra, P. Chemotaxonomic Features Associated with Flavanoids of Cannabinoid-Free Cannabis (*Cannabis sativa* subsp. *sativa* L.) in Relation to Hops. *Nat. Prod. Lett.* **2002**, *16*, 57-63.

Van Rompaey, P.; Nauwelaerts, K.; Vanheusden, V.; Rozenski, J.; Munier-Lehmann, H.; Herdwijn, P.; Van Calenbergh, S. *Mycobacterium tuberculosis* Thymidine Monophosphate Kinase Inhibitors: Biological Evaluation and Conformational Analysis of 2'- and 3'-Modified Thymidine Analogues. *Eur. J. Org. Chem.* **2003**, *15*, 2911-2918.

Vanheusden, V.; Van Rompaey, P.; Munier-Lehmann, H.; Pochet, S.; Herdewijn, P.; Van calenbergh, S. Thymidine and Thymidine-5'-O-monophosphate Analogues as Inhibitors of *Mycobacterium tuberculosis* Thymidylate Kinase. *Bioorg. Med. Chem. Lett.* **2003**, *13*, 3045-3048.

Kim, S.-K.; Gao, Z.-G.; Van Rompaey, P.; Gross, A. S.; Chen, A.; Van Calenbergh, S.; Jacobson, K. A. Modeling the Adenosine Receptors: Comparison of Binding Domains of the A_{2A} Agonists and Antagonists. *J. Med. Chem.* **2003**, *46*, 4847-4859.

Ohno, M.; Gao, Z.-G.; Van Rompaey, P.; Tchilibon, S.; Kim, S.-K.; Harris, B. A.; Gross, A. S.; Duong, H. T.; Van Calenbergh, S.; Jacobson, K. A. Modulation of Adenosine Receptor Affinity and Intrinsic Efficacy in Adenosine Nucleosides Substituted at the 2- and N^6-Position. *Bioorg. Med. Chem.* **2004**, *12*, 2995-3007.

Van Rompaey, P.; Jacobson, K. A.; Gross, A. S.; Gao, Z.-G.; Van Calenbergh, S. Exploring Human Adenosine A_3 Receptor Complementarity and Activity for Adenosine Analogues Modified in the Ribose and Purine Moiety. *Bioorg. Med. Chem.* **2004**, Accepted.

APPENDIX: AMINO ACIDS

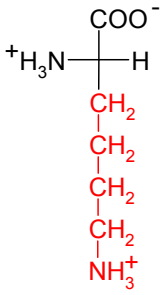

Lys or K

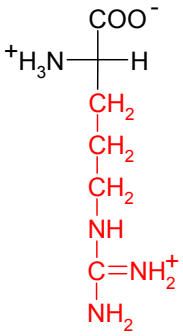

Arg or R

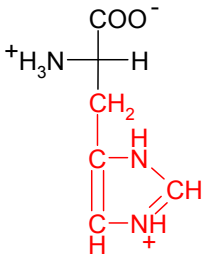

His or H

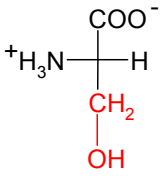

Ser or S

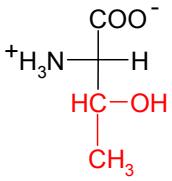

Thr or T

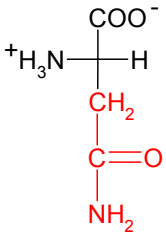

Asp or N

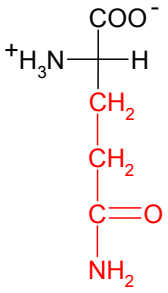

Gln or Q

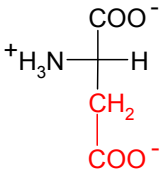

Asp or D

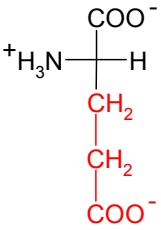

Glu or E

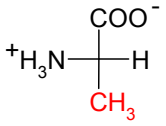

Ala or A

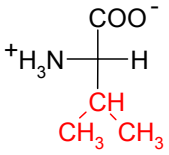

Val or V

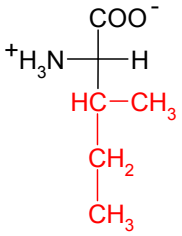

Ile or I

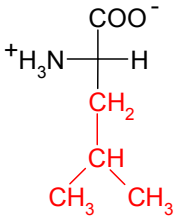

Leu or L

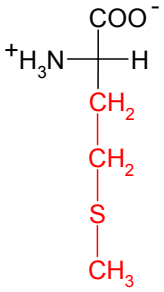

Met or M

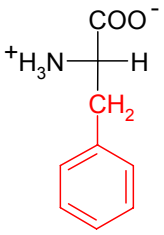

Phe or F

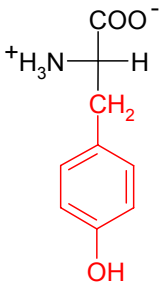

Tyr or T

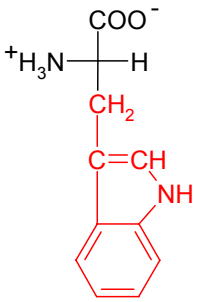

Trp or W

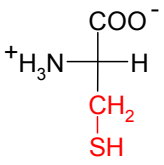

Cys or C

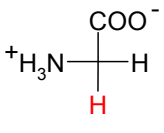

Gly or G

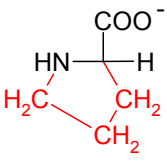

Pro or P

SAMENVATTING

In **Deel I** (**Hoofdstuk 1**-**2**) van dit werk beschreven we de synthese van gemodificeerde adenosine en thymidine analogen (zie Figuur 1). Deze verbindingen werden als moleculaire *probes* gebruikt voor de biologische evaluatie van adenosine-receptoren (ARn, **Deel II**, **Hoofdstuk 3**-**6**), die behoren tot de G-proteïne gekoppelde receptor (GPCR) superfamilie, en als inhibitoren voor thymidine-monofosfaat kinase (**Deel III**, **Hoofdstuk 7**-**8**), een potentieel antituberculose doelwit.

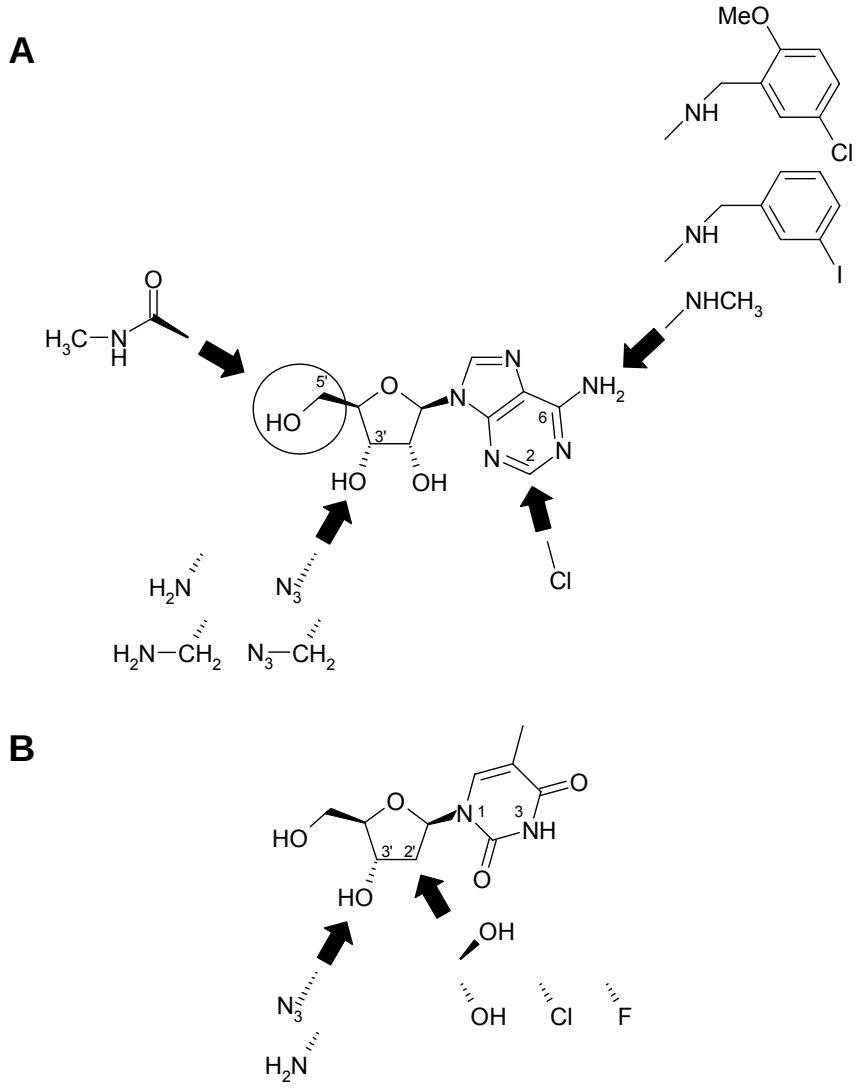

Figuur 1 Overzicht van de verrichte adenosine (**A**) en thymidine modificaties (**B**)

Deel II richtte zich voornamelijk op de adenosine A_3 receptor (A_3AR), de meest recente AR. Reeds vele structurele variaties van het adenosine-skelet werden onderzocht met het oog op A_3AR affiniteit en selectiviteit, waaronder N^6-benzyl-

substituties en kleinere functionele groepen in 2-positie van het purine gedeelte, al of niet in combinatie met de introductie van een 5'-methylcarbamoyl in het ribofuranose deel.

Door bovengenoemde veranderingen aan het adenosine-skelet te combineren met 3'-azido/amino(methyl)-modificaties (zie Figuur 1**A**), wilden we de invloed bestuderen van dergelijk (gecombineerd) substitutiepatroon op de A_3AR selectiviteit, affiniteit en intrinsieke activiteit. Vele van de gesynthetiseerde analogen vertoonden matige tot hoge A_3AR affiniteit en selectiviteit. Het beste derivaat uit deze serie was analoog **4.19** (K_i hA_3AR = 27 nM en A_1/A_3 selectiviteit > 350). Interessant bij deze verbindingen was dat de intrinsieke activiteit gemoduleerd kon worden afhankelijk van de substituent in 3'-positie:

- een 3'-aminogroep (zoals bv. **4.14**, **4.16** en **4.19**) resulteerde in (sterk) partieel agonisme;
- de azide precursoren (zoals bv. **4.11**, **4.13** en **4.17**) waren allen antagonisten; en
- introductie van een methylene-*spacer* zoals bij **4.1**-**10**, **4.12**, **4.15**, **4.18** en **4.20** ging ten koste van de intrinsieke activiteit.

Ook bestudeerden we de rol van deze gemodificeerde adenosine analogen als *tools* voor het structuurgebaseerd onderzoek van ARn. Door organische synthese en moleculaire modeling te integreren in het "neoceptor-neoligand" concept, konden we (in samenwerking met dr. Kenneth A. Jacobson) meer inzicht verwerven in de moleculaire complementariteit van wild-type en gemuteerde A_3 (**Hoofdstuk 5**) en A_{2A} (**Hoofdstuk 6**) ARn. In afwezigheid van exacte structurele kennis van verschillende GPCRn, liet deze aanpak toe met behulp van verbindingen zoals **4.7** en **5.14** de (A_{2A}AR en A_3AR) homologie modellen van de te valideren.

Bovendien, toonden we in **Hoofdstuk 5** aan dat de affiniteit van 3'-amino gemodificeerde adenosine analogen (neoliganden) hoger was voor de H272E gemuteerde A_3AR (neoceptor) dan voor de wild-type A_3AR. Hiermee bewezen we dat de A_3AR (of GPCRn in het algemeen) ontworpen kunnen worden om selectief met synthetische liganden te interageren.

In **Hoofdstuk 6** beschreven we de verschillende A_{2A}AR-bindingskarakteristieken voor agonisten en antagonisten op basis van het ontworpen 3-D homologie model. Een model dat gevalideerd werd door nieuwe neoceptor (T88D)-neoligand-paren te beschrijven.

In **Deel III** (**Hoofdstukken 7**-**8**) bestudeerden we het potentieel van 2',3'-gemodificeerde thymidine analogen als inhibitoren voor Mycobacterium *tuberculosis* thymidine-monofosfaat kinase, een nieuw antituberculose doelwit. De (onverwacht) lage affiniteit (d.i. K_i tussen 118 en 1260 μM) van deze verbindingen, spoorde ons aan om hun conformationele eigenschappen nader te bestuderen. De conformationele analyse van verbindingen **8.7** en **8.8** (respectievelijk met K_i's = 118 en 190 μM) toonde een mogelijk verband aan tussen de matige affiniteit en een suboptimale positionering van de 2'- en 3'-substituenten, toe te schrijven aan de uitgesproken voorkeur voor de noord conformatie.